Magnetic Resonance Imaging (MRI) Biomarkers for Therapeutic Response Prediction in Rectal Cancer

Trang Thanh Pham

A thesis in fulfilment of the requirements for the degree of

Doctor of Philosophy

Faculty of Medicine
South Western Sydney Clinical School

2020

Thesis/Dissertation Sheet

Surname/Family Name	:	**Pham**
Given Name/s	:	**Trang Thanh**
Abbreviation for degree as give in the University calendar	:	**PhD**
Faculty	:	**Faculty of Medicine**
School	:	**South Western Sydney Clinical School**
Thesis Title	:	**Magnetic resonance imaging (MRI) biomarkers for therapeutic response prediction in rectal cancer**

Abstract 350 words maximum:

Prediction of chemoradiotherapy (CRT) response in rectal cancer would enable stratification of management whereby responders could undergo 'watch-and-wait' to avoid surgical morbidity, and non-responders could have early treatment intensification to improve therapeutic outcomes. Functional MRI can assess tumour function and heterogeneity, and may improve therapeutic response prediction. The aims of this PhD were to (i) prospectively evaluate multi-parametric MRI at 3.0 tesla *in vivo* combining diffusion weighted imaging (DWI) and dynamic contrast enhanced (DCE) MRI for prediction of CRT response and 2 year disease-free survival (DFS), and (ii) examine diffusion tensor imaging (DTI) MRI biomarkers of rectal cancer extent and heterogeneity at ultra-high field 11.7 tesla *ex vivo* in order to establish a pipeline for MRI biomarker discovery from ultra-high field to clinical field.

Patients with locally advanced rectal cancer undergoing CRT followed by surgery underwent multi-parametric MRI before, during, and after CRT. A whole tumour voxel-wise histogram analysis of apparent diffusion co-efficient (ADC) and K^{trans} heterogeneity was performed and correlated with histopathology tumour regression grade. After CRT (before surgery) ADC 75^{th} and 90^{th} quantiles were significantly higher in responders than non-responders. Patients with higher K^{trans} values after CRT or greater increase in K^{trans} values from before to after CRT had a significantly higher risk of distant metastases, and lower 2 year DFS.

Biobank tissue from patients with rectal cancer were examined at 11.7 tesla and DTI-MRI results correlated with histopathology. This work established a discovery framework for screening Biobank cancer tissue for novel MRI biomarkers of tumour extent and heterogeneity, and resulted in good preservation of tissue integrity and MRI-histopathology alignment. DTI-MRI derived fractional anisotropy (FA) was able to differentiate between tumour and desmoplasia, fibrous tissue, and muscularis propria, allowing for more accurate delineation of rectal cancer tumour extent and stromal heterogeneity *ex vivo*.

In conclusion, DWI-MRI was predictive of CRT response, DCE-MRI was predictive of 2 year DFS, and DTI-MRI was able to more accurately define tumour extent and heterogeneity in rectal cancer. These findings could be useful for stratification of patients for individualised treatment based on accurate assessment of tumour extent and therapeutic response prediction.

ORIGINALITY STATEMENT

'I hereby declare that this submission is my own work and to the best of my knowledge it contains no materials previously published or written by another person, or substantial proportions of material which have been accepted for the award of any other degree or diploma at UNSW or any other educational institution, except where due acknowledgement is made in the thesis. Any contribution made to the research by others, with whom I have worked at UNSW or elsewhere, is explicitly acknowledged in the thesis. I also declare that the intellectual content of this thesis is the product of my own work, except to the extent that assistance from others in the project's design and conception or in style, presentation and linguistic expression is acknowledged.'

Signed ……..

Date ……..

COPYRIGHT STATEMENT

Signed .....

Date .....

AUTHENTICITY STATEMENT

'I certify that the Library deposit digital copy is a direct equivalent of the final officially approved version of my thesis. No emendation of content has occurred and if there are any minor variations in formatting, they are the result of the conversion to digital format.'

Signed .....

Date .....

INCLUSION OF PUBLICATIONS STATEMENT

UNSW is supportive of candidates publishing their research results during their candidature as detailed in the UNSW Thesis Examination Procedure.

Publications can be used in their thesis in lieu of a Chapter if:

- The student contributed greater than 50% of the content in the publication and is the "primary author", ie. the student was responsible primarily for the planning, execution and preparation of the work for publication
- The student has approval to include the publication in their thesis in lieu of a Chapter from their supervisor and Postgraduate Coordinator.
- The publication is not subject to any obligations or contractual agreements with a third party that would constrain its inclusion in the thesis

Please indicate whether this thesis contains published material or not.

☐ *This thesis contains no publications, either published or submitted for publication*

☐ *Some of the work described in this thesis has been published and it has been documented in the relevant Chapters with acknowledgement*

☒ *This thesis has publications (either published or submitted for publication) incorporated into it in lieu of a chapter and the details are presented below*

CANDIDATE'S DECLARATION

I declare that:

- I have complied with the Thesis Examination Procedure
- where I have used a publication in lieu of a Chapter, the listed publication(s) below meet(s) the requirements to be included in the thesis.

Name	Signature	Date (dd/mm/yy)
Trang Pham		

Postgraduate Coordinator's Declaration (to be filled in where publications are used in lieu of Chapters)

I declare that:

- the information below is accurate
- where listed publication(s) have been used in lieu of Chapter(s), their use complies with the Thesis Examination Procedure
- the minimum requirements for the format of the thesis have been met.

PGC's Name	PGC's Signature	Date (dd/mm/yy)
Roberto Forero		

For each publication incorporated into the thesis in lieu of a Chapter, provide all of the requested details and signatures required

Details of publication #1: *Full title:* Review Article: Functional MRI for quantitative treatment response prediction in locally advanced rectal cancer. *Authors:* ***Trang T Pham***, Gary Liney, Karen Wong, Michael Barton. *Journal or book name: British Journal of Radiology* *Volume/page numbers:* 2017; 90(1072) *Date accepted/ published:* 3 January 2017						
Status	*Published*	X	*Accepted and In press*		*In progress (submitted)*	
The Candidate's Contribution to the Work Candidate performed and wrote the entire literature review publication						
Location of the work in the thesis and/or how the work is incorporated in the thesis: Chapter 2.1 Literature Review						
Primary Supervisor's Declaration I declare that: • the information above is accurate • this has been discussed with the PGC and it is agreed that this publication can be included in this thesis in lieu of a Chapter • All of the co-authors of the publication have reviewed the above information and have agreed to its veracity by signing a 'Co-Author Authorisation' form.						
Supervisor's name Michael Barton	*Supervisor's signature*		*Date (dd/mm/yy)*			

Details of publication #2: *Full title:* Study protocol: multi-parametric magnetic resonance imaging for therapeutic response prediction in rectal cancer. *Authors:* ***Trang T. Pham***, Gary Liney, Karen Wong, Robba Rai, Mark Lee, Daniel Moses, Christopher Henderson, Michael Lin, Joo-Shik Shin, Michael Barton *Journal or book name:* BMC Cancer *Volume/page numbers:* 2017;17:465 *Date accepted/ published: 26 June 2017*						
Status	*Published*	*X*	*Accepted and In press*		*In progress (submitted)*	
The Candidate's Contribution to the Work Candidate was primary author, designed all aspects of the study protocol and contributed to the majority of work in the publication						
Location of the work in the thesis and/or how the work is incorporated in the thesis: Chapter 3.11						
Primary Supervisor's Declaration I declare that: • the information above is accurate • this has been discussed with the PGC and it is agreed that this publication can be included in this thesis in lieu of a Chapter • All of the co-authors of the publication have reviewed the above information and have agreed to its veracity by signing a 'Co-Author Authorisation' form.						
Supervisor's name Michael Barton	*Supervisor's signature*		*Date (dd/mm/yy)*			

Details of publication #3:

Full title: Ultra-high field MRI at 11.7 tesla for evaluation of rectal cancer stromal heterogeneity ex vivo: correlation with histopathology.

Authors: ***Trang T Pham,*** Timothy Stait-Gardner, Cheok Soon Lee, Michael Barton, Petra Graham, Gary Liney, Karen Wong, William S Price.

Journal or book name: Scientific Reports

Volume/page numbers: 2019;9:9311

Date accepted/ published: 4 June 2019

Status	*Published*	*X*	*Accepted and In press*		*In progress (submitted)*	

The Candidate's Contribution to the Work

Candidate was the primary author, contributed the majority of the work in all aspects of the study protocol design, experimentation work, results analysis and publication

Location of the work in the thesis and/or how the work is incorporated in the thesis:

Chapter 7 Results and discussion (ex vivo study): Ultra-high field MRI aided biomarker discovery in rectal cancer. The publication contains detailed methods, results and discussion for the *ex vivo* ultra-high field study.

Note that the previous Chapter 6 Methods expands on the patients/clinical/Biobank tissue collection methods for this study.

Primary Supervisor's Declaration

I declare that:

- the information above is accurate
- this has been discussed with the PGC and it is agreed that this publication can be included in this thesis in lieu of a Chapter
- All of the co-authors of the publication have reviewed the above information and have agreed to its veracity by signing a 'Co-Author Authorisation' form.

Supervisor's name	*Supervisor's signature*	*Date (dd/mm/yy)*
Michael Barton		

Table of Contents

Acknowledgements

Firstly, I would like to thank my primary supervisor Professor Michael Barton for his mentorship. I am fortunate to have a great mentor who has been an inspiration, supported my progression, and always fostered quality, innovation and collaboration. I would like to thank Michael for his guidance, and for encouraging and allowing me to be creative and explore new ideas. I would also like to thank my co-supervisors, A/Professor Gary Liney, who has been a great teacher and taught me so much about MRI, and Dr Karen Wong for her guidance, patience and invaluable support during my PhD.

The most rewarding part of my PhD journey has been the people I have had the opportunity to work with along the way, they have made the exploratory work and long hours enjoyable. I would like to thank Professor Bill Price, who has been an enormous support and an inspiration to work with, and Dr Timothy Stait-Gardner for his enthusiasm and making the exploratory work enjoyable. I would also like to thank the CONCERT Biobank, Professor Soon Lee for sharing his knowledge and ideas, Dr Nicole Caixeiro for helping with the tissue work, and Dr Petra Graham for the biostatistical work and her generosity with time. I am grateful to my colleagues at Liverpool Hospital including Ms. Robba Rai, Professor Christopher Henderson, Dr Mark Lee, Dr Stephanie Lim and Dr Michael Lin for their dedication and input into this work.

I would also like to thank my family - Mum, Dad, Khoi and Khoa; I am forever grateful for their love, support and inspiration.

Abstract

Prediction of chemoradiotherapy (CRT) response in rectal cancer would enable stratification of management whereby responders could undergo 'watch-and-wait' to avoid surgical morbidity, and non-responders could have early treatment intensification to improve therapeutic outcomes. Functional MRI can assess tumour function and heterogeneity, and may improve therapeutic response prediction. The aims of this PhD were to (i) prospectively evaluate multi-parametric MRI at 3.0 tesla *in vivo* combining diffusion weighted imaging (DWI) and dynamic contrast enhanced (DCE) MRI for prediction of CRT response and 2 year disease-free survival (DFS), and (ii) examine diffusion tensor imaging (DTI) MRI biomarkers of rectal cancer extent and heterogeneity at ultra-high field 11.7 tesla *ex vivo* in order to establish a pipeline for MRI biomarker discovery from ultra-high field to clinical field.

Patients with locally advanced rectal cancer undergoing CRT followed by surgery underwent multi-parametric MRI before, during, and after CRT. A whole tumour voxel-wise histogram analysis of apparent diffusion co-efficient (ADC) and K^{trans} heterogeneity was performed and correlated with histopathology tumour regression grade. After CRT (before surgery) ADC 75^{th} and 90^{th} quantiles were significantly higher in responders than non-responders. Patients with higher K^{trans} values after CRT or greater increase in K^{trans} values from before to after CRT had a significantly higher risk of distant metastases, and lower 2 year DFS.

Biobank tissue from patients with rectal cancer were examined at 11.7 tesla and DTI-MRI results correlated with histopathology. This work established a discovery framework for screening Biobank cancer tissue for novel MRI biomarkers of tumour extent and heterogeneity, and resulted in good preservation of tissue integrity and MRI-histopathology alignment. DTI-MRI derived fractional anisotropy (FA) was able to differentiate between tumour and desmoplasia, fibrous tissue, and muscularis propria, allowing for more accurate delineation of rectal cancer tumour extent and stromal heterogeneity *ex vivo*.

In conclusion, DWI-MRI was predictive of CRT response, DCE-MRI was predictive of 2 year DFS, and DTI-MRI was able to more accurately define tumour extent and heterogeneity in rectal cancer. These findings could be useful for stratification of patients for individualised treatment based on accurate assessment of tumour extent and therapeutic response prediction.

Publications, awards and presentations arising from PhD work

Publications

1. ***Pham TT,*** Liney G, Wong K, Barton M. Review Article: Functional MRI for quantitative treatment response prediction in locally advanced rectal cancer. *British Journal of Radiology* 2017; 90(1072) https://doi.org/10.1259/bjr.20151078

2. ***Pham TT***, Liney G, Wong K, Rai R, Lee M, Moses D, Henderson C, Lin M, Shin J, Barton M. Study protocol: multi-parametric magnetic resonance imaging for therapeutic response prediction in rectal cancer. *BMC Cancer* 2017;17:465. https://doi.org/10.1186/s12885-017-3449-4

3. ***Pham TT***, Stait-Gardner T, Lee S, Barton M, Graham P, Liney G, Wong K, Price, W.S. Ultra-high field MRI at 11.7 tesla for evaluation of rectal cancer stromal heterogeneity ex vivo: correlation with histopathology. *Scientific Reports* 2019;9:9311. https://doi.org/10.1038/s41598-019-45450-2

4. Fernando S, Lin M, ***Pham TT***, Chong S, Ip E, Wong K, Chua W, Ng W, PhD, Lin P, Lim S. Prognostic utility of serial ^{18}F-FDG-PET/CT in patients with locally advanced rectal cancer who underwent tri-modality treatment. *British Journal of Radiology* 2019 2019 Oct 23:20190455. https://doi.org/10.1259/bjr.20190455

Grants and Awards

1. **Withers and Peters Research Grant (RANZCR) 2014**

   Royal Australian and New Zealand College of Radiology Grant awarded for most able and committed young researcher. $25 000 grant awarded to undertake the research project 'Multi-parametric MRI Biomarkers for Therapeutic Response Prediction in Rectal Cancer'

2. **Elekta Award 2018 – Best scientific paper that shows advances in the use of technology in radiation therapy**

   Multi-parametric MRI biomarkers for radiotherapy response prediction in rectal cancer

3. **Ingham Institute Bowel Cancer Grant 2018** - $16000 awarded to undertake "Clinical Translation of MRI Biomarkers for Prediction of Tumour Extent and Radiotherapy Response in Rectal Cancer"

   PIs: Dr Trang Pham, Professor William S. Price

   AIs: Professor Soon Lee, Dr Timothy Stait-Gardner, Professor Michael Barton, Associate Professor Gary Liney and Dr Nicole Caixeiro

4. **National Health and Medical Research Council (NHMRC) Program Grant 2018 – 2022:** ***The Australian MRI-Linac Program: Transforming the science and clinical practice of cancer radiotherapy***

   Chief Investigators: Prof Paul Keall, Prof Michael Barton, Prof Stuart Crozier

   Research Collaborators*:* Dr Trang Pham, et al.

Conference Presentations

1. ***Pham TT***, Liney G, Roach D, Wong, K., Moses, D., Schmitt, B., Barton, M. Analysis of multi-parametric MRI at 3.0 tesla for the prediction of treatment response in rectal cancer. *3rd MR in RT Symposium 2015, Lund, Sweden.*

2. ***Pham TT***, Liney G, Wong K, Roach D, Moses D, Henderson C, Lee M, Rai R, Barton M. Multi-parametric MRI at 3.0 Tesla for the prediction of treatment response in rectal cancer. ESTRO 35 abstract. *Radiotherapy and Oncology* 2016; S874. *European Society for Radiotherapy and Oncology ESTRO 35, 2016. Turin, Italy*

3. ***Pham TT***, Barton M, Roach D, Wong K, Moses D, Henderson C, Lee M, Rai R, Schmitt B, Liney G. Multi-parametric MRI at 3.0 tesla for the prediction of treatment response in rectal cancer. *International Society for Magnetic Resonance in Medicine (ISMRM) 24th Annual Meeting 2016, Singapore*

4. ***Pham TT***, Stait-Gardner T, Lee S, Liney G, Barton M, Wong K, Price WS. High field diffusion tensor imaging for ex vivo evaluation of rectal cancer. *5th MR in RT Symposium 2017, Sydney, Australia*

5. ***Pham TT***, Stait-Gardner T, Lee S, Barton M, Liney G, Wong K, Price, W.S. Ultra-high field MRI for evaluation of rectal cancer stroma ex vivo: correlation with histopathology. ESTRO 37 Abstract. *Radiotherapy and Oncology* 2018; 127: S541–S542. *Barcelona, Spain*

6. ***Pham TT***, Liney G, Wong K, Henderson C, Shin J, Rai R, Lee M, Graham P, Hudson M, Borok N, Truong M, Barton M. Rectal cancer: multiparametric MRI assessment of tumour heterogeneity and chemoradiotherapy response. ESTRO 37 Abstract. *Radiotherapy and Oncology* 2018; 127: S410. *Barcelona, Spain*

7. ***Pham TT,*** Liney G, Wong K, Henderson C, Rai R, Graham P, Hudson M, Borok N, Truong M, Lee M, Shin J, Barton M. Rectal cancer: multi-parametric MRI 3-dimensional assessment of intra-tumour heterogeneity and chemoradiotherapy response prediction. *International Society for Magnetic Resonance in Medicine (ISMRM) Annual Meeting 2018, Paris, France*

8. ***Pham TT,*** Stait-Gardner T, Lee S, Barton M, Liney G, Wong K, Price W.S. Functional MRI at ultra-high field strength (11.7 T) for evaluation of rectal cancer stromal heterogeneity ex vivo: correlation with histopathology. *International Society for Magnetic Resonance in Medicine (ISMRM) Annual Meeting 2018, Paris, France*

9. ***Pham TT***, Liney G, Wong K, Henderson C, Rai R, Graham P, Hudson M, Borok N, Truong M, Shin J, Barton M. Multi-parametric MRI biomarkers for radiotherapy response prediction in rectal cancer. Abstract. *JMIRO* 2018. *Canberra, Australia*

10. ***Pham TT***, Liney G, Wong K, Henderson C, Rai R, Graham P, Hudson M, Borok N, Truong M, Lee M, Shin J, Barton M. MRI tumour heterogeneity analysis for prediction of chemoradiotherapy response and disease free survival in rectal cancer. *Australian MR in RT 2019, Noosa, Australia*

11. ***Pham TT***, Stait-Gardner T, Lee S, Barton M, Graham P, Liney G, Wong K, Gupta A, Price WS. Ultra-high field MRI aided biomarker discovery in rectal cancer. A*ustralian MR in RT 2019, Noosa, Australia*

Book chapter

1. *Barton MB, **Pham TT**, Harris G* "Will we still need radiotherapy in 20 years?" in MRI for Radiotherapy Planning, Delivery, and Response Assessment. Liney, Gary, van der Heide, Uulke (Eds.). Springer August 5, 2019 ISBN 978-3-030-14442-5

Abbreviations and Symbols

CRT	Chemoradiotherapy
Before CRT	Before chemoradiotherapy
During CRT	During chemoradiotherapy
After CRT	After chemoradiotherapy
ADC	Apparent diffusion co-efficient
ΔADC	Change in apparent diffusion co-efficient
ΔK^{trans}	Change in K^{trans}
FA	Fractional anisotropy
LARC	Locally advanced rectal cancer
DWI	Diffusion weighted imaging
DCE	Dynamic contrast enhanced
DTI	Diffusion tensor imaging
MRI	Magnetic resonance imaging
MR	Magnetic resonance
MRS	Magnetic resonance spectroscopy
mpMRI	Multi-parametric magnetic resonance imaging
ROI	Region of interest
3-D	Three-dimensional
DFS	Disease-free survival
HR	Hazard ratio
TRG	Tumour regression grade
FOV	Field of view
H&E	Haematoxylin and eosin
eVG	elastic Van Gieson
T	tesla
ns	non-significant
AJCC	American Joint Committee on Cancer

List of Figures

List of Tables

Chapter 1 Introduction and hypotheses

1.1 Introduction

Colorectal cancer is the third most common cancer diagnosed and the second most common cause of cancer death in Australia. Rectal cancer accounts for about 30% of colorectal cancer cases (1). The 5 year relative survival for rectal cancer in Australia between 2011 and 2015 was 70%. The addition of pre-operative radiotherapy with or without chemotherapy to primary surgery for treatment of locally advanced rectal cancer (LARC) has decreased locoregional recurrence rates (2-6), and increased overall survival (3, 7). Neoadjuvant chemo-radiotherapy (CRT) followed by a 6 - 8 week period before surgery has the advantage of tumour downstaging, with a pathologic complete response (pCR) achieved in 15-27% of patients (8). Tumour responses vary considerably following CRT and the reasons for this are not clearly understood. Fifty-four to seventy-five percent of patients will have tumour downstaging, however the remaining patients will have no treatment response (9). In patients with locally advanced (T3 – 4) resectable rectal cancer, distant metastases still dominate with a 5 year cumulative incidence of 30% in a pooled analysis of 5 randomised control trials (10). There is significant morbidity associated with locally advanced rectal cancer treatment, and about a third of patients will have a permanent colostomy as a result of surgery. At present, there is no accurate method of predicting response to CRT. Current predictive models require pathological staging, making them unsuitable for use as a pre-treatment decision support tool (10, 11). Non-invasive predictive biomarkers, such as MRI biomarkers, are required to guide individualisation of patient treatment in order to maximise therapeutic outcomes and minimise treatment toxicity.

Early imaging prediction of CRT response would enable a personalised treatment approach, to potentially improve therapeutic response and avoid treatment morbidity. Prediction of a complete clinical response to CRT prior to surgery would enable these patients to undergo a ‘watch-and-wait’ approach, avoiding the morbidity of surgery. Early detection of non-responders to CRT would provide the opportunity for these

patients to undergo dose escalation strategies, intensification of systemic therapies, or to proceed directly to surgery and avoid futile treatment.

Functional MRI assessment of tumour heterogeneity

Functional magnetic resonance imaging (MRI) has enabled the assessment of different biological tumour characteristics and is an important advance in imaging evaluation in oncology. Tumours are biologically heterogeneous, and this can affect therapeutic response. Tumour characteristics that can affect therapeutic response include cellularity, perfusion, hypoxia and the tumour extracellular matrix microenvironment. MRI can provide a virtual 'whole tumour biopsy' capturing information on intra-tumoural heterogeneity, and this can potentially aid with personalisation of treatment based on the patient's tumour characteristics. Volumetric measurements based on standard morphologic MRI (T2-weighted) lack sufficient accuracy for the differentiation of treatment responders from non-responders because of their inability to detect small residual tumour deposits within areas of radiation-induced fibrosis. Changes on morphologic MRI in response to treatment also occur late, making it unsuitable for early stratification of management. Functional MRI biomarkers have been documented to have greater potential compared to standard T2-weighted sequences in the assessment of therapeutic response prediction in LARC (12). The clinical utility of these functional MRI biomarkers in rectal cancer incorporating a whole tumour heterogeneity analysis for therapeutic early response prediction needs to be further explored.

MRI has a major benefit of imaging the whole tumour, capturing information on heterogeneity avoiding the sampling errors that occur with biopsies. Tumours are biologically heterogeneous, and information on intra-tumoural heterogeneity could improve therapeutic response prediction. Most published MRI response prediction studies in rectal cancer report single summary parameters from either diffusion or perfusion MRI. Summary measures such as mean values do not provide information on tumour heterogeneity. Tumour heterogeneity could be analysed using a whole tumour voxel-wise histogram analysis method, from which parameters such as percentiles, skewness and kurtosis could be extracted.

This PhD thesis explores the role of diffusion weighted imaging (DWI), dynamic contrast enhanced (DCE) and diffusion tensor imaging (DTI) MRI in the assessment of rectal cancer heterogeneity and response to CRT. It examines the role of ultra-high field MRI in screening promising MRI biomarkers.

Diffusion weighted imaging (DWI) MRI

DWI is a functional MRI technique which measures the movement of water through the tissue. The apparent diffusion coefficient (ADC) is the quantitative parameter of water diffusion through tissue derived from DWI-MRI and shows an inverse relationship with tissue cellularity. Viable tumour cells restrict the mobility of water molecules, whereas necrotic tumour cells allow freer diffusion of water through tissue. High tumour cellularity and architectural distortion of the extracellular space leads to restricted diffusion and lower ADC values, and these values are expected to correlate with tumour cellularity and grade(13). Radiotherapy related cellular damage leading to necrosis can occur within days of commencing treatment. ADC has been shown to be able to differentiate viable tumour from inflammation and necrosis, making it potentially a useful tool to monitor early effects of radiotherapy (13).

A number of prospective studies have evaluated the use of DWI in the assessment of response to CRT in LARC (14-16), and demonstrated ADC to be useful for the prediction and early assessment of pathologic response to CRT. However, ADC cut-off values for response were chosen on an ad-hoc basis and still require prospective validation. There are limited prospective studies examining the value of DWI during CRT (14, 15). Diagnostic performance of after CRT ADC values for predicting pCR varied between studies, ranging from 83-100% for sensitivity, and 67 - 93% for specificity (15-17). A meta-analysis demonstrated that DWI had a mean sensitivity of 83.6% (95% CI 61.7 to 94.2%) and specificity of 84.8% (95% CI 74.2 to 91.5%) (12).

Dynamic contrast enhanced (DCE) MRI

DCE-MRI provides information on micro-vessel density, perfusion, permeability and extracellular-extravascular space composition. Regions of interest may be interrogated to produce enhancement-time curves with malignant tumours, due to their abnormal

microvasculature, demonstrating a rapid wash-in and wash-out of contrast, and a greater increase in signal intensity than normal tissues (18, 19). K^{trans} (contrast medium exchange in the Tofts pharmacokinetic model) is a quantitative measure of 'wash-in' of contrast. Early DCE studies in rectal cancer have shown correlation of DCE parameters with tumour angiogenesis, as indicated by micro-vessel density and VEGF, and tumour downstaging (20-24). DCE may be useful in assessing biological factors of the functional tumour vascular microenvironment that influence radiotherapy response.

Diffusion tensor imaging (DTI) MRI

DTI-MRI is a variant of diffusion MRI which provides a rotationally invariant description of tissue diffusion and can probe diffusion direction and tissue organisation (also known as anisotropy). Fractional anisotropy (FA) of the diffusion tensor is a measure of tissue organisation that yields information about fibril organisation and the stromal microenvironment. Most tumours typically have relatively isotropic (disorganised) diffusion, whereas organised tissues have anisotropic diffusion. Tumour stroma evolves during cancer progression, and can be associated with increased deposition of extracellular matrix and fibrosis. As DTI-MRI examines tissue organisation, it may provide information on cancer stroma that could help in more accurately defining tumour extent in rectal cancer. There are currently no published studies on DTI-MRI in rectal cancer.

Multi-parametric MRI

Multi-parametric MRI combines multiple MRI sequences in an examination, yielding multiple functional parameters and thereby providing a more comprehensive biologically assessment of tumour. For example, multi-parametric MRI combining DWI and DCE would yield information on tumour cellularity and vascularity from a single MRI scan. This could be useful as there are likely multiple biological characteristics in tumours that may affect therapeutic response. There are only limited studies in multi-parametric MRI combining DWI and DCE for prediction of CRT response in rectal cancer.

Ultra-high field MRI

Ultra-high field MRI at 11.7 to 14.0 tesla has the capability to image cancer morphology and function at microscopic resolutions of 100 – 200 µm. MRI analysis of tissue samples *ex vivo* results in no tissue destruction, allowing for direct correlation with histopathologic analysis of the same tissue sample after MRI analysis. The microscopic resolutions images can be directly correlated with histopathology as a 'ground-truth' basis for screening of potential MRI biomarkers of tumour extent, heterogeneity, and function. Findings can then be subsequently translated to lower clinically relevant field strengths for clinical practice. Biobank cancer tissue samples could be analysed at ultra-high field to screen for novel MRI biomarkers. Important considerations include appropriate Biobank tissue handling and preparation methods to ensure tissues are suitable for MRI analysis, and the co-registration of MR images with histopathology for accurate correlation. Ultra-high field MRI analysis of Biobank tissue could be used as 'ground-truth' exploration for biomarkers of clinical need. In rectal cancer, further MRI sequences are required for more accurate assessment of tumour extent, and radiotherapy response prediction. There are currently no rectal cancer studies in DTI-MRI. Ultra-high field MRI analysis of rectal cancer Biobank tissue *ex vivo* could provide microscopic DTI-MRI images to be correlated with histopathology, and exploration of whether FA of the stromal microenvironment is useful in assessment of tumour extent and radiotherapy response.

1.2 PhD HYPOTHESES AND AIMS

Hypothesis A (Clinical MRI Study)

Multi-parametric MRI, consisting of DWI and DCE, performed before, during and after CRT is predictive of treatment outcome in locally advanced rectal cancer, with histopathology of the resected tumour being the reference standard.

Aim 1

To prospectively evaluate before, during and after CRT multi-parametric MRI (DWI and DCE) at 3.0 tesla for therapeutic response prediction in locally advanced rectal cancer. A whole tumour heterogeneity analysis will be performed, and MRI biomarkers will be correlated with histopathology tumour regression grade (TRG).

Hypothesis B (Clinical MRI study)

Functional MRI (DWI and DCE) is predictive of 2 year disease-free survival in patients with locally advanced rectal cancer.

Aim 2

To correlate functional MRI biomarkers (DWI and DCE) performed before, during, and after CRT with 2 year disease-free survival.

Hypothesis C (*Ex-vivo* ultra-high field MRI study)

Ultra-high field MRI can image Biobank cancer tissue at microscopic resolutions, thereby allowing for correlation with histopathology 'ground-truth' and screening for novel MRI biomarkers of tumour extent, heterogeneity and treatment response. *Ex vivo* findings will form the basis for the development of novel *in vivo* MRI techniques, establishing a translational pathway from ultra-high field MR into the clinic for assessment of tumour extent and prediction of treatment response.

DTI-MRI can assess stromal heterogeneity in rectal cancer, thereby allowing for more accurate delineation of rectal cancer extent and staging.

Aim 3

To establish a framework for diffusion MRI analysis of Biobank cancer tissue *ex vivo* for MRI biomarker discovery.

Aim 4

To examine DTI-MRI derived imaging biomarkers of rectal cancer stromal heterogeneity and tumour extent, *ex vivo*. Specifically, the stromal microstructure of rectal cancer and adjacent normal rectum will be examined by ultra-high field DTI-MRI at 11.7 tesla *ex vivo*, and the MRI findings correlated with histopathology.

Chapter 2 Literature review

This chapter comprises:

1. A published literature review that was completed for this PhD research on the role of functional MRI for therapeutic response prediction in rectal cancer (submitted on 23 December 2015, and accepted for publication on 3 January 2017).
2. An updated literature review on functional MRI for therapeutic response prediction in rectal cancer.
3. An updated literature review on ultra-high field MRI in rectal cancer.

2.1 Literature Review Publication.

Review Article: Functional MRI for quantitative treatment response prediction in locally advanced rectal cancer. *British Journal of Radiology.* 2017; 90: 20151078 https://doi.org/10.1259/bjr.20151078

Authors:

1. Trang T. Pham
2. Gary P. Liney
3. Karen Wong
4. Michael B. Barton

BJR

Received:
23 December 2015

Revised:
15 December 2016

Accepted:
3 January 2017

https://doi.org/10.1259/bjr.20151078

Cite this article as:
Pham TT, Liney GP, Wong K, Barton MB. Functional MRI for quantitative treatment response prediction in locally advanced rectal cancer. *Br J Radiol* 2017; **90**: 20151078.

REVIEW ARTICLE

Functional MRI for quantitative treatment response prediction in locally advanced rectal cancer

[1,2,3,4]TRANG T PHAM, MB BS, FRANZCR, [1,3,4,5]GARY P LINEY, PhD, [1,3,4]KAREN WONG, PhD, FRANZCR and [1,3,4]MICHAEL B BARTON, MD, FRANZCR

[1]Department of Radiation Oncology, Liverpool Hospital, Sydney, NSW, Australia
[2]Sydney West Radiation Oncology Network, Westmead, Blacktown and Nepean Hospitals, Sydney, NSW, Australia
[3]Faculty of Medicine, University of New South Wales, Sydney, NSW, Australia
[4]Ingham Institute for Applied Medical Research, Sydney, NSW, Australia
[5]Faculty of Radiation and Medical Physics, University of Wollongong, NSW, Australia

Address correspondence to: Dr Trang T Pham
E-mail: *trang.pham@sswahs.nsw.gov.au*

ABSTRACT

Despite advances in multimodality treatment strategies for locally advanced rectal cancer and improvements in locoregional control, there is still a considerable variation in response to neoadjuvant chemoradiotherapy (CRT). Accurate prediction of response to neoadjuvant CRT would enable early stratification of management according to good responders and poor responders, in order to adapt treatment to improve therapeutic outcomes in rectal cancer. Clinical studies in diffusion-weighted imaging (DWI) and dynamic contrast-enhanced (DCE) MRI have shown promising results for the prediction of therapeutic response in rectal cancer. DWI allows for assessment of tumour cellularity. DCE-MRI enables evaluation of factors of the tumour microvascular environment and changes in perfusion in response to treatment. Studies have demonstrated that predictors of good response to CRT include lower tumour pre-CRT apparent diffusion coefficient (ADC), greater percentage increase in ADC during and post CRT, and higher pre-CRT K^{trans}. However, the mean ADC and K^{trans} values do not adequately reflect tumour heterogeneity. Multiparametric MRI using quantitative DWI and DCE-MRI in combination, and a histogram analysis technique can assess tumour heterogeneity and its response to treatment. This strategy has the potential to improve the accuracy of therapeutic response prediction in rectal cancer and warrants further investigation.

INTRODUCTION

Advances in multimodality treatment strategies over the past decades have contributed to an improvement of outcomes for patients with rectal cancer. The combination of neoadjuvant chemoradiotherapy (CRT) and standardized surgical technique (total mesorectal excision) has led to an improvement in locoregional control, with local recurrence rates dropping from 20–30% to 7–10% for patients with locally advanced disease (T3–4 and/or N1–2).[1,2] Neoadjuvant CRT followed by a 6- to 8-week break prior to surgery has the advantage of tumour downstaging, with a pathological complete response (pCR) achieved in 15–27% of patients.[3] Despite these advances, tumour responses to CRT still vary considerably, with 54–75% of patients having tumour downstaging and the remainder having no treatment response.[4] The reason for this variation in treatment response is not well understood, and at present, there is no accurate method of predicting treatment response. Furthermore, distant metastases still predominate with a 5-year cumulative incidence of 30% in locally advanced (T3–4) resectable rectal cancer shown in a pooled analysis of five Phase III randomized trials.[2]

More accurate imaging biomarkers for the prediction and assessment of radiotherapy response would enable early stratification of patients into different prognostic groups and a personalized treatment approach. Identification of patients with a clinical complete response prior to surgery would enable optimization of the surgical approach with "organ-preserving" procedures, which would result in a reduction in surgical morbidity. It has been proposed that patients with a clinical complete response may be able to avoid surgery with a "wait and watch" policy;[5] however, accurate identification of patients with complete response is crucial for this approach to minimize the risk of recurrence. Early detection of poor responders to CRT would provide the opportunity for these patients to proceed directly to surgery thereby avoiding morbidity of CRT or for

intensified treatment regimens such as second-line chemotherapy or higher radiation dose to maximize therapeutic response.

Functional imaging predictive biomarkers may be able to guide individualization of patient treatment in order to maximize therapeutic outcomes and minimize treatment toxicity. MRI has the benefit of sampling the whole tumour and can be repeated on multiple occasions unlike biopsy. Conventional pre-operative staging investigations and histological examination of tissue biopsies are not capable of predicting individual treatment response. Although MRI using standard morphological sequences (T_2 weighted) is important for staging and treatment planning,[6] it is inadequate for prediction and assessment of individual response to CRT. Current predictive models require pathological staging, making them unsuitable for use as a pre-treatment decision support tool.[2,7] Recent research efforts have focused on using physiological information from functional MRI techniques to more accurately predict treatment response; however, the clinical role of functional MRI is yet to be defined.

This expert review assesses the current status on functional MRI, from the clinical utility in prediction of CRT response through to the *ex vivo* analysis and characterization of rectal cancer. This review summarizes the existing literature on clinical potential of diffusion-weighted imaging (DWI) and dynamic contrast-enhanced (DCE) MRI in prediction of CRT response, prognosis and biological characterization of tumour and the *ex vivo* high-field MR spectroscopy (MRS) in the metabolic characterization of rectal cancer.

Potential benefits of MRI/MR spectroscopy biomarkers

The development and discovery of MRI/MRS biomarkers can improve the clinical management of rectal cancer. The foreseeable benefits are:

(i) MRI/MRS provides a non-invasive technique that can assess the entire tumour region, thereby yielding information about tumour heterogeneity and avoiding sampling error associated with conventional biopsy techniques.
(ii) New MRI/MRS biomarkers will better reflect patient prognosis and response to different treatment options, thus facilitating individually tailored medical management and monitoring of outcomes. This can enable early stratification of patients into high-risk groups, for de-escalation of treatment (*e.g.* exclusion of surgery or sphincter-sparing techniques in patients with pCR) or low-risk groups for intensification of treatment.

FUNCTIONAL MRI FOR CLINICAL THERAPEUTIC RESPONSE PREDICTION AND ASSESSMENT IN RECTAL CANCER

The development of functional MRI sequences has enabled the assessment of different biological tumour characteristics and is an important advance in imaging evaluation in oncology. Standard morphological MRI (T_2 weighted) has been shown to have significant correlation with survival outcomes in the MRI and Rectal Cancer European Equivalence (MERCURY) study,[8] a large prospective trial assessing the prognostic significance of post-CRT MRI assessment of tumour regression grade (TRG). However, volumetric measurements based on standard morphological MRI lack sufficient accuracy for the differentiation of treatment responders from non-responders because of their inability to detect small residual tumour deposits within areas of radiation-induced fibrosis. Functional MRI biomarkers have been documented to have greater potential compared with standard T_2 weighted sequences in the assessment of therapeutic response in patients with locally advanced rectal cancer undergoing neoadjuvant CRT.[9] The clinical utility of these functional MRI biomarkers in rectal cancer is still yet to be defined.

DIFFUSION-WEIGHTED MRI

DWI is a functional MRI technique which is sensitive to the movement of water molecules through the body. The apparent diffusion coefficient (ADC), a quantitative parameter used for assessment of water diffusion through tissue, shows an inverse relationship with tissue cellularity.[10] Viable tumour cells restrict the mobility of water, whereas necrotic tumour cells allow increased diffusion of water molecules. Increasing tumour cellularity and architectural distortion of the extracellular space will contribute to decreased ADC values. The ADC values have been shown to correlate with tumour cellularity and grade.[11] The ADC has been shown to differentiate post-treatment persistent tumour from inflammation and necrosis, making it a useful tool to monitor effects of radiotherapy. Radiotherapy-related cellular damage leading to necrosis can occur within days of initiating therapy. The ability to detect changes in tumour microstructure allows DWI to be used for early treatment predictions.[12,13]

Prediction and assessment of primary tumour response

Prospective studies have evaluated the use of DWI in the prediction and assessment of primary response to CRT in rectal cancer. The majority of these studies demonstrated ADC to be useful for distinguishing good responders from poor responders, with the standard histological reference based on TRG. The key findings in prospective studies of DWI for assessment of CRT response are shown in Table 1. In general, studies demonstrated predictors for good responders have a lower pre-CRT ADC value and a greater percentage increase in ADC during and post CRT. Performance of pre-treatment ADC values for prediction of good responders is variable between small prospective studies, with sensitivities, specificities, positive-predictive values (PPVs) and negative-predictive values (NPVs) ranging from 62% to 100%, 86–91%, 67–79%, and 62–100%, respectively.[13–15] One study[16] demonstrated that pre-treatment ADC was not a significant predictor of treatment response. The performance of post-treatment percentage increase (41–59%) in ADC for detection of good responders produced PPV and NPV ranging from 82 to 91% and from 43 to 94%, respectively.[15,16] In another study,[17] a post-treatment mean ADC cut-off of $1.045 \times 10^{-3}\,mm^2\,s^{-1}$ was associated with a sensitivity and specificity of 75% and 100%, respectively. These DWI studies used echo planar imaging (EPI) and multiple *b*-values (range between 0 and 1000). However, there were a number of differences that may account for the variations in results observed between studies. The standardization of MRI protocols is important to compare quantitative studies; the differences in the number of *b*-values

Table 1. Diffusion-weighted imaging (DWI) MRI studies—assessment of neoadjuvant chemoradiotherapy response

Study	*n*	MRI time points	MRI variable	Histopathology response	Result—direction of correlation with histopathology	Significance
Primary tumour response						
Barbaro et al (2012)[13]	62	1.5 T Pre, during and post	ADC (median) %ΔADC	TRG (Mandard)	Pre-ADC $<1\times10^{-3}$mm^2 s^{-1} correlation (+) with TRG4	$p = 0.0011$
				Good responders TRG1–2 *vs* non-responders TRG3–5	During: higher %ΔADC correlation (+) with responders	$p < 0.0001$
Intven et al (2013)[15]	59	3 T Pre	ADC (median)	TRG (Mandard)	Pre-ADC (0.95 good response *vs* 1.12 moderate response)	$p < 0.001$
				Good response TRG1–2 *vs* moderate response TRG3–5	Post-ADC	NS
					ΔADC (%) (50 *vs* 23)	$p < 0.001$
					ΔADC (absolute) (0.43 *vs* 0.26)	$p < 0.001$
Monguzzi et al (2013)[16]	31	1.5 T Pre and post	ADC (median)	TRG (Mandard)	Pre-ADC	NS
			ΔADC	Good responders TRG1–2 *vs* non-responders TRG3–5	Post-ADC (1.3 *vs* 1.2)	$p = 0.004$
					ΔADC (%)	NS
					ΔADC (absolute) (0.5 *vs* 0.4)	$p < 0.05$
Kim et al (2011)[55]	34	3 T Pre, during and post	ADC	TRG (Mandard)	Pre-ADC	NS
				Good responders TRG1–2 *vs* non-responders TRG3–5	Early ΔADC	NS
Cai et al (2013)[56]	15	1.5 T Pre CRT, weekly during CRT	ADC (mean)	TRG (Dworak)	Pre-ADC	$p = 0.021$
				Good response TRG3–4	Weekly ADC—comparison with pre-ADC:	
				Poor response TRG0–2	Week 1 ADC	NS
					Week 2 ADC (increase-correlation with GR)	$p = 0.004$
					Week 3 ADC	NS
					Week 4 ADC	NS
					Week 5 ADC	NS
Musio et al (2013)[57]	22	3 T Pre, during, post	ADC (mean)	Histological responders: Downstaging/reduction in T or N staging Non-responders: stable or progressive disease	Pre-ADC—no significant difference	NS
					Responders: ΔADC from pre to during in responders	$p < 0.05$
					Non-responders: ΔADC	NS
Carbone et al (2012)[58]	14	1.5 T Pre, post	DWI volume	TRG (Mandard)	Pre-V_{DWI}	NS
			(V_{DWI}) *vs* T2W volume (V_c)	Good responders TRG1–2 *vs* non-responders TRG3–5	Post-V_{DWI} (4 responders *vs* 13 non-responders)	$p = 0.004$
Nodal response						
Lambregts et al (2011)[18]	30	1.5 T Post	ADC (mean)	Histological malignant nodes *vs* benign nodes	DWI *vs* T2W or DWI + T2W: no improvement in identification of malignant nodes	NS

ADC, apparent diffusion coefficient; NS, not significant; T2W, T_2 weighted; TRG, tumour regression grade.

and *b*-values used in the protocols could result in differences in the ADC maps produced, making it difficult to compare studies. The imaging analyses and quantification methods varied between studies; Lambrecht et al[14] defined the region of interest (ROI) on $b = 0$ and $b = 1000$ images; Barbaro et al[13] defined the ROI on ADC maps, matching with corresponding T_2 weighted images, and Intven et al[15] used in-house software for their analysis.

A meta-analysis by van de Paardt et al,[9] which included six DWI studies, has compared the performance of DWI with standard morphological MRI (T_2 weighted) in assessment of treatment response post CRT. DWI showed significantly better results for tumour re-staging compared with standard morphological sequences. They found that DWI had a mean sensitivity of 83.6% (95% CI 61.7–94.2%) and specificity of 84.8% (95% CI 74.2–91.5%). Studies with experienced observers showed significantly better results, with higher sensitivity for re-staging, than studies with less experienced observers.

There are limited prospective studies examining the value of DWI during CRT.[13,14] These studies showed that the percentage increase in ADC during Week 2 of CRT was predictive of response. This is potentially useful in identifying poor responders early during treatment, to provide an opportunity to change the treatment approach and to prevent them from proceeding with likely futile treatment. Further investigation of DWI performed during CRT is warranted.

ADC cut-off values for response in studies were chosen on an *ad hoc* basis and still require prospective validation in larger patient populations. Furthermore, there was a wide variation in performance of ADC values demonstrated between studies. Although promising, DWI currently lacks sufficient accuracy for clinical use to stratify patients into adaptive management pathways. The above rectal cancer diffusion studies used conventional single-shot EPI. More recent improvements in these sequences, such as readout segmented diffusion technique (RESOLVE), have improved detail and decreased image distortion compared with standard EPI diffusion. The benefit of RESOLVE for therapeutic response prediction warrants further investigation in rectal cancer.

Assessment of nodal response

The van der Paardt meta-analysis found that MRI, including standard morphological sequences and DWI studies, cannot discriminate nodal response to treatment.[9] However, it was not specified how many DWI studies formed part of this analysis. One DWI prospective study of 30 patients by Lambregts et al[18] specifically assessed the performance of ADC for nodal staging after completion of CRT. They found that DWI on its own was not reliable and did not improve accuracy of nodal staging when performed in addition to T_2 weighted sequences.

Identification of pathological complete response

Between 15% and 27% of patients will have a pCR following CRT. This represents an important subgroup of patients in whom surgery could be avoided with a "wait and watch" policy, or morbidity of surgery can be reduced with sphincter-sparing surgical techniques. Accurate identification of these patients is of great importance prior to considering more conservative management options. There are only 5 small prospective studies[14,15,19–21] assessing the role of DWI in detection of pCR; the remainder of studies are retrospective series.[22–24] The key findings from these studies are summarized in Table 2. The majority of these studies have shown that it is possible to identify patients with pCR through early prediction pre CRT or assessment post CRT.

Multiple studies[14,15,19] have found that a lower pre-treatment mean ADC had value in prediction of patients who went on to have a pCR, although this was not significant in Genovesi et al.[19] Lambrecht et al[14] studied DWI performed at multiple time points for the assessment of pCR in a prospective study of 20 patients. They found that pre-CRT ADC had a sensitivity of 100% and specificity of 86% in prediction of pCR.

In the post-CRT assessment of CRT response, Intven et al[15] and Genovesi et al[19] found that change in the ADC post CRT could identify pCR, with diagnostic accuracy of 98% and 91% in the studies, respectively. Lambrecht et al[14] found that ΔADC post CRT was also useful in the detection of pCR. These results have not always been replicated, with some investigators finding that DWI does not unequivocally determine pCR.[20] A large retrospective multicentre study[22] of 120 patients found that the addition of DWI to standard morphological sequences improved the selection of pCR after CRT. DWI analysis by observers in this study was qualitative and therefore did not use the ADC values. With T_2 weighted MRI alone, the sensitivity for identification of pCR was poor ranging from 0% to 40%. The addition of DWI improved the sensitivity to 52–65% and had a specificity of 89–98%.

It is difficult to accurately identify pCR on DWI alone, and this modality may need to be combined with another modality. It is expected that in patients with no residual tumour, diffusion will be freer and restriction will not remain on the post-CRT scan. However, a study[25] assessing the post-CRT DWI of patients with confirmed pCR has shown that this is not always the case. Jang et al[25] retrospectively reviewed post-CRT DWI of 43 patients who had undergone neoadjuvant CRT, subsequent surgery and achieved pCR. They reported diffusion restriction remained in 42% of patients with pCR. Radiation proctitis and fibrosis, demonstrated on histopathology, were significant independent predictors of diffusion restriction in patients achieving pCR after CRT. This study has shown that even in the absence of residual tumour, restricted diffusion can still occur as a result of radiation-induced fibrosis, making it difficult to accurately identify all patients with pCR on DWI alone. A study by Maas et al[21] on 50 patients found that post CRT, qualitative T_2 weighted imaging and DWI had low sensitivity of 35% and specificity of 94% for the prediction of pCR. However, combining MRI with clinical assessment, consisting of digital rectal examination and endoscopy, improved the prediction of pCR with a post-test probability for predicting pCR of 98%. This study demonstrated that DWI alone is poor at detecting pCR and needs to be combined with another modality.

Joye et al[26] performed a systematic review on the role of DWI in the prediction of pCR in response to CRT. Pooled data from

Table 2. Diffusion-weighted imaging (DWI) MRI studies—identification of pathological complete response (pCR)—ypT0 *vs* non-pCR after chemoradiotherapy

Study	*n*	MRI timing	MRI variable	Result	Significance
Lambrecht et al (2012)[14]	20	1.5 T Pre, during, post	ADC (mean)	Pre-ADC (0.94 pCR *vs* 1.19 non-pCR)	$p < 0.003$
			ΔADC (%)	During ΔADC (72 *vs* 16) and post-ΔADC (88 *vs* 26) higher in pCR	$p = 0.0006$
					$p = 0.0011$
Genovesi et al (2013)[19]	28	Pre, post	ADC (mean)	ΔADC (%) (77.2 pCR *vs* 36 non-pCR)	$p = 0.05$
			ΔADC (%)	ΔADC (%) better than T2W Δvolume (%) in detection of pCR	$p = 0.022$
Engin et al (2012)[20]	30	Pre, post	DWI qualitative—SI, ADC (mean)	Post-ΔSI and Post-ΔADC	NS
Maas et al (2015)[21]	50	1.5 T Post	T2W and DWI—qualitative	Detection of pCR: sensitivity 35%, specificity 94%	
				Combining T2W, DWI and clinical assessment improves detection of pCR post-test probability 98%	
Lambregts et al (2011)[22]	120 (multicentre)	1.5 T Post	Qualitative	Detection of pCR: DWI *vs* T2W alone (sensitivity 52–64% *vs* 0–40%, specificity the same 89–98%)	
Sassen et al (2013)[23]	70	1.5 T Pre, post	T2W *vs* addition DWI—qualitative	DWI improved interobserver agreement	$p = 0.005$
Curvo-Semedo et al (2011)[24]	50 (single centre)	1.5 T Pre, post	ADC ΔADC (%) ADC volume *vs* T2W volume	ADC and ΔADC (%)	NS
				Post-ADC volume (0.03 pCR *vs* 1.5 non-pCR) and Δvolume (−100 *vs* −90) better than T2W in detection pCR	$p < 0.001$ $p < 0.001$
Ha et al (2013)[59]	100	1.5 T Pre, post	V_{DWI} (pCR: Dworak grade 4)	Pre-V_{DWI}—no significant difference	NS
				Post-V_{DWI} (0.8 pCR *vs* 3.5 non-pCR)	$p < 0.001$
				Pre-ADC—no significant difference	NS
				Post-ADC (1.33 *vs* 1.13)	0.002

ADC, apparent diffusion coefficient; NS, not significant; SI, signal intensity; T2W, T_2 weighted; V_{DWI}, DWI volume.

9 studies with a combined total of 226 patients demonstrated that the ADC pre CRT was unable to predict for pCR with a sensitivity of 69%, specificity of 68%, PPV of 35% and NPV of 90%. Pooled data from 10 studies with a combined total of 315 patients found that the ADC post CRT had sensitivity of 78%, specificity of 72%, PPV of 47% and NPV of 91% for detection of pCR. However, the lack of standardization of MRI protocols and image quantification methods between different centres would limit the potential of pooled analysis.

DYNAMIC CONTRAST-ENHANCED MRI

DCE-MRI provides functional information on tumour microvessel perfusion, permeability and extracellular-extravascular space composition by assessing the changes in signal intensity over time following intravenous injection of a paramagnetic contrast agent. ROIs may be interrogated to produce enhancement–time curves with malignant tumours, due to their abnormal microvasculature, demonstrating a rapid washin and washout of contrast and a greater increase in signal intensity than in normal tissues.[10,27] DCE-MRI may be able to assess characteristics of the tumour vascular microenvironment, such as hypoxia and microvascular density that influence radiotherapy response, and also vascular changes induced by radiotherapy. DCE-MRI can potentially assess tumour downstaging, therefore distinguishing good responders from poor responders to treatment. The perfusion characteristics on DCE-MRI can be analysed either in a quantitative[28] or qualitative technique, hence the published studies are difficult to compare. Quantitative analysis involves modelling the

pharmacokinetics of an intravenously administered contrast agent and requires correction for T_1 pre-contrast. Investigation into DCE-MRI is sparse, and its clinical role in response prediction and assessment and optimal evaluation technique is yet to be established.

Prediction of therapeutic response

Several quantitative studies assessing tumour response with DCE-MRI have shown that higher contrast exchange rates pre CRT, which indicates higher tumour permeability, are associated with better therapeutic response to CRT. Key findings from studies evaluating the role of DCE-MRI in therapeutic response assessment are shown in Table 3. In a prospective study of 95 patients, a higher pre-treatment K_{21} (contrast medium exchange in the Brix pharmacokinetic model) was significantly associated with good treatment response, defined as post-treatment pT0-2N0 Union for International Cancer Control (UICC) stage.[29] On multivariate analysis, a higher 75th percentile K_{21} was associated with a higher tumour response rate, whereas the DCE-MRI quantitative parameters—amplitude and time to peak—were not associated with tumour response. In addition, mucinous tumour morphology was significantly associated with poorer response to treatment. Other quantitative studies demonstrated higher pre-CRT K^{trans} (contrast medium exchange in the Tofts pharmacokinetic model) was predictive of tumour response.[30,31] Intven et al[30] found in a study of

Table 3. Dynamic contrast-enhanced (DCE) MRI studies—assessment of chemoradiotherapy response and prognosis

Study	*n*	MRI time points	MRI variable	Histopathological Physiological variable	Result	Significance
De Vries et al (2014)[38]	83	1.5 T Pre	Semi-quantitative PI	Responders: ypT0-2 Non-responders: ypT3 DFS OS	PI lower in responders than non-responders (7.6 *vs* 9.8) Mean follow-up 71 (±29) months PI-predicted DFS (HR 1.85) PI-predicted OS (HR 1.42)	$p < 0.001$ $p < 0.001$ $p = 0.04$
Martens et al (2014)[33]	30	1.5 T Pre, post	Semi-quantitative Initial slope Initial peak Late slope AUC 60, 90, 120 s	TRG (Mandard): Good responders TRG1–2 Non-responders TRG3–5	Late slope (-0.05×10^{-3} GR *vs* 0.62×10^{-3} PR) Other parameters—no significant difference	$p < 0.001$ NS
Oberholzer et al (2013)[29]	95	1.5 T Pre	Quantitative/ semi-quantitative K_{21} A TTP	Responder—downshift in UICC stage *vs* non-responder—no downshift Good responder ypT0–2N0	K_{21}—higher in responders *vs* non-responders TTP—difference between responders and non-responders A—75th percentile lower in responders K_{21}—high 75th percentile—higher response	$p < 0.001$ $p < 0.025$ $p = 0.016$ $p = 0.019$
Intven et al (2014)[30]	51	3 T Pre, post	Quantitative K^{trans} Median (50th percentile) p25 (25th percentile) p75 (75th percentile)	TRG (Mandard) Good responder TRG1–2 *vs* non-responder TRG3–5	Pre-K^{trans} median (0.48 GR *vs* 0.39 PR) Post-K^{trans} median (0.33 GR *vs* 0.39 PR) ΔK^{trans} (%) (−34 GR *vs* −1.2 PR)	$p = 0.024$ $p = 0.024$ $p < 0.001$
Lim et al (2012)[32]	39	3 T Pre, during, post	Quantitative K^{trans} V_e	TRG good responder TRG1–2 *vs* non-responder TRG3–5 TNM down-staging	K^{trans} no significant correlation with TRG good-responders *vs* non-responders Pre- and early-K^{trans} higher in TNM downstaging V_e—no correlation	NS $p = 0.0215$ NS

A, amplitude; AUC, area under the curve; HR, hazard ratio; NS, not significant; PI, perfusion index; TRG, tumour regression grade; TTP, time-to-peak signal intensity; PR, poor responder; GR, good responder; DFS, disease free survival; K^{trans}, transfer constant between blood plasma and extravascular extracellular space; V_e, extravascular extracellular fractional volume; OS, overall survival.

51 patients that pre-CRT K^{trans} (50th percentile) was significantly higher in patients with good therapeutic response as defined by Mandard TRG 1–2. Similarly, George et al[31] showed that responsive tumours had higher pre-treatment K^{trans} than non-responsive tumours. This result was also demonstrated in Lim et al,[32] although not significant. Results on the predictive value of post-CRT DCE-MRI were less clear, with Intven et al[30] and George et al[31] demonstrating a correlation between a reduction in post-CRT K^{trans} and good response, and Lim et al showing no correlation.

The role of DCE-MRI derived quantitative parameters in the prediction of therapeutic response to CRT was explored in a study of 30 patients by Martens et al.[33] Six semi-quantitative parameters from pre-CRT and post-CRT DCE-MRI were investigated: (i) initial slope, (ii) initial peak, (iii) areas under the first 60, 90 and 120 s of the enhancement curve and (iv) late slope. Only pre-CRT late slope was able to discriminate between good and poor responders to treatment (-0.05×10^{-3} *vs* 0.62×10^{-3}, $p < 0.001$).

There are a variety of quantitative measurements that can be obtained from DCE-MRI that can be obtained through a simple approach or through pharmacokinetic quantification models. A simple analysis uses a curve descriptor to characterize the signal intensity curve.[34] Examples of this include area under curve and initial peak used in the study by Martens et al.[33] Pharmacokinetic modelling includes the Brix and the Tofts models. K_{21} is derived from the original Brix model,[35] a simple linear two-compartment model that does not require T_1 mapping or arterial input function measurements. K_{21} can measure the rate constant between the extravascular extracellular space and plasma, but a major disadvantage is that it does not measure perfusion. There has been a shift towards using the Tofts model, which provides values that more closely represent pathophysiological processes, such as perfusion. K_{ep} in the Tofts model can measure rate constant between extravascular extracellular space and plasma, a value similar to K_{21} in the Brix model. K^{trans} in the Tofts model is the influx volume transfer constant from the plasma into the extravascular extracellular space. The calculation of K^{trans} requires pre-contrast T_1 measurement and takes into account the arterial input factor, hence this parameter more closely represents physiological perfusion.[28,36] At present, K^{trans} appears to be the most promising parameter for the prediction of treatment response in rectal cancer.

Most DCE-MRI studies assess therapeutic response in the primary tumour. There is a lack of studies on the potential of DCE-MRI in nodal therapeutic response assessment. The ability of DCE-MRI to assess nodal response to treatment has been explored only in a study of 55 patients who underwent DCE-MRI following completion of CRT. In this study, Alberda et al[37] assessed the accuracy of qualitative DCE-MRI methods, with histopathological assessment of nodes being the standard reference. They found that early incomplete arterial phase enhancement on DCE-MRI was a significant indicator of malignant nodes.

Prognostic value

The prognostic value of DCE-MRI in rectal cancer has been investigated by DeVries et al.[38] In a prospective study of 83 patients with T3 rectal cancer undergoing neo-adjuvant CRT, DeVries et al investigated the value of the pre-CRT perfusion index, a microcirculatory parameter which integrates information on flow and permeability, in the prediction of therapeutic disease-free survival and overall survival. A lower pre-treatment mean perfusion index was found to be significantly predictive of therapy response (defined as ypT0-2). After a mean follow-up of 71 ± 29 months, the perfusion index significantly predicted disease-free survival (hazard ratio 1.84, $p < 0.001$) and overall survival (hazard ratio 1.42, $p = 0.04$), with patients with lower perfusion index having worse survival.

Biological correlation

DCE-MRI allows functional characterization of biological changes in the tumour microvasculature.[27] The findings from studies correlating DCE-MRI with tumour biological characteristics are summarized in Table 4. Clinical DCE-MRI studies in rectal cancer have shown correlation of DCE-MRI parameters with variables of tumour angiogenesis relevant to radiation response.[29,31,39–41] A prospective study[39] of 17 patients showed that DCE-MRI can be used to assess radiation-induced changes in tumour vasculature. Radiotherapy inhibits tumour angiogenesis, which correlated with a significantly lower microvessel density (MVD) compared with non-irradiated tumours. Similarly, K_{ps}, the endothelial transfer coefficient, was found to be 77% ($p = 0.03$) lower in the radiotherapy-treated group. Hong et al[42] also showed that DCE-MRI could be used to assess tumour angiogenesis. The semi-quantitative parameter of E_{max} (maximal enhancement) had a significant correlation with microvessel count.

Yeo et al[40] performed a retrospective analysis of pre-operative DCE-MRI in 31 patients undergoing surgery alone, and pre-CRT and post-CRT DCE-MRI in 15 patients undergoing CRT. Quantitative parameters including K^{trans}, K_e, K^{trans}, K_{ep}, extravascular extracellular fractional volume (V_e), and initial area under the concentration curve in 60 seconds (iAUC) were correlated with histological markers of tumour aggressiveness [expression of epidermal growth factor receptor (EGFR) and *KRAS* gene mutations], tumour angiogenesis (MVD) and vascular endothelial growth factor (VEGF). They found that a higher mean K^{trans} and K_{ep} correlated with increased tumour aggressiveness, as indicated by the presence of an EGFR mutation. Furthermore, the mean K_{ep} from the high K^{trans} area had a significant positive correlation with MVD (higher mean K_{ep}, correlated with greater MVD). However, there was no correlation between DCE-MRI and VEGF in this study. In another study by George et al,[31] there was a correlation in K^{trans} and VEGF before treatment; however, this correlation was no longer present after the commencement of treatment.

MR SPECTROSCOPY: METABOLIC IMAGING

MRS is an important tool for studying cancer metabolism. It can improve the understanding of the altered metabolic pathways in cancer and identify new metabolic biomarkers for treatment response prediction, prognosis and novel therapeutic targets. The discovery of an activated choline metabolic pathway in cancer was mostly due to MRS studies of tumours in the 1980s.[43] This pathway is characterized by increased choline-containing compounds, such as phosphocholine, glycerophosphocholine and total choline-containing compounds, which are detectable by

Table 4. Dynamic contrast-enhanced (DCE) MRI studies—correlation with biological characteristics

Study	*n*	MRI time points	MRI variable	Histopathological Physiological variable	Result	Significance
de Lussanet et al (2005)[39]	17	1.5 T	K_{ps}	Micro-vessel density (MVD) (scored by CD31, CD34) Tumour cell and endothelial cell proliferation (scored by expression of Ki67 protein) Treated ($n = 7$)—long radiotherapy Non-treated ($n = 10$)—short radiotherapy or no radiotherapy	K_{ps} 77% lower in treated than non-treated MVD 37% lower in treated than non-treated Tumour cell proliferation reduced in both long RT and short RT	$p = 0.03$ $p = 0.03$
George et al (2001)[31]	31	1.5 T	ln K^{trans}	Serum VEGF Radiological (MR) response by World Health Organization criteria: CR *vs* partial response (50% decrease in size), progressive disease (increase ≥25% size or new lesions, stable disease	Pre-ln K^{trans} correlated with VEGF Post-ln K^{trans} no correlation with VEGF Pre-ln K^{trans} higher in responders than non-responders (−0.46 *vs* −0.72) Post-ln K^{trans}—significant reduction in responders compared with pre-ln K^{trans} (−0.86)	$p = 0.01$ NS $p = 0.03$ $p = 0.04$
Zhang et al (2008)[41]	38	3 T	ER_{peak} T_{peak} $T_{first\text{-}enhance}$ Uptake rate	Histopathological MVD, VEGF	Rectal cancer *vs* normal rectum: ER_{peak} higher Uptake rate higher T_{peak} earlier T_{peak} negative correlation with MVD T_{peak} earlier for VEGF+ ER_{peak}, uptake rate and T_{peak} no correlation with MVD/VEGF	$p < 0.001$ $p < 0.001$ $p = 0.027$ $p = 0.01$ $p = 0.021$ NS

CR, complete response; ER_{peak}, peak enhancement ratio; NS, not significant; T_{peak}, time to peak enhancement; RT, radiotherapy; $T_{first\text{-}enhance}$, first enhancement time; VEGF, vascular endothelial growth factor; K_{ps}, endothelial transfer co-efficient; K^{trans}, volume transfer constant between blood plasma and extravascular extracellular space.

non-invasive MRS. The increased choline compounds are caused by malignant transformation and the hypoxic and acidic micro-environment of tumour. Enzymes of choline metabolism, such as choline kinase, may provide novel therapeutic targets.

MRS is a unique technique that can be applied with high resolution, as an initial *ex vivo* metabolic screening tool on tissue samples, and then translated into lower resolution *in vivo* MRS protocols for clinical use. MRS can identify the "spectral fingerprint" of cancer subtypes due to its ability to detect multiple tissue-specific metabolites in a single experiment. It is a quantitative technique with the intensities of MRS signal being directly related to metabolite concentration.[44] Analysis of intact tissue using standard MRS techniques result in spectra with lower resolution than normal liquid-state spectra. The resolution of tissue spectra can be improved by applying high-resolution magic angle spinning, a specialized MRS technique that detects high-resolution spectra by spinning solid tissue samples at the angle of 54.7°. High-resolution magic angle spinning profiling of intact tissue produces spectra that approach the resolution of solution-state samples.[45] An advantage of this technique is that tissue sample preparation results in minimal tissue destruction, allowing for correlation with histological and molecular analysis of the same tissue sample post MR analysis.

Ex vivo MR spectroscopy: prediction of disease behaviour and survival

A small number of studies have highlighted the potential of metabolic profile derived from *ex vivo* MRS tissue analysis in predicting disease behaviour[46] and survival outcomes.[47,48] The key findings are summarized in Table 5. Pacholczyki-Sienicka et al[47] analysed frozen tissue samples from surgical specimens of 52 patients with colorectal cancer who underwent surgery using 700.33-MHz (16.4-T) proton (^{1}H) MRS. Survival time was defined as the interval from surgery until death or the end of a 5.5-year observation period. They found that long-term survival in patients was characterized by lower levels of choline

compounds (choline, phosphocholine, glycerylphosphorylcholine), glycine, lactate and myo-inositol compared with non-survivors. Choline compounds have been found to be associated with malignant transformation, therefore this finding of a lower level of choline compounds in long-term survivors is biologically plausible. In addition, they found that an increase in taurine/glycine (sensitivity 64% and specificity 96%) and taurine/myo-inositol (sensitivity 65% and specificity 100%) ratios were significantly higher in survivors than in non-survivors.

Jimenez et al[48] also found that metabolic profiling of colorectal cancer samples was predictive of 5-year survival. However, this study found that metabolic changes predictive of survival occurred in tumour-adjacent macroscopically normal colon, 5–10 cm from the tumour. The authors suggest this represents a "field cancerization" effect, whereby the tumour affects the metabolism of its surroundings. However, the metabolic profile within the tumour specimens was not predictive of survival.

MRS metabolic profiling can potentially predict patients at risk of tumour recurrence.[46] Minicozzi et al proposed a marker of malignancy (MRS-tm) based on the metabolic findings in a study by Chan et al.[49] MRS-tm was defined as the ratio between the sum of the amplitudes of increasing components with peak between 3.0 and 3.8 ppm (including choline-containing compounds, taurine, scyllo-inositol and glycine) to the amplitude of the lipid methylene at 1.3 ppm. 4.7-T ^{1}H-MRS was performed on 29 surgical specimens. The MRS-tm was calculated for each specimen for tumour compared with healthy mucosa. The results demonstrated that MRS-tm was higher in tumour than normal mucosa. At 5-year follow-up, they reported statistical significance for tumour MRS-tm when patients were discriminated according to disease progression (either local recurrence or distant metastases). 5 of 6 patients with disease progression had a tumour MRS-tm <0.1, whereas 16 of 18 disease-free patients had MRS-tm >0.1 ($p = 0.04$).

Clinical MR spectroscopy

One published study[50] assessed the use of MRS *in vivo* in patients with rectal cancer. Kim et al[50] performed ^{1}H-MRS at 3 T with a 6-channel phased-array pelvic coil in 34 patients with rectal cancer at diagnosis and after neoadjuvant CRT. They found that the choline peak at 3.2 ppm was characteristic of rectal cancer at diagnosis. Following CRT, the choline peak disappeared and only the lipid peaks remained in 33 patients post CRT. The study identified three spectral types and found that 67% of patients with a post-CRT spectral type containing lipid peaks at 1.3 and 0.9 ppm at both long and short echo times

Table 5. *Ex vivo* high-field MR spectroscopy (MRS) studies of colorectal cancer

Study	*n*	Methods	Tumour findings (relative to normal bowel)/prognostic findings	Other findings
Minicozzi et al (2013)[46]	29 CRC (29 colon, 2 RC, 5 RC after neoadjuvant chemoradiotherapy)	^{1}H HR-MAS NMRS 4.7 T Surgical specimens Proposed marker of malignancy (MRS-tm)—ratio between sum of amplitudes of increasing components and amplitude of lipid methylene	↑ MRS-tm 5-year follow-up: Local recurrence or distant disease progression: MRS-tm <0.1 in 5/6 cases Disease-free patients: MRS-tm ≥0.1 in 16/18 cases	
Pacholczyk-Sienicka et al (2014)[47]	52 CRC (22 survivors, 30 non-survivors)	^{1}H HR-MAS NMRS 16.4T Frozen tissue samples	Long-term survival: ↓ glycine, choline, phosphocholine, myo-inositol, lactate, glycerophosphocholine ↑ creatine, glucose, aspargine Long-term survival: ↑ taurine/glycine, and taurine/myo-inositol ratio	Rectal cancer: ↑ formate
Jimenez et al (2013)[48]	26 CRC (6 RC, 20 colon)	^{1}H HR-MAS NMRS 400-MHz Frozen tissue samples	↑ isoglutamine, choline, phosphocholine, taurine, lactate, tyrosine, phenylalanine ↓ lipids, triglycerides	Lymph node positive disease: ↑creatine, scyllo-inositol, ↓triglycerides "Field cancerization" Tumour-adjacent mucosa had unique metabolic field changes distinguishing TN stage, 5-year survival prediction

CRC, colorectal cancer; RC, rectal cancer; ^{1}H HR-MAS, proton high-resolution magic angle spinning; NMRS, nuclear MRS.

had histological residual tumour. The lipid in normal controls was present at short echo time only, and the authors hypothesized that the nature of the lipid was different in patients with residual tumour compared with normal controls. This study showed that MRS metabolic profiling *in vivo* may have the potential to identify tumour at diagnosis and changes in the metabolic profile post CRT may be used to assess treatment response.

Translation of *ex vivo* to clinical MR spectroscopy

Choline is currently the most investigated metabolite in *ex vivo* and clinical studies. *Ex vivo* studies have shown higher levels of choline-containing compounds in colorectal tumour.[46,49] *Ex vivo* studies have demonstrated lower levels of choline-containing compounds and glycine, and higher taurine ratios in surgical specimens were associated with longer survival in patients with colorectal cancer.[47] The clinical MRS study found choline to be a potential biomarker of treatment response, with results showing a choline peak characteristic of rectal cancer at diagnosis and disappearance of this peak post CRT.[50] However, further clinical studies are required to translate high field *ex vivo* findings to clinical protocols and to assess whether choline would be a useful biomarker in the assessment of response to CRT (good *vs* poor response) and prediction of survival. Clinical studies are also required to assess whether taurine and glycine are useful clinical biomarkers in rectal cancer treatment response. Furthermore, there are some challenges in the translation of *ex vivo* MRS findings to MRI protocols to current clinical strengths (1.5–3 T) that need to be overcome. Localization of metabolite, weak metabolite signal relative to the larger water signal, *in vivo* can present challenges to clinical translation.[44]

FUTURE DIRECTIONS: MULTIPARAMETRIC MRI AND HISTOGRAM ANALYSIS

Although the evidence for DWI and DCE-MRI is promising, results from either of these techniques alone currently lack sufficient accuracy and standardization to be routinely used to alter clinical patient management. There is a wide variation reported in the performance of functional MRI in response prediction. Parameter thresholds obtained from studies require prospective validation of *post hoc* values in larger prospective studies. Most published studies have measured single parameter values from either diffusion or perfusion MRI. Single-parameter measurements, such as mean ADC or K^{trans} of pixels in the ROI, do not reflect tumour heterogeneity.

Figure 1. Diffusion-weighted imaging (DWI) MRI histogram analysis—apparent diffusion coefficient (ADC) colour-coded maps and histograms of a patient with good response following neoadjuvant chemoradiotherapy for rectal cancer. Example of ADC histogram analysis using Siemens OncoTreat (WIP), Erlangen, Germany. This patient had histological American Joint Committee on Cancer (7th edition) tumour regression grade 1 (moderate response, single cells or small groups of cancer cells). A voxel-by-voxel technique was used to assess changes in the entire region of interest. (a, c, e) Representative axial colour-coded ADC maps for MRI pre-chemoradiotherapy (CRT), Week 3 of CRT and post CRT, respectively. (b, d, f) Colour-coded histograms for every voxel within the segmented region of interest for DWI-MRI pre-CRT, Week 3 of CRT and post-CRT, respectively. Colour code: blue voxels, ADC values $<1000\times10^{-6}$; green voxels, ADC values $1000-1500\times10^{-6}$; red voxels, ADC values $>1500\times10^{-6}$. The histograms demonstrate an increase in the absolute ADC values of voxels over the time points.

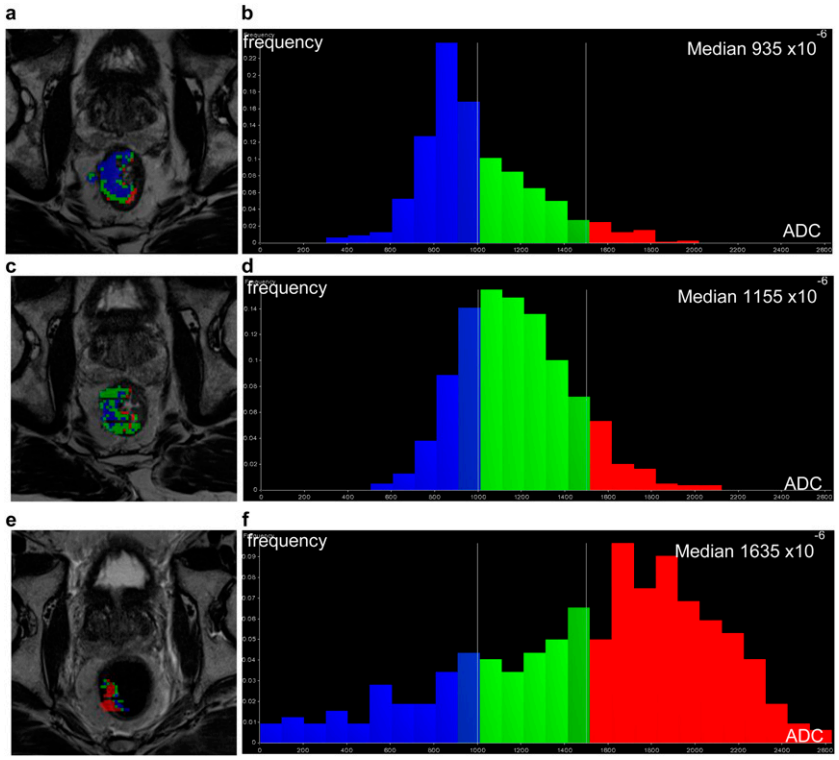

Multiparametric MRI combining multiple functional parameters can provide a more complete physiological assessment of tumour, which may improve accuracy in response prediction. A combined analysis of DWI and DCE-MRI would provide complementary information on tumour microarchitecture and cellularity (DWI) and angiogenesis and perfusion (DCE-MRI).[51] For example, in the case of pCR, the presence of radiation-induced fibrosis may cause restricted diffusion resulting in low ADC and inability to detect pCR on DWI. The addition of DCE-MRI would allow assessment of perfusion within this region; the absence of perfusion or low K^{trans} would indicate the absence of residual tumour, which may improve the detection of pCR. Multiparametric functional MRI for response prediction is an emerging area, and currently, there are limited studies assessing the role of DWI and DCE-MRI in combination in rectal cancer CRT response prediction. Intven et al demonstrated that good responders to CRT had a larger decrease in median K^{trans} and larger increase in median ADC post CRT than non-responders. However, the addition of DCE-MRI did not improve the detection of good responders compared with the use of DWI alone.[52] A histogram analysis that incorporates a voxel-by-voxel technique to calculate MRI functional parameters for every voxel within the ROI would provide a more accurate representation of intratumour heterogeneity.[53] A histogram technique can be sensitive to a shift in distribution of ADC or K^{trans} values of all voxels within the entire tumour region over the time points, thereby providing information on any heterogeneity in tumour response to treatment. Other information such as mean, mode, skewness and percentile distributions can also be extracted. Overall trends from histogram studies have shown that following treatment, DWI (ADC) histograms demonstrate a shift to the right with decreased skewness and kurtosis, and DCE-MRI histograms shift to the left with narrower and increased peak height.[53] A new analysis software is being investigated that allows this analysis to be conducted for multiple parameters, allowing for multiparametric histogram analysis. An example of voxel-by-voxel histogram analysis is shown in Figures 1 and 2. Furthermore, semi-automated segmentation tools can also reduce interobserver variability in defining a three-dimensional ROI and lead to more reproducible results.

The fundamental aspect to multiparametric imaging is achieving a standardized imaging protocol that provides consistent and reliable data sets for quantification. For voxel-wise analysis of multiple functional MRI sequences, selection of imaging parameters that minimize distortion is essential to ensure geometrically accurate data. For DWI, RESOLVE is one method to minimize distortion.[54] For DCE-MRI, short temporal resolution of between 5 and 10 s would enable adequate sampling of the rapid "washin" of contrast into tumour, and

Figure 2. Dynamic contrast-enhanced (DCE) MRI histogram analysis—K^{trans} colour-coded maps and histogram of the same patient with good response following neoadjuvant chemoradiotherapy for rectal cancer. Example of K^{trans} histogram analysis using Siemens OncoTreat (WIP) for the same patient as in Figure 1. A voxel-by-voxel technique was used. (a, c, e) Representative axial colour-coded K^{trans} maps for MRI pre-chemoradiotherapy (CRT), Week 3 of CRT and post CRT, respectively. (b, d, f) Colour-coded histograms for every voxel within the segmented region of interest for DCE-MRI pre CRT, Week 3 of CRT and post CRT, respectively. Colour code: blue voxels, K^{trans} values $<100\times10^{-3}$; green voxels, K^{trans} values $100-500\times10^{-3}$; red voxels, K^{trans} values $>500\times10^{-3}$. The histograms demonstrate a marked reduction in the absolute K^{trans} values of voxels over the time points.

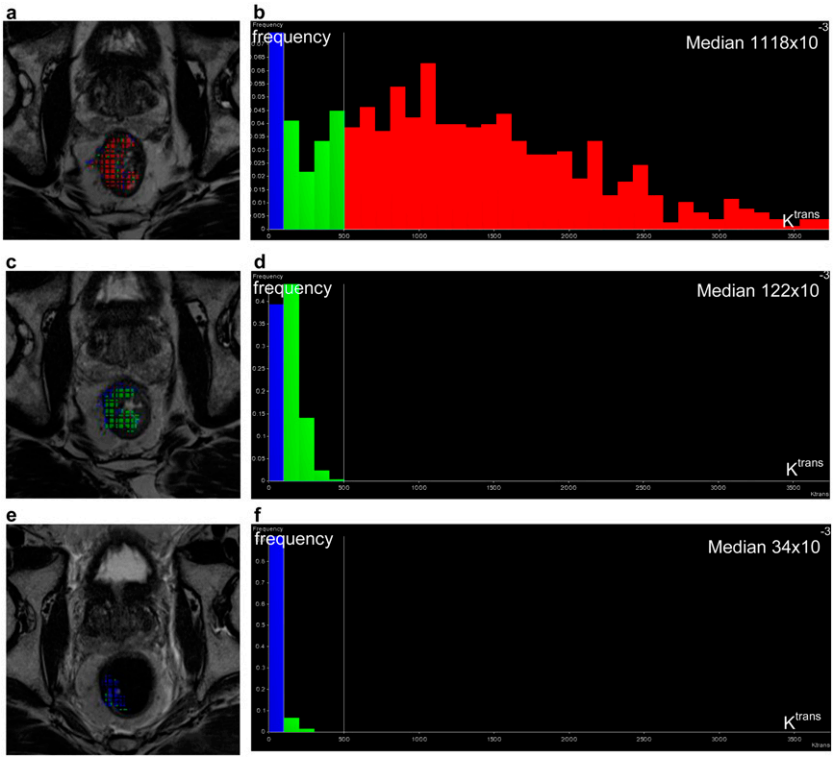

acquisition of pre-contrast T_1 flip angle scans would enable calculation of native T_1, allowing for more accurate assessment of perfusion using the Tofts two-compartment model. Although multiple parameters can be obtained from DWI and DCE-MRI, at present, ADC and K^{trans} appear to be the most promising parameters for clinical prediction of radiotherapy response in rectal cancer. Standardization of imaging protocols and analysis methods is essential in order to establish optimal thresholds of ADC and K^{trans} and to permit the clinical role of multiparametric MRI for treatment prediction to be properly evaluated.

CONCLUSION

Functional MRI is emerging as an important and promising tool for assessment of physiological characteristics of the tumour microenvironment. MRI has the benefit of sampling the whole tumour and can be repeated on multiple occasions unlike biopsies.

DWI has been shown to be superior to morphological MRI in the assessment of therapeutic response of the primary tumour in rectal cancer. In general, studies have demonstrated that lower primary tumour pre-CRT ADC value and greater percentage increase in ADC during CRT are predictors for good response. There is limited prospective data on the use of DWI for identification of patients with pCR, an important subgroup of patients in whom early MRI detection of CR would enable optimization of the surgical approach and reduction in surgical related sphincter morbidity. DCE studies have demonstrated that high tumour K^{trans} pre-CRT is a predictor for response. The role of MRS in the clinical management of rectal cancer remains yet to be defined. Although published *ex vivo* studies have identified colorectal cancer-specific metabolic profiles that can aid with prediction of disease behaviour, there is only one clinical rectal MRS study which identified choline as a potential biomarker of CRT response.

Multiparametric MRI assessing diffusion and perfusion in combination using a histogram analysis technique can assess tumour heterogeneity and its response to treatment. This strategy has the potential to improve the accuracy of therapeutic response prediction and facilitate individualized management for patients with rectal cancer.

ACKNOWLEDGMENTS

The authors thank Siemens for providing the OncoTreat WIP software.

REFERENCES

1. Zeestraten EC, Kuppen PJ, van de Velde CJ, Marijnen CA. Prediction in rectal cancer. *Semin Radiat Oncol* 2012; **22**: 175–83. doi: https://doi.org/10.1016/j.semradonc.2011.12.005
2. Valentini V, van Stiphout RG, Lammering G, Gambacorta MA, Barba MC, Bebenek M, et al. Nomograms for predicting local recurrence, distant metastases, and overall survival for patients with locally advanced rectal cancer on the basis of European randomized clinical trials. *J Clin Oncol* 2011; **29**: 3163–72. doi: https://doi.org/10.1200/JCO.2010.33.1595
3. Maas M, Nelemans PJ, Valentini V, Das P, Rödel C, Kuo LJ, et al. Long-term outcome in patients with a pathological complete response after chemoradiation for rectal cancer: a pooled analysis of individual patient data. *Lancet Oncol* 2010; **11**: 835–44. doi: https://doi.org/10.1016/S1470-2045(10)70172-8
4. Valentini V, Coco C, Cellini N, Picciocchi A, Fares MC, Rosetto ME, et al. Ten years of preoperative chemoradiation for extraperitoneal T3 rectal cancer: acute toxicity, tumor response, and sphincter preservation in three consecutive studies. *Int J Radiat Oncol Biol Phys* 2001; **51**: 371–83. doi: https://doi.org/10.1016/S0360-3016(01)01618-2
5. Maas M, Beets-Tan RG, Lambregts DM, Lammering G, Nelemans PJ, Engelen SM, et al. Wait-and-see policy for clinical complete responders after chemoradiation for rectal cancer. *J Clin Oncol* 2011; **29**: 4633–40. doi: https://doi.org/10.1200/JCO.2011.37.7176
6. Beets-tan RG, Lambregts DM, Maas M, Bipat S, Barbaro B, Caseiro-alves F, et al. Magnetic resonance imaging for the clinical management of rectal cancer patients: recommendations from the 2012 European Society of Gastrointestinal and Abdominal Radiology (ESGAR) consensus meeting. *Eur Radiol* 2013; **23**: 2522–31.
7. Dhadda AS, Bessell EM, Scholefield J, Dickinson P, Zaitoun AM. Mandard tumour regression grade, perineural invasion, circumferential resection margin and post-chemoradiation nodal status strongly predict outcome in locally advanced rectal cancer treated with preoperative chemoradiotherapy. *Clin Oncol* 2014; **26**: 197–202. doi: https://doi.org/10.1016/j.clon.2014.01.001
8. Patel UB, Taylor F, Blomqvist L, George C, Evans H, Tekkis P, et al. Magnetic resonance imaging-detected tumor response for locally advanced rectal cancer predicts survival outcomes: MERCURY experience. *J Clin Oncol* 2011; **29**: 3753–60. doi: https://doi.org/10.1200/JCO.2011.34.9068
9. van der Paardt MP, Zagers MB, Beets-Tan RG, Stoker J, Bipat S. Patients who undergo preoperative chemoradiotherapy for locally advanced rectal cancer restaged by using diagnostic MR imaging: a systematic review and meta-analysis. *Radiology* 2013; **269**: 101–12. doi: https://doi.org/10.1148/radiol.13122833
10. Metcalfe P, Liney G, Holloway L, Walker A, Barton M, Delaney G, et al. The potential for an enhanced role for MRI in radiation-therapy treatment planning. *Technol Cancer Res Treat* 2013; **12**: 429–46. doi: https://doi.org/10.7785/tcrt.2012.500342
11. Gibbs P, Liney GP, Pickles MD, Zelhof B, Rodrigues G, Turnbull LW. Correlation of ADC and T2 measurements with cell density in prostate cancer at 3.0 Tesla. *Invest Radiol* 2009; **44**: 572–76. doi: https://doi.org/10.1097/RLI.0b013e3181b4c10e
12. Evans J, Patel U, Brown G. Rectal cancer: primary staging and assessment after chemoradiotherapy. *Semin Radiat Oncol* 2011; **21**: 169–77. doi: https://doi.org/10.1016/j.semradonc.2011.02.002
13. Barbaro B, Vitale R, Valentini V, Illuminati S, Vecchio FM, Rizzo G, et al. Diffusion-weighted magnetic resonance imaging in monitoring rectal cancer response to neoadjuvant chemoradiotherapy. *Int J Radiat Oncol Biol Phys* 2012; **83**: 594–9. doi: https://doi.org/10.1016/j.ijrobp.2011.07.017

14. Lambrecht M, Vandecaveye V, De Keyzer F, Roels S, Penninckx F, Van Cutsem E, et al. Value of diffusion-weighted magnetic resonance imaging for prediction and early assessment of response to neoadjuvant radiochemotherapy in rectal cancer: preliminary results. *Int J Radiat Oncol Biol Phys* 2012; **82**: 863–70. doi: https://doi.org/10.1016/j.ijrobp.2010.12.063
15. Intven M, Reerink O, Philippens M. Diffusion-weighted MRI in locally advanced rectal cancer. *Strahlenther Onkol* 2013; **189**: 117–22. doi: https://doi.org/10.1007/s00066-012-0270-5
16. Monguzzi L, Ippolito D, Bernasconi DP, Trattenero C, Galimberti S, Sironi S. Locally advanced rectal cancer: value of ADC mapping in prediction of tumor response to radiochemotherapy. *Eur J Radiol* 2013; **82**: 234–40. doi: https://doi.org/10.1016/j.ejrad.2012.09.027
17. Song I, Kim SH, Lee SJ, Choi JY, Kim MJ, Rhim H. Value of diffusion-weighted imaging in the detection of viable tumour after neoadjuvant chemoradiation therapy in patients with locally advanced rectal cancer: comparison with T2 weighted and PET/CT imaging. *Br J Radiol* 2012; **85**: 577–86. doi: https://doi.org/10.1259/bjr/68424021
18. Lambregts DM, Maas M, Riedl RG, Bakers FC, Verwoerd JL, Kessels AG, et al. Value of ADC measurements for nodal staging after chemoradiation in locally advanced rectal cancer—a per lesion validation study. *Eur Radiol* 2011; **21**: 265–73. doi: https://doi.org/10.1007/s00330-010-1937-x
19. Genovesi D, Filippone A, Ausili Cefaro G, Trignani M, Vinciguerra A, Augurio A, et al. Diffusion-weighted magnetic resonance for prediction of response after neoadjuvant chemoradiation therapy for locally advanced rectal cancer: preliminary results of a mono-institutional prospective study. *Eur J Surg Oncol* 2013; **39**: 1071–8. doi: https://doi.org/10.1016/j.ejso.2013.07.090
20. Engin G, Sharifov R, Gural Z, Sagam EK, Saglam S, Balik E, et al. Can diffusion-weighted MRI determine complete responders after neoadjuvant chemoradiation for locally advanced rectal cancer? *Diagn Interv Radiol* 2012; **18**: 574–81. doi: https://doi.org/10.4261/1305-3825.dir.5755-12.1
21. Maas M, Lambregts DM, Nelemans PJ, Heijnen LA, Martens MH, Leijtens JW, et al. Assessment of clinical complete response after chemoradiation for rectal cancer with digital rectal examination, endoscopy, and MRI: selection for organ-saving treatment. *Ann Surg Oncol* 2015; **22**: 3873–80. doi: https://doi.org/10.1245/s10434-015-4687-9
22. Lambregts DM, Vandecaveye V, Barbaro B, Bakers FC, Lambrecht M, Maas M, et al. Diffusion-weighted MRI for selection of complete responders after chemoradiation for locally advanced rectal cancer: a multicenter study. *Ann Surg Oncol* 2011; **18**: 2224–31. doi: https://doi.org/10.1245/s10434-011-1607-5
23. Sassen S, de Booij M, Sosef M, Berendsen R, Lammering G, Clarijs R, et al. Locally advanced rectal cancer: is diffusion weighted MRI helpful for the identification of complete responders (ypT0N0) after neoadjuvant chemoradiation therapy? *Eur Radiol* 2013; **23**: 3440–9. doi: https://doi.org/10.1007/s00330-013-2956-1
24. Curvo-Semedo L, Lambregts DM, Maas M, Thywissen T, Mehsen RT, Lammering G, et al. Rectal cancer: assessment of complete response to preoperative combined radiation therapy with chemotherapy—conventional MR volumetry *versus* diffusion-weighted MR imaging. *Radiology* 2011; **260**: 734–43.
25. Jang KM, Kim SH, Choi D, Lee SJ, Park MJ, Min K. Pathological correlation with diffusion restriction on diffusion-weighted imaging in patients with pathological complete response after neoadjuvant chemoradiation therapy for locally advanced rectal cancer: preliminary results. *Br J Radiol* 2012; **85**: e566–72. doi: https://doi.org/10.1259/bjr/24557556
26. Joye I, Deroose CM, Vandecaveye V, Haustermans K. The role of diffusion-weighted MRI and (18)F-FDG PET/CT in the prediction of pathologic complete response after radiochemotherapy for rectal cancer: a systematic review. *Radiother Oncol* 2014; **113**: 158–65. doi: https://doi.org/10.1016/j.radonc.2014.11.026
27. Zahra MA, Hollingsworth KG, Sala E, Lomas DJ, Tan LT. Dynamic contrast-enhanced MRI as a predictor of tumour response to radiotherapy. *Lancet Oncol* 2007; **8**: 63–74. doi: https://doi.org/10.1016/S1470-2045(06)71012-9
28. Tofts PS, Brix G, Buckley DL, Evelhoch JL, Henderson E, Knopp MV, et al. Estimating kinetic parameters from dynamic contrast-enhanced T(1)-weighted MRI of a diffusable tracer: standardized quantities and symbols. *J Magn Reson Imaging* 1999; **10**: 223–32. doi: https://doi.org/10.1002/(SICI)1522-2586(199909)10:3<223::AID-JMRI2>3.0.CO;2-S
29. Oberholzer K, Menig M, Pohlmann A, Junginger T, Heintz A, Kreft A, et al. Rectal cancer: assessment of response to neoadjuvant chemoradiation by dynamic contrast-enhanced MRI. *J Magn Reson Imaging* 2013; **38**: 119–26. doi: https://doi.org/10.1002/jmri.23952
30. Intven M, Reerink O, Philippens ME. Dynamic contrast enhanced MR imaging for rectal cancer response assessment after neo-adjuvant chemoradiation. *J Magn Reson Imaging* 2015; **41**: 1646–53. doi: https://doi.org/10.1002/jmri.24718
31. George M, Dzik-Jurasz A, Padhani A, Brown G, Tait D, Eccles S, et al. Non-invasive methods of assessing angiogenesis and their value in predicting response to treatment in colorectal cancer. *Br J Surg* 2001; **88**: 1628–36. doi: https://doi.org/10.1046/j.0007-1323.2001.01947.x
32. Lim JS, Kim D, Baek SE, Myoung S, Choi J, Shin SJ, et al. Perfusion MRI for the prediction of treatment response after preoperative chemoradiotherapy in locally advanced rectal cancer. *Eur Radiol* 2012; **22**: 1693–700. doi: https://doi.org/10.1007/s00330-012-2416-3
33. Martens MH, Subhani S, Heijnen LA, Lambregts DM, Buijsen J, Maas M, et al. Can perfusion MRI predict response to preoperative treatment in rectal cancer? *Radiother Oncol* 2015; **114**: 218–23. doi: https://doi.org/10.1016/j.radonc.2014.11.044
34. Luna A, Vilanova JC, Hygino Da Cruz LC Jr, Rossi SE. *Functional imaging in oncology: biophysical basis and technical approaches*. Vol. **1**. Berlin, Germany: Springer; 2013.
35. Brix G, Semmler W, Port R, Schad LR, Layer G, Lorenz W. Pharmacokinetic parameters in CNS Gd-DTPA enhanced MR imaging. *J Comput Assist Tomogr* 1991; **15**: 621–8. doi: https://doi.org/10.1097/00004728-199107000-00018
36. Tofts PS. Modeling tracer kinetics in dynamic Gd-DTPA MR imaging. *J Magn Reson Imaging* 1997; **7**: 91–101. doi: https://doi.org/10.1002/jmri.1880070113
37. Alberda WJ, Dassen HP, Dwarkasing RS, Willemssen FE, van der Pool AE, de Wilt JH, et al. Prediction of tumor stage and lymph node involvement with dynamic contrast-enhanced MRI after chemoradiotherapy for locally advanced rectal cancer. *Int J Colorectal Dis* 2013; **28**: 573–80. doi: https://doi.org/10.1007/s00384-012-1576-6
38. DeVries AF, Piringer G, Kremser C, Judmaier W, Saely CH, Lukas P, et al. Pretreatment evaluation of microcirculation by dynamic contrast-enhanced magnetic resonance imaging predicts survival in primary rectal cancer patients. *Int J Radiat Oncol Biol Phys* 2014; **90**: 1161–7. doi: https://doi.org/10.1016/j.ijrobp.2014.07.042
39. de Lussanet QG, Backes WH, Griffioen AW, Padhani AR, Baeten CI, van Baardwijk A, et al. Dynamic contrast-enhanced magnetic resonance imaging of radiation therapy-induced microcirculation changes in rectal

cancer. *Int J Radiat Oncol Biol Phys* 2005; **63**: 1309–15. doi: https://doi.org/10.1016/j.ijrobp.2005.04.052

40. Yeo DM, Oh SN, Jung CK, Lee MA, Oh ST, Rha SE, et al. Correlation of dynamic contrast-enhanced MRI perfusion parameters with angiogenesis and biologic aggressiveness of rectal cancer: preliminary results. *J Magn Reson Imaging* 2015; **41**: 474–80. doi: https://doi.org/10.1002/jmri.24541
41. Zhang XM, Yu D, Zhang HL, Dai Y, Bi D, Liu Z, et al. 3D dynamic contrast-enhanced MRI of rectal carcinoma at 3T: correlation with microvascular density and vascular endothelial growth factor markers of tumor angiogenesis. *J Magn Reson Imaging* 2008; **27**: 1309–16. doi: https://doi.org/10.1002/jmri.21378
42. Hong HS, Kim SH, Park HJ, Park MS, Kim KW, Kim WH, et al. Correlations of dynamic contrast-enhanced magnetic resonance imaging with morphologic, angiogenic, and molecular prognostic factors in rectal cancer. *Yonsei Med J* 2013; **54**: 123–30. doi: https://doi.org/10.3349/ymj.2013.54.1.123
43. Glunde K, Bhujwalla ZM, Ronen SM. Choline metabolism in malignant transformation. *Nat Rev Cancer* 2011; **11**: 835–48. doi: https://doi.org/10.1038/nrc3162
44. Serkova NJ, Brown MS. Quantitative analysis in magnetic resonance spectroscopy: from metabolic profiling to *in vivo* biomarkers. *Bioanalysis* 2012; **4**: 321–41. doi: https://doi.org/10.4155/bio.11.320
45. O'Connell TM. Recent advances in metabolomics in oncology. *Bioanalysis* 2012; **4**: 431–51. doi: https://doi.org/10.4155/bio.11.326
46. Minicozzi A, Mosconi E, Cordiano C, Rubello D, Marzola P, Ferretti A, et al. Proton magnetic resonance spectroscopy: *ex vivo* study to investigate its prognostic role in colorectal cancer. *Biomed Pharmacother* 2013; **67**: 593–7. doi: https://doi.org/10.1016/j.biopha.2013.05.002
47. Pacholczyk-Sienicka B, Fabiańska A, Pasz-Walczak G, Kordek R, Jankowski S. Prediction of survival for patients with advanced colorectal cancer using (1)H high-resolution magic angle spinning nuclear MR spectroscopy. *J Magn Reson Imaging* 2014; **41**: 1669–74.
48. Jimenez B, Mirnezami R, Kinross J, Cloarec O, Keun HC, Holmes E, et al. (1)H HR-MAS NMR spectroscopy of tumor-induced local metabolic "field-effects" enables colorectal cancer staging and prognostication. *J Proteome Res* 2013; **12**: 959–68.
49. Chan EC, Koh PK, Mal M, Cheah PY, Eu KW, Backshall A, et al. Metabolic profiling of human colorectal cancer using high-resolution magic angle spinning nuclear magnetic resonance (HR-MAS NMR) spectroscopy and gas chromatography mass spectrometry (GC/MS). *J Proteome Res* 2009; **8**: 352–61. doi: https://doi.org/10.1021/pr8006232
50. Kim MJ, Lee SJ, Lee JH, Kim SH, Chun HK, Kim SH, et al. Detection of rectal cancer and response to concurrent chemoradiotherapy by proton magnetic resonance spectroscopy. *Magn Reson Imaging* 2012; **30**: 848–53. doi: https://doi.org/10.1016/j.mri.2012.02.013
51. Li SP, Padhani AR. Tumor response assessments with diffusion and perfusion MRI. *J Magn Reson Imaging* 2012; **35**: 745–63. doi: https://doi.org/10.1002/jmri.22838
52. Intven M, Monninkhof EM, Reerink O, Philippens ME. Combined T2w volumetry, DW-MRI and DCE-MRI for response assessment after neo-adjuvant chemoradiation in locally advanced rectal cancer. *Acta Oncol* 2015; **54**: 1729–36. doi: https://doi.org/10.3109/0284186X.2015.1037010
53. Just N. Improving tumour heterogeneity MRI assessment with histograms. *Br J Cancer* 2014; **111**: 2205–13. doi: https://doi.org/10.1038/bjc.2014.512
54. Liney GP, Holloway L, Harthi TM, Sidhom M, Moses D, Juresic E, et al. Quantitative evaluation of diffusion-weighted imaging techniques for the purposes of radiotherapy planning in the prostate. *Br J Radiol* 2015; **88**: 20150034. doi: https://doi.org/10.1259/bjr.20150034
55. Kim YC, Lim JS, Keum KC, Kim KA, Myoung S, Shin SJ, et al. Comparison of diffusion-weighted MRI and MR volumetry in the evaluation of early treatment outcomes after preoperative chemoradiotherapy for locally advanced rectal cancer. *J Magn Reson Imaging* 2011; **34**: 570–6. doi: https://doi.org/10.1002/jmri.22696
56. Cai G, Xu Y, Zhu J, Gu WL, Zhang S, Ma XJ, et al. Diffusion-weighted magnetic resonance imaging for predicting the response of rectal cancer to neoadjuvant concurrent chemoradiation. *World J Gastroenterol* 2013; **19**: 5520–7. doi: https://doi.org/10.3748/wjg.v19.i33.5520
57. Musio D, De Felice F, Magnante AL, Ciolina M, De Cecco CN, Rengo M, et al. Diffusion-weighted magnetic resonance application in response prediction before, during, and after neoadjuvant radiochemotherapy in primary rectal cancer carcinoma. *Biomed Res Int* 2013; **2013**: 740195. doi: https://doi.org/10.1155/2013/740195
58. Carbone SF, Pirtoli L, Ricci V, Venezia D, Carfagno T, Lazzi S, et al. Assessment of response to chemoradiation therapy in rectal cancer using MR volumetry based on diffusion-weighted data sets: a preliminary report. *Radiol Med* 2012; **117**: 1112–24. doi: https://doi.org/10.1007/s11547-012-0829-3
59. Ha HI, Kim AY, Yu CS, Park SH, Ha HK. Locally advanced rectal cancer: diffusion-weighted MR tumour volumetry and the apparent diffusion coefficient for evaluating complete remission after preoperative chemoradiation therapy. *Eur Radiol* 2013; **23**: 3345–53. doi: https://doi.org/10.1007/s00330-013-2936-5

2.2 Literature review update January 2015 – June 2019: Functional MRI for therapeutic response prediction in rectal cancer

DWI-MRI for prediction of primary tumour response

PubMed and MEDLINE were used for the search. The inclusion criteria for this search were (i) rectal cancer, (ii) chemoradiotherapy, (iii) diffusion weighted MRI, (iv) quantitative analysis, and (v) prospective study. Radiomics (high-throughput computer analyses generating hundreds of parameters) studies were not included in this search. The cut-off date was June 2019.

An additional 4 prospective DWI-MRI studies assessing ADC for CRT response prediction were found. The results of these studies are summarised in Table 2.1. These studies support the potential of quantitative analysis of DWI-MRI for prediction of CRT response in rectal cancer. One of these studies developed a multivariate model from a total of 18 T2-weighted volumetry and 18 DWI-MRI variables (25, 26) in a development cohort of 85 patients (25, 26), and tested the model on a validation cohort of 55 patients undergoing CRT (26). The final MRI model consisted of 2 T2-weighted volumetric parameters (T2-weighted volume % change and diameter of sphere post CRT) and 2 DWI parameters (average ADC post-CRT and average ADC ratio) and testing of the model on the validation cohort showed high predictive performance.

DCE-MRI for prediction of primary tumour response

The inclusion criteria for this search were (i) rectal cancer, (ii) chemoradiotherapy, (iii) DCE-MRI (iv) (semi-)quantitative analysis, and (iv) prospective study. Radiomics studies were excluded.

An additional 3 prospective DCE-MRI studies were found that assessed the role of DCE-MRI in prediction of CRT response in patients with locally advanced rectal cancer (Table 2.2). These studies showed the ability of DCE-MRI (semi-)quantitative parameters in the prediction of CRT response.

Table 2.1 DWI-MRI studies prediction of chemoradiotherapy response

Prospective quantitative studies 2015 – 2019

Study	N	MRI time points	MRI variable	Histopathology response	Result	Significance
Joye et al (2017) (25) and Bulens et al (2018) (26)	85 (development cohort) 55 (validation cohort)	3.0 T Pre, post-CRT	Model included T2-weighted Δvolume% and sphere_post and ADCaverage_post and ADC ratio_average	Near pCR (ypT0-1N0) vs. not	Development cohort area under curve (AUC) = 0.89 Validation cohort AUC = 0.88	CI 0.80 – 0.98 CI 0.79 – 0.98
De Felice et al (2017) (27)	37	3.0 T Pre, during, post	ADC (mean) ΔADC	pCR (ypT0N0) vs. no pCR	Mean ADC ΔADC + in pCR	p = ns p < 0.05
Iannicelli et al (2016) (28)	34	1.5 T Pre, post-CRT	ADC (mean)	TRG (Mandard) Responders TRG 1-2 Non-responders (TRG 3-5)	Mean ADC pre Mean ADC post (higher in responders) ΔADC + in responders	p = ns p = 0.001 P = 0.01
Birlik et al (2015) (29)	43	1.5 T Pre, post CRT	ADC mean ΔADC	TRG (Ryan) Responders (TRG 1) Nonresponders (TRG 2-3)	Mean ADC pre lower in responders ΔADC higher in responders	p < 0.001 p = 0.001

Table 2.2 DCE-MRI studies prediction of chemoradiotherapy response

Prospective (semi-)quantitative studies 2015 – 2019

Study	N	MRI time points	MRI variable	Histopathology response	Result	Significance
Palmisano et al (2018) (30)	21	Pre-CRT 1.5 T	K^{trans} and Ve Histogram 25^{th}, 50^{th}, 75^{th} percentile, mean, skewness and kurtosis	Rodel's TRG Responders TRG 3 – 4 Non-responders TRG 0 – 2	Ve skewness and kurtosis higher in non-responders Other parameters	p = 0.003 p = 0.011 p = ns
Tong et al (2015) (31)	38	Pre and post-CRT 3.0 T	Mean K^{trans}, K_{ep}, V_e	pCR (ypT0N0) vs. non-pCR	Pre-CRT K^{trans} lower in pCR Pre-CRT K_{ep} – higher in pCR Pre-V_e – higher in pCR Post-CRT K^{trans}, K_{ep}, V_e	p = 0.01 p = 0.02 p = 0.01 p = ns
Petrillo et al (2015) (32)	74	Pre and post-CRT 1.5 T	Median maximal signal difference (MSD) Time to peak (TTP) WII (wash-in intercept) WOI (Wash-out intercept) WIS (wash-in slope) WOS / WIS WOI / WII	TRG mandard Responders (TRG 1 – 2) Non-responders (TRG 3 – 5)	ΔMSD + in responders ΔWOS + in responders Other parameters	p = 0.001 p = 0.0001 p = ns

Multi-parametric MRI for prediction of primary tumour response

The inclusion criteria for this search were (i) rectal cancer, (ii) chemoradiotherapy, (iii) multi-parametric MRI (DWI and DCE-MRI), (iv) quantitative analysis, and (v) prospective study. Radiomics (high-throughput computer analyses) studies were not included in this search.

Intven et al (33) studied multi-parametric MRI combining DWI and DCE at 3.0 tesla in a prospective study in rectal cancer, and this study is described in the above review. One other prospective study was found assessing multi-parametric MRI (DWI and DCE) for response prediction in rectal cancer. De Cecco et al (34) assessed multi-parametric MRI (DWI and DCE) before CRT in 12 patients. The parameters analysed were T2-weighted texture kurtosis (of ROI on single slice), ADC, and DCE-MRI derived K^{trans}, K_{ep}, V_e, and areas under the concentration curve of contrast agent over 90 s (IAUGC90). They found that pre-CRT kurtosis ($p = < 0.001$) and mean Ve ($p = 0.04$) were predictive of pCR.

MRI histogram analysis of whole tumour heterogeneity

There have not been any published prospective DWI-MRI histogram studies in rectal cancer. The DWI-MRI studies that analysed whole tumour heterogeneity using a histogram analysis were retrospective (35-37). Enkhbaatar et al found that post-CRT skewness of ADC histogram was useful for predicting response to CRT (35). Cho et al (37) and Choi et al (36) found that low percentile ADC values post-CRT were useful for predicting CRT response.

For prospective DCE-MRI studies, Palmisano et al analysed DCE-MRI K^{trans} and Ve histogram parameters 25^{th}, 50^{th}, 75^{th} percentiles, skewness and kurtosis in 21 patients, and found that of these parameters, Ve skewness and kurtosis could predict CRT response with an AUC 0.988 and 0.963 (30). De Cecco et al included a heterogeneity analysis in their methods of their study of 12 patients by assessing the before CRT highest 10^{th} and 25^{th} quantiles of voxels for the DCE-MRI parameters, but not of DWI-MRI, although these specific results were not reported in the publication (34).

Overall, this literature review update supports the conclusions in the published literature review. The additional studies found have shown promise in the ability of DWI and DCE-MRI performed before CRT and after CRT for prediction of CRT response in patients with locally advanced rectal cancer. The majority of studies assessed summary MRI parameters, such as mean ADC or K^{trans} values. There were still a limited number of studies assessing DWI and DCE in combination for the multi-parametric MRI assessment of CRT response. There were no prospective studies investigating the potential of multi-parametric MRI (combining multiple functional parameters such as diffusion and perfusion) assessment of whole tumour heterogeneity for CRT response prediction and this remains an area to be investigated.

2.3 Literature review: ultra-high field MRI in rectal cancer

The majority of *ex vivo* ultra-high field MRI studies in rectal cancer have been reported in the field of MR spectroscopy as part of colorectal studies, and a description of these studies is contained in the review article. There have been no published studies in rectal cancer using MRI sequences other than spectroscopy at fields ≥ 7.0 tesla. There has been a preliminary report (abstract form) on a study of patients who underwent neoadjuvant CRT for rectal cancer (Hoendergangers et al ESTRO 37 EP-2094). This study explored chemical exchange saturation transfer (CEST) MRI at 7.0 tesla on 5 patients and surgical specimens, however correlation work with pathology is ongoing.

To the best of our knowledge, there have been no published studies examining DTI-MRI in rectal cancer *ex vivo* or *in vivo*. DTI-MRI ultra-high field work has been performed in other gastrointestinal tumour sites. Yamada et al have examined DTI-MRI on oesophageal and gastric cancer specimens at 7.0 tesla and found this technique to be feasible for assessing mural depth of tumour invasion (38-40).

This literature review has shown that the potential of ultra-high field MRI in screening promising rectal cancer biomarkers remains yet to be explored.

Chapter 3 Methods (clinical study): Multi-parametric MRI for radiotherapy response prediction in locally advanced rectal cancer

3.1 Introduction

The objectives of this study were to:

(1) Prospectively evaluate multi-parametric MRI using diffusion weighted imaging and dynamic contrast enhanced MRI at 3.0 tesla performed before, during and after chemoradiotherapy (CRT) for therapeutic response prediction in locally advanced rectal cancer. MRI biomarkers were correlated with histopathology tumour regression grade (TRG) according to AJCC 7th edition criteria.

(2) Correlate functional MRI biomarkers (DWI and DCE) performed before, during and after CRT with 2 year disease-free survival.

Patients with locally advanced rectal cancer undergoing CRT followed by surgery prospectively underwent multi-parametric MRI before CRT, during CRT (week 3), and after CRT (within 1 week before surgery). Histopathological assessment of the surgical specimen was undertaken to assess tumour response to CRT. Tumour Regression Grade (TRG) was defined according to the modified classification of Ryan et al (41) as set out in the AJCC 7th Edition tumour regression grading criteria (42) (see below section 3.8).

A complete protocol using quantitative diffusion weighted imaging (DWI) and dynamic contrast enhanced (DCE) imaging in combination, and a voxel-by-voxel histogram analysis strategy was developed for multi-parametric MRI prediction of treatment response in rectal cancer. The developed protocol enables 3-dimensional assessment of tumour heterogeneity and its changes in response to CRT in rectal cancer.

3.2 Study design

This study was a prospective, single-arm, cohort study to investigate the value of multi-parametric MRI (combining DWI and DCE) in the prediction of CRT response. Patients received standard treatment for their malignancy.

3.3 Study population

Patients with Stage II or III rectal adenocarcinoma undergoing neoadjuvant CRT followed by primary surgery were eligible for this prospective study. The inclusion criteria were (i) age >18 years, (ii) locally advanced rectal adenocarcinoma defined as Stage II or III (T3 – T4 and / or N1 – 2), without distant metastases staged as per TNM AJCC 7th edition (42), (iii) neoadjuvant CRT (radiotherapy 50.4Gy in 28 fractions concurrent with infusional 5-fluorouracil or oral capecitabine), and surgery 6 – 12 weeks after completion of CRT. The exclusion criteria were: (i) prior malignancy, (ii) active inflammatory bowel disease, (iii) contraindication to MRI from implanted ferromagnetic metal, pacemaker / implantable defibrillator or extreme claustrophobia.

3.4 Study schematic

All patients received standard treatment consisting of neoadjuvant CRT followed by primary surgery, and had MRI performed at 3 time-points; before CRT, during CRT (week 3 of CRT) and after CRT (within 1 week prior to surgery). The study schema (Figure 3.1) included FDG-PET and circulating tumour cells (CTC) as this study was part of a multi-disciplinary trial.

Figure 3.1 Study schematic

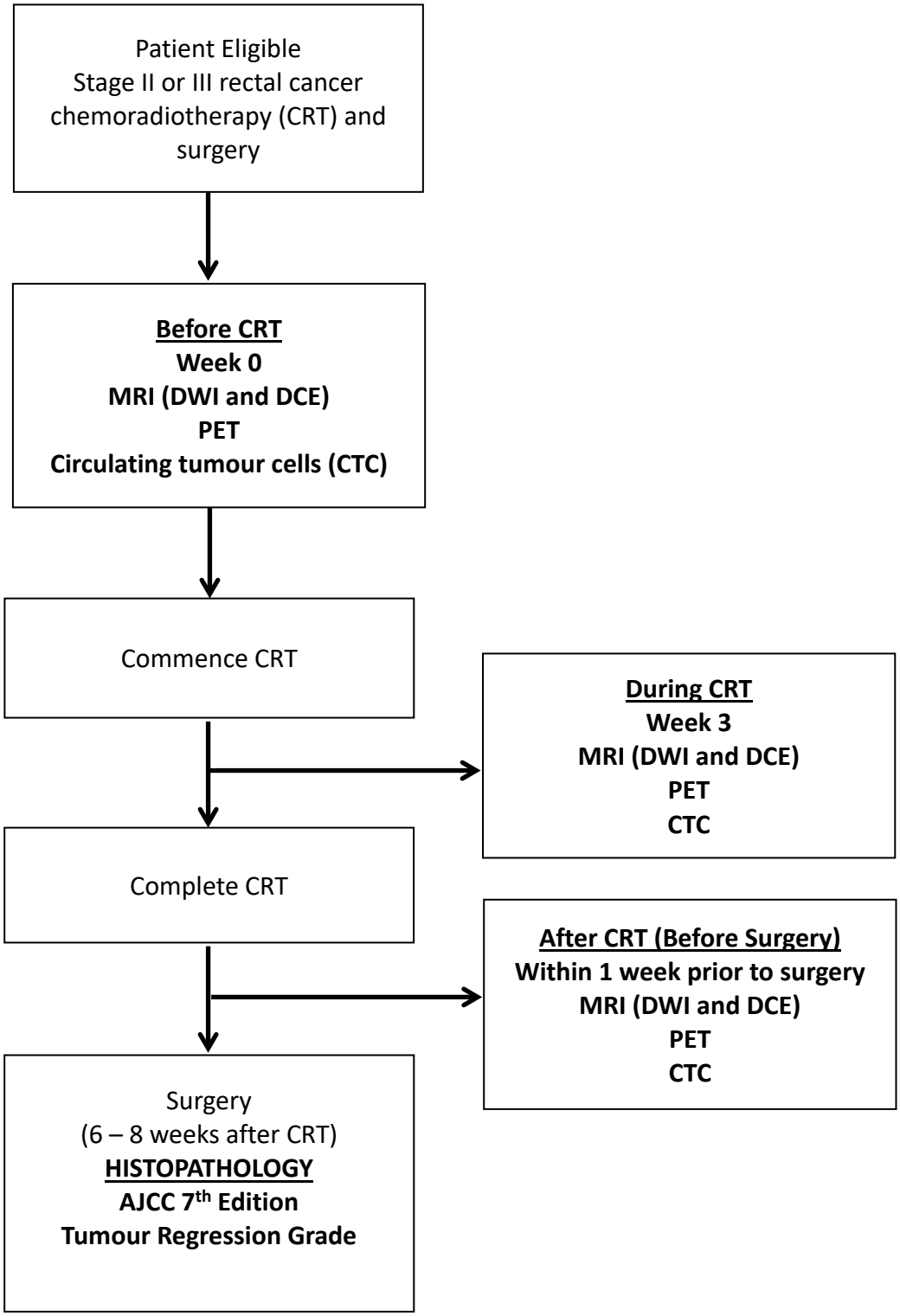

3.5 MRI technique

Patients underwent MRI consisting of DWI and DCE at 3 time-points: (i) Before CRT, (ii) during CRT week 3 after 9 – 10 fractions of radiotherapy, and (iii) after CRT, within 1 week prior to surgery. All MRIs were acquired on the 3.0 tesla Siemens Skyra radiotherapy dedicated MRI-Simulator in the Liverpool Cancer Therapy Radiation Oncology department. A 32-channel RF coil in the patient table was used in combination with an 18-channel phase array coil strapped firmly around the pelvis.

T2-weighted (T2-w) turbo spin echo images were acquired in 3 planes with 2mm slice thickness and bandwidth 440Hz/Px in 1 concatenation: (i) sagittal, (ii) axial oblique, angulated perpendicular to the long tumour axis, and (iii) axial orthogonal. The field of view encompassed primary tumour and pelvic nodes. A T2-w HASTE sequence was additionally acquired in the coronal plane.

Butylscopolamine (Buscopan) 20mg was administered intravenously prior to acquisition of functional sequences to reduce rectal motion. Functional sequences were acquired with in-plane resolution of 1.1 x 1.1 mm and 4 mm slice thickness (20 or 26 slices for DWI, 26 slices for DCE). The field of view was 22cm (axial) and encompassed the primary tumour (20 or 26 slices for DWI and 26 slices for DCE). DWI was acquired using a readout segmented diffusion technique (RESOLVE), in the axial orthogonal plane with b-values 50 and 800 s/mm^2, bandwidth 870Hz/Px, and 1 & 3 averages respectively. ADC maps and calculated b = 1400 mm/s^2 images were produced as part of protocol. DCE consisted of pre-contrast T1-weighted VIBE scans with TR 4.09ms, TE 1.35ms, bandwidth 440Hx/Px and flip angles 2^o and 15^o to calculate native T1. DCE utilised a time-resolved angiography with stochastic trajectories (TWIST) technique acquired over 60 phases, with a temporal resolution of 5.28 seconds, bandwidth 440 Hz/Px, TR 3.67ms and TE 1.48ms. Gadoversetamide (Optimark 0.5mmol/ml) gadolinium-based contrast 0.1mM/kg capped at a maximum 7.5mmol (15ml) was injected at rate 4 ml/s followed by a 20ml normal saline flush at a rate 4 ml/s after 3 phases were acquired. The contrast dose was kept consistent across all time-points for each patient. If patients had renal

impairment (eGFR<60ml/s) or prior allergic reaction to gadolinium-based contrast, the DCE sequence was omitted.

The 'Rectal study multi-parametric MRI study sequences' protocol for this study is in Appendix 1.

3.6 Clinical assessment and acute toxicity grading

Radiation oncology clinical assessments and formal acute toxicity soring according to the Common terminology criteria for adverse events (CTCAE) version 4.0 was performed before commencement of CRT, weekly during radiotherapy treatment reviews, 2 weeks after completion of CRT. The acute toxicity scoring form is in Appendix 2.

All patients were followed every 3 months for 2 years from the date of surgery, then 6 monthly. A routine blood test including CEA was done at every follow-up visit. A CT scan of the chest, abdomen and pelvis was performed every 6 months during follow-up. Colonoscopy and biopsy during the follow-up period was performed at the surgeon's discretion.

3.7 Imaging analysis

Rigid body registration of flip-angle images to dynamic images was performed. Images were manually pre-registered using commercial 3D visualisation software (Siemens). Subsequently, the registered images were exported off-line and using in-house code were re-assigned a full DICOM header to enable these images to be analysed in Tissue 4D (Siemens). Tissue 4D was used to produce K^{trans} maps by first pre-selecting an appropriate arterial input function, scaled by dose, based on chi-squared goodness of fit, and using a two-compartment Tofts model (43). ADC and K^{trans} parameter maps were exported in DICOM format and registered to T2-w axial orthogonal images in OncoTreat (works-in-progress, Siemens). Semi-automated segmentation was used to define the region of interest (ROI) from the entire hyper-intense tumour on the b-value 1400mm/s^2 images. A radiation oncologist (TP) with sub-specialization in gastrointestinal malignancies performed all segmentation. The raw voxel-wise data was exported from

OncoTreat WIP and cleaned prior to analysis. A voxel-by-voxel technique was used to produce colour-coded maps and histograms of ADC and K^{trans}, and combined scatterplots for each time-point.

3.8 Histopathology

Histopathological assessment was undertaken by a dedicated pathology team, with all reporting of tumour regression grade (TRG) assessment by pathologists with sub-specialisation in gastrointestinal pathology. Two dedicated pathologists (CH and JS) examined each case and reached a consensus on TRG. Examination of the specimen was undertaken as per the guidelines set out in the Royal College of Pathologists of Australasia Structured Reporting Protocol for Colorectal Cancer (44). For the study it was a universal requirement that the whole of the original tumour site should be embedded for microscopic assessment. TRG was recorded using the modified classification of Ryan et al (41) set out in the AJCC Cancer Staging Manual, 7th Edition (42) as follows:

TRG 0 (complete response) – no viable cancer cells
TRG 1 (moderate response) – single cells or small groups of cancer cells
TRG 2 (minimal response) – residual cancer outgrown by fibrosis
TRG 3 (poor response) – minimal or no tumour kill; extensive residual cancer.

Patients with TRG 0–1 were categorised as 'responders' and those with TRG 2–3 were categorised as 'non-responders' to CRT.

Histologic subtype was assessed. Histology was categorised as adenocarcinoma, mucinous adenocarcinoma, or not assessable (in case of pathologic complete response (pCR)). Tumours were classified as mucinous adenocarcinoma if the tumour contained >50% mucin as per WHO definition.

The histopathology reporting form is in Appendix 3.

3.9 Statistical analysis

The target number of patients was 35. For estimated pCR rate of 25%, 35 patients provided 80% power to detect an area under the curve (AUC) ≥ 80%. Poor responders rate were estimated to be in the range of 25-45% (9). For estimated poor responder rate of 25%, 35 patients provided 80% power to detect an AUC ≥80%. For estimated poor responder rate of 45%, 35 patients provided 80% power to detect an AUC ≥ 76%.

All analyses were performed using R version 3.5.1 (R Core Team, 2013) using various packages including rms (F. Harrell, 2014) for analysis, ggplot2 for plotting (histogram and scatterplots) and knitr (Xie, 2013) for reproducible research. Whole tumour voxel-wise raw data (cleaned) was used for analysis. In the case of ADC, pixels in the ROI with value below 10 were trimmed before calculating the median. In the case of K^{trans}, medians of transformed ROI values (after first excluding voxels with recorded K^{trans} of 0) using the cube-root (symmetrising) transformation were used. A continuous variable analysis was performed. Whole tumour ADC and K^{trans} distributions were produced for each patient, and histogram quantiles (10^{th}, 25^{th}, 50^{th}, 75^{th}, 90^{th}), skewness (measure of asymmetry of the distribution (45)) and kurtosis (sharpness of the peak of the distribution and a measure of the shape of the distribution (45)) were extracted from ADC and K^{trans} distributions for analysis in order to determine if the statistics differed between groups by response status or was changing over time. Tumour heterogeneity was assessed by using objective cut-points defined by quantiles.

Correlation of MRI with response status

For statistical analyses, patients were categorized according to response status: responders (TRG 0 – 1) versus non-responders (TRG 2 – 3). Logistic regressions were performed to investigate the association of median ADC, and median K^{trans} with response status, by individual parameter and time-point, and by joint combination of parameters and time-point. Paired t-tests were used to analyse change in medians of ADC and K^{trans} from baseline to week 3, and from baseline to post-treatment according to response status. Bivariate logistic regressions were also performed to investigate the association between the ADC and K^{trans} histogram parameters 10^{th}, 25^{th}, 75^{th} and 90^{th}

quantiles, skewness, and kurtosis at all time-points, and response status. As these analyses were considered exploratory, multiple comparison adjustments were not employed and a p value < 0.05 was considered statistically significant.

Tables of data categorized by blue (low value) / green (medium value) / red voxels (high value) for ADC and K^{trans} were created using cut-points set at lower and upper quartiles using all patients. The frequencies of blue / green / red voxels for each time-point was calculated for ADC and K^{trans}. Whole tumour voxel-wise ADC and K^{trans} colour-coded histograms and combined scatterplots were produced for all patients. For the multi-parametric MRI analysis, multi-variate analysis was used to assess the relationship between combination of ADC and K^{trans}, and response status.

Correlation of MRI with disease-free survival

Disease-free survival was defined as the interval from date of surgery to date of relapse (loco-regional relapse or distant metastasis), or death from rectal cancer. The associations between ADC and K^{trans} at 3 time-points (before CRT, during CRT, and after CRT) with time to relapse (loco-regional or distant) were analysed as a continuous variable using a Cox proportional hazard model. P value < 0.05 was considered statistically significant. To investigate the relevance of heterogeneities of ADC and K^{trans} before CRT, during CRT, and after CRT (before surgery) percentile values (10^{th}, 25^{th}, 50^{th}, 75^{th} and 90^{th}) were analysed for relapse. Receiver-operator characteristics (ROC) curve analysis with Youden's index was used to determine the best cut-point for ADC and K^{trans}.

Mucinous adenocarcinomas

Mucinous adenocarcinomas were analysed as a separate group. Mucinous tumours contain predominately mucin which has diffusion and perfusion characteristics similar to water. Mucinous tumours have different MR diffusion and perfusion characteristics to that of solid adenocarcinomas, and hence mucinous tumours were analysed separately using descriptive analysis due to small sample size. Similar methods to the methods used in non-mucinous adenocarcinoma group described above were used for the mucinous adenocarcinoma group.

3.10 Ethics approval

This project was approved by the South Western Sydney Local Health District Human Research and Ethics Committee (HREC) as part of the 'Circulating tumour cells in cancer management' meta-project on 11th September 2013.

An ethics amendment for the administration of gadolinium-based MRI contrast was approved on 20th May 2014.

Ethics reference: HREC/13/LPOOL/158, local project number 13/097a, 13/097b, 13/097c, Sub-study Rectal Cancer.

3.11 Study protocol publication

Study protocol: multi-parametric magnetic resonance imaging for therapeutic response prediction in rectal cancer. ***BMC Cancer 2017;17:465.*** https://doi.org/10.1186/s12885-017-3449-4

Authors:

1. Trang T. Pham
2. Gary Liney
3. Karen Wong
4. Robba Rai
5. Mark Lee
6. Daniel Moses
7. Christopher Henderson
8. Michael Lin
9. Joo-Shik Shin
10. Michael Barton

Pham et al. BMC Cancer (2017) 17:465
DOI 10.1186/s12885-017-3449-4

BMC Cancer

STUDY PROTOCOL Open Access

Study protocol: multi-parametric magnetic resonance imaging for therapeutic response prediction in rectal cancer

Trang Thanh Pham[1,2,3,4,7*], Gary Liney[1,3,4,9], Karen Wong[1,3,4], Robba Rai[1,4], Mark Lee[1,3], Daniel Moses[3,5], Christopher Henderson[3,6,7], Michael Lin[3,7,8], Joo-Shik Shin[6,7] and Michael Bernard Barton[1,3,4]

Abstract

Background: Response to neoadjuvant chemoradiotherapy (CRT) of rectal cancer is variable. Accurate imaging for prediction and early assessment of response would enable appropriate stratification of management to reduce treatment morbidity and improve therapeutic outcomes. Use of either diffusion weighted imaging (DWI) or dynamic contrast enhanced (DCE) imaging alone currently lacks sufficient sensitivity and specificity for clinical use to guide individualized treatment in rectal cancer. Multi-parametric MRI and analysis combining DWI and DCE may have potential to improve the accuracy of therapeutic response prediction and assessment.

Methods: This protocol describes a prospective non-interventional single-arm clinical study. Patients with locally advanced rectal cancer undergoing preoperative CRT will prospectively undergo multi-parametric MRI pre-CRT, week 3 CRT, and post-CRT. The protocol consists of DWI using a read-out segmented sequence (RESOLVE), and DCE with pre-contrast T1-weighted (VIBE) scans for T1 calculation, followed by 60 phases at high temporal resolution (TWIST) after gadoversetamide injection. A 3-dimensional voxel-by-voxel technique will be used to produce colour-coded ADC and K^{trans} histograms, and data evaluated in combination using scatter plots. MRI parameters will be correlated with surgical histopathology. Histopathology analysis will be standardized, with chemoradiotherapy response defined according to AJCC 7th Edition Tumour Regression Grade (TRG) criteria. Good response will be defined as TRG 0–1, and poor response will be defined as TRG 2–3.

Discussion: The combination of DWI and DCE can provide information on physiological tumour factors such as cellularity and perfusion that may affect radiotherapy response. If validated, multi-parametric MRI combining DWI and DCE can be used to stratify management in rectal cancer patients. Accurate imaging prediction of patients with a complete response to CRT would enable a 'watch and wait' approach, avoiding surgical morbidity in these patients. Consistent and reliable quantitation from standardised protocols is essential in order to establish optimal thresholds of ADC and K^{trans} and permit the role of multi-parametric MRI for early treatment prediction to be properly evaluated.

Trial registration: Australian New Zealand Clinical Trials Registry (ANZCTR) number ACTRN12616001690448 (retrospectively registered 8/12/2016).

Keywords: MRI, Rectal cancer, Radiotherapy, Response, Chemoradiotherapy, Diffusion weighted imaging, Dynamic contrast enhanced, Diffusion, Perfusion

* Correspondence: Trang.Pham@health.nsw.gov.au
[1]Department of Radiation Oncology, Liverpool Cancer Therapy Centre, Liverpool Hospital, South Western Sydney Local Health District, Sydney, Australia
[2]Sydney West Radiation Oncology Network, Westmead, Blacktown and Nepean Hospitals, Sydney, Australia
Full list of author information is available at the end of the article

Background

Locally advanced rectal cancer (LARC) requires multi-modality treatment consisting of neoadjuvant chemoradiotherapy (CRT) and standardized surgical technique (total mesorectal excision) [1–3]. Response to neoadjuvant therapy is variable; 15–27% of patients will have a pathologic complete response (pCR) [4], whilst 25–45% will have a poor response with minimal tumour regression [5]. In patients with locally advanced rectal cancer undergoing CRT and surgery, 45% of patients will require permanent colostomy [6]. Accurate imaging for prediction and early assessment of response would enable appropriate stratification of management to reduce treatment morbidity and improve therapeutic outcomes. In patients with a clinical complete response to CRT, substitution of surgery by a 'watch-and-wait' approach has emerged as a management option [7–9]. Prediction of poor response could permit trials of dose escalation strategies or curtailment of futile treatment.

Functional magnetic resonance imaging (MRI) has shown promising results for prediction of CRT response in rectal cancer. Diffusion weighted imaging (DWI) has demonstrated greater potential compared with morphologic T2-weighted (T2-w) imaging for the assessment of therapeutic response in rectal cancer patients [10]. However, a systematic review by Joye et al. found that pre-CRT quantitative DWI alone was unable to predict pCR with sensitivity and specificity of 69% and 68%, respectively. Quantitative DWI post-CRT had sensitivity and specificity of 78–80% and 72–78%, respectively, for detecting pCR [11]. Some dynamic contrast enhanced (DCE) MRI studies have shown that higher contrast exchange rate pre-treatment, as indicated by higher K^{trans}, is associated with better response to CRT [12, 13]. One study did not find a correlation between pre-treatment K^{trans} and therapeutic response [14]. Use of either DWI or DCE alone currently lacks sufficient accuracy for clinical use to guide individualized treatment in rectal cancer.

Multi-parametric MRI combining DWI and DCE may have potential to improve the accuracy of therapeutic response prediction and assessment. Most published studies describe mean values of a region of interest (ROI) from either DWI or DCE. Single parameter measurements, such as mean apparent diffusion co-efficient (ADC) or K^{trans}, do not adequately reflect intra-tumour heterogeneity. A three-dimensional analysis of the tumour volume would provide information on tumour heterogeneity. Development and standardization of multi-parametric imaging protocols is required to provide robust serial imaging datasets and reliable quantitative assessment of treatment response.

Study hypothesis

Multi-parametric MRI, consisting of DWI and DCE, performed pre-, during- and post- neoadjuvant CRT is predictive of treatment outcome in locally advanced rectal cancer, with histopathology being the standard reference.

Methods/design

Study objectives

Primary objective

To prospectively evaluate pre-, during- and post-CRT multi-parametric MRI (DWI and DCE) at 3 Tesla for therapeutic response prediction in LARC. MRI biomarkers will be correlated with histopathology tumour regression grade (TRG).

Secondary objectives

1. To prospectively evaluate the role of DCE MRI for therapeutic response prediction and assessment in LARC.
2. To prospectively evaluate the role of DWI MRI (RESOLVE) for therapeutic response prediction and assessment in LARC.
3. To evaluate the different contributions of MRI and PET for therapeutic prediction and assessment in LARC.
4. To correlate MRI biomarkers with 2 year disease-free survival and overall survival.

Study design

The study design is a prospective, single-arm, cohort study to investigate the value of multi-parametric MRI (combining DWI and DCE) in the prediction and assessment of CRT response. Patients will receive standard treatment for their malignancy. This study does not involve a treatment intervention.

Study schematic

All patients will receive standard treatment consisting of neoadjuvant CRT followed by surgery, and have MRI and PET performed at three time-points (Fig. 1); pre-CRT, during-CRT (week 3 of CRT), and post-CRT (within 1 week prior to surgery).

Patient selection

Inclusion criteria

1. Age greater than 18
2. Stage II or III rectal adenocarcinoma, defined as T3 - T4 and/or node positive disease (N1–2), without distant metastatic disease (M0)
3. No evidence of metastatic disease on computed tomography (CT) chest/abdomen/pelvis
4. Undergoing treatment regimen consisting of neoadjuvant CRT (Radiotherapy 50.4Gy in 28 fractions delivered using 3D–conformal or VMAT

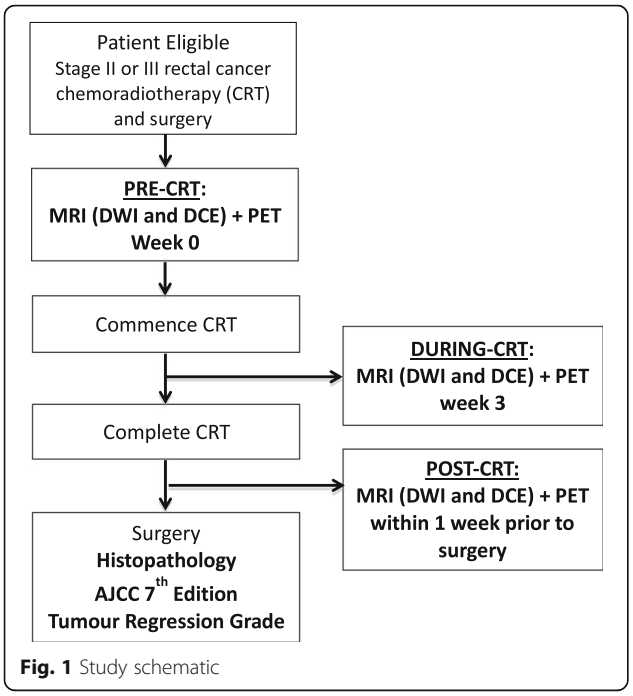

Fig. 1 Study schematic

technique concurrent with infusional 5-fluorouracil or oral capecitabine) followed by primary surgery.

Exclusion criteria

1. Other malignancy
2. Active inflammatory bowel disease
3. Contraindication to MRI:
    - Implanted ferromagnetic metal eg. Intraocular metal
    - Pacemaker/Implantable defibrillator
    - Extreme claustrophobia

Treatment

Patients are to undergo standard treatment, consisting of neo-adjuvant long course CRT (as detailed above) followed by surgery, as recommended by treating team. There will be no change to the patient's treatment from participating in this study.

Imaging study procedures

Timing of multi-parametric MRI and PET

1. Pre-CRT: week −2 to 0
2. During-CRT: Week 3 of CRT (early as possible during week 3)
3. Post-CRT: Post completion of CRT, within 1 week prior to surgery

MRI technique

All MRI scans will be acquired on the 3 Tesla Siemens Skyra (Magnetom, Erlangen, Germany) dedicated MRI-Simulator within the Radiation Oncology department. A 32-channel spine coil integrated in the patient table will be used in combination with an 18-channel phase array surface coil strapped firmly around the pelvis. Butylscopolamine (Buscopan) 20 mg will be administered intravenously prior to acquisition of functional sequences (DWI and DCE) to reduce rectal motion.

MRI safety screening

All patients will undergo MRI safety screening.

Screening of suitability for gadolinium-based MRI contrast

1. Require documentation of normal renal function within three months (eGFR > = 60 ml/min/1.73 m2
2. Contra-indications to use of gadolinium-based MRI contrast/DCE:
    1. Renal impairment eGFR <60 ml/min/1.73 m2
    2. Acute kidney injury
    3. Previous allergic reaction to gadolinium-based MRI contrast.

MRI sequences

T2-weighted turbo spin echo images - Acquired in 3 planes with 2 mm slice thickness and bandwidth 440 Hz/Px in 1 concatenation: (i) sagittal, (ii) axial oblique, angulated perpendicular to the long tumour axis, and (iii) axial. A T2-w HASTE sequence is additionally acquired in the coronal plane.

Diffusion weighted imaging (DWI)

- Readout segmented diffusion technique (RESOLVE)
- Axial orthogonal plane with b-values 50 and 800 s/mm^2, and 1 & 3 signal averages respectively.
- ADC maps and calculated b = 1400 mm/s^2 images produced as part of protocol.
- In-plane resolution of 1.1 × 1.1 mm and 4 mm slice thickness.

Dynamic contrast enhanced (DCE) imaging

- Pre-contrast T1-weighted VIBE scans with TR 4.09 ms, TE 1.35 ms, and flip angles 2° and 15° to calculate native T1.
- DCE acquired with time-resolved angiography with stochastic trajectories (TWIST) technique acquired over 60 phases, with a temporal resolution of 5.28 s, bandwidth 440 Hz/Px, TR 3.67 ms and TE 1.48 ms. Gadoversetamide (Optimark) 0.1 mM/kg injected after 3 phases acquired.

PET/CT technique

^{18}F–FDG PET/CT will be acquired on the GE Discovery-710 PET-CT. Patients need to fast for at least 4 h prior to 4.29 ± 0.34 (mean ± SD) MBq/kg ^{18}F -FDG injection and have blood glucose levels <10 mmol/L. All PET scans will be acquired in three-dimensional mode from the mid-brain to proximal femora with an acquisition time of 1.5–2.5 min per bed position, after an ^{18}F–FDG uptake time of 60 min. PET data will be reconstructed into a 256 × 256 matrix size with slice thickness of 3.3 mm using GE VUE Point FX (Time of Flight) algorithm. All PET/CT scans will be evaluated on the Advantage Workstation (GE Healthcare) using the AW VolumeShare 5 software and PET-VCAR (Volume Computer-Assisted Reading) protocol.

Clinical assessment and acute toxicity grading

1. Radiation Oncology clinical assessments and formal acute toxicity scoring will be performed at the following time points:
   a. Pre-CRT: Baseline assessment prior to commencement of treatment
   b. During-CRT: Weekly during radiotherapy treatment reviews
   c. Post-CRT: At 2 weeks post-completion of CRT, and within 1 week prior to surgery (ideally at time of post-CRT MRI).
2. Acute toxicity will be scored according to the 'Common Terminology Criteria for Adverse Events (CTCAE) Version 4.0.

Histopathology and tumour regression grade criteria

Histopathological assessment will be undertaken by a dedicated pathology team, with all reporting/TRG assessment by pathologists with sub-specialisation in gastrointestinal pathology. For the study it is a requirement that the whole of the original tumour site should be embedded for microscopic assessment.

MRI will be correlated with histopathological TRG using the modified classification of Ryan et al. [15] set out in the AJCC Cancer Staging Manual, 7th Edition as follows:

TRG 0 (complete response) – no viable cancer cells.

TRG 1 (moderate response) – single cells or small groups of cancer cells.

TRG 2 (minimal response) – residual cancer outgrown by fibrosis.

TRG 3 (poor response) – minimal or no tumour kill; extensive residual cancer.

Patients with TRG 0–1 will be categorized as 'good responders' and those with TRG 2–3 categorized as 'poor responders' to CRT.

Multi-parametric imaging analysis

A Radiation Oncologist with sub-specialization in gastrointestinal malignancies and a Radiologist with sub-specialization in pelvic MRI will perform all segmentations. K^{trans} maps will be produced by first pre-selecting an appropriate arterial input function, scaled by dose, based on chi-squared goodness of fit, and using a two-compartment Tofts model [16]. ADC and K^{trans} parameter maps will be exported in DICOM format and registered to T2-w axial images.

The region of interest for analysis will be defined on the entire hyper-intense primary tumour on the b-value 1400 mm/s s^2 images. A voxel-by-voxel technique will be used to produce colour-coded maps and histograms of ADC and K^{trans}, and combined scatterplots for each time-point.

Statistical considerations

A target of 35 patients will be recruited; this is estimated to take 24 months. For estimated pCR rate of 25%, 35 patients will provide 80% power to detect an AUC ≥ 80%. Poor responders rate is estimated to be in the range of 25–45% [5]. For estimated poor responder rate of 25%, 35 patients will provide 80% power to detect an AUC ≥ 80%. For estimated poor responder rate of 45%, 35 patients will provide 80% power to detect an AUC ≥ 76%.

Univariate analysis will be performed to investigate the association between each MRI parameter and tumour regression grade (AJCC 7th edition). Each MRI parameter will be correlated with pathologic complete responders (pCR - TRG 0) using a 2 × 2 Table. A similar analysis will be performed for good responders (TRG0–1) vs. poor responders (TRG 2–3). Receiver operator characteristics curves will be used to obtain an optimal threshold for each MRI parameter (ADC and K^{trans}).

Multivariate analysis will be performed to investigate the association between multi-parametric MRI and tumour regression grade. The multi-parametric MRI parameters that will be used for multivariate analysis are ADC and K^{trans}.

Discussion

MRI offers a variety of functional parameters, with each parameter offering information on various biological aspects of tumour. Multi-parametric image analysis has become increasingly relevant in cancer therapy response predication, as analysis of multiple parameters can provide a more complete physiological assessment of tumour [17]. The rectum is a particularly challenging anatomy to image and provide robust functional datasets that can be examined in a serial manner. In order to provide reliable quantitative assessment of treatment response, it is important to have a standardized protocol that minimizes organ motion and provides robust serial image datasets. This study protocol describes standardized imaging procedures combining DWI and DCE, and a 3D voxel-wise multi-

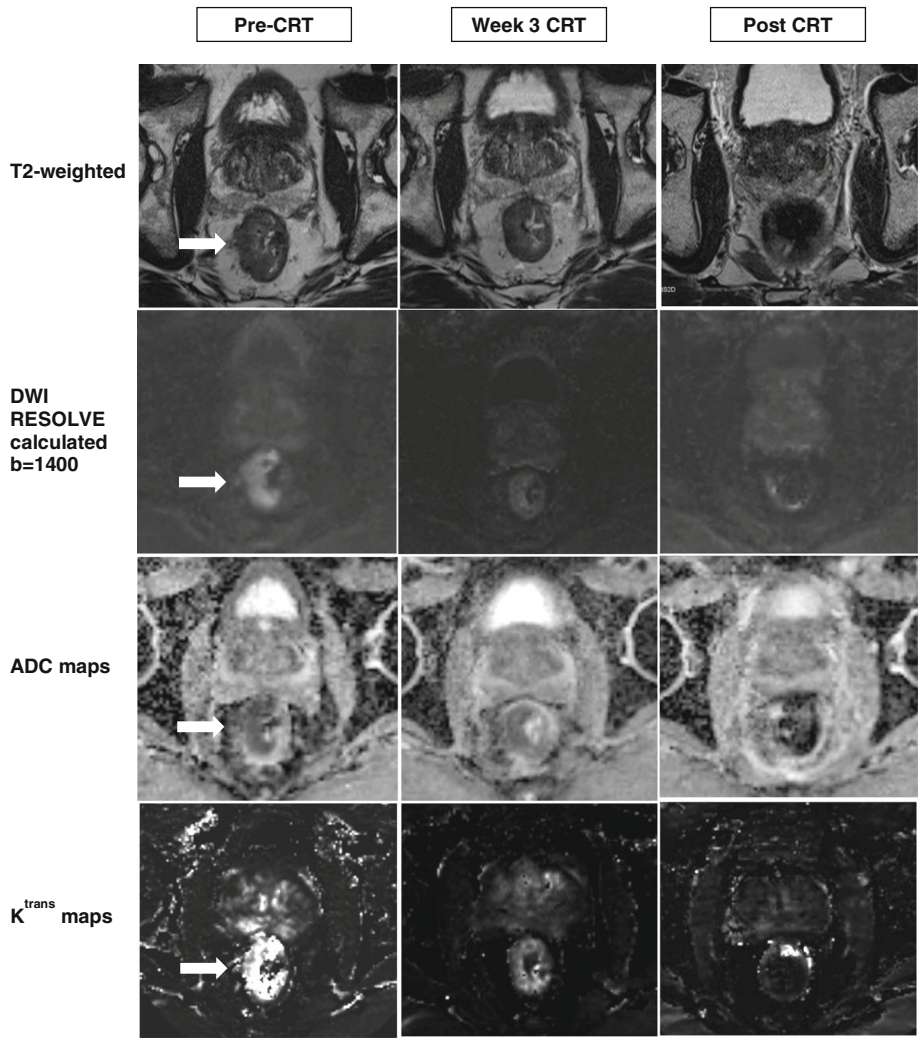

Fig. 2 MRI images and functional parameter maps produced as per study protocol. Images for a patient with good response to chemoradiotherapy (CRT) with histopathology tumour regression grade 1 (AJCC 7th Edition). The rectal tumour is indicated by the arrow. In the T2-weighted week 3 image, it was difficult to distinguish residual tumour deposits within areas of radiation-induced necrosis. Early tumour response to therapy can be seen in the functional sequences. In the DWI-RESOLVE images, there was a reduction in tumour signal enhancement in week 3. The calculated b = 1400 mm/s2 images demonstrated increased signal intensity in tumour relative to surrounding normal tissues. Ktrans maps were produced in Siemens Tissue 4D and a reduction in K^{trans} was seen in week 3

parametric analysis strategy for the assessment of tumour heterogeneity, and prediction of response to CRT in rectal cancer. Both DWI and DCE techniques in this protocol have improvements compared to previously used techniques. The DWI RESOLVE sequence used in this study protocol has previously been shown to be more robust with respect to geometrical distortions, compared to DWI standard echo planar images [18]. The calculated b = 1400 mm/s^2 images gains from both extra sensitivity and reduced noise of a calculated high b-value. The short temporal resolution of 5.28 s in DCE-TWIST will enable adequate sampling of the rapid wash-in of contrast into tumour. For acquisition of DCE images, the administration of butylscopolamine is crucial in eliminating rectal motion and ensuring accurate signal intensity for each pixel over the 60 time-points. Figure 2 shows examples of the good quality functional images with minimal distortion and corresponding parameter maps that are able to be acquired with this study protocol.

If validated, multi-parametric MRI combining DWI and DCE can be used to stratify management in rectal cancer patients. Accurate imaging prediction of patients with a complete response to CRT would enable a 'wait and watch' approach, avoiding surgical morbidity in these patients. Consistent and reliable quantitation from standardized protocols is essential in order to establish optimal thresholds of ADC and K^{trans} and permit the role of multi-parametric MRI for early treatment prediction to be properly evaluated.

Abbreviations
ADC: Apparent diffusion co-efficient; CRT: Chemoradiotherapy; CT: Computed tomography; DCE: Dynamic contrast enhanced; DWI: Diffusion weighted imaging; LARC: Locally advanced rectal cancer; MRI: Magnetic resonance imaging; pCR: Pathologic complete response; RESOLVE: Read-out segmented sequence; ROI: Region of interest; T2-W: T2-weighted; TRG: Tumour regression grade; TWIST: Time-resolved angiography with stochastic trajectories

Acknowledgments
Not applicable.

Funding
This study has been funded by the Royal Australian and New Zealand College of Radiologists (RANZCR) with a Withers and Peters $25,000 competitive research grant. RANZCR was not involved in the design of this study protocol and will not be involved in data collection or analysis.

Availability of data and materials
Not applicable.

Authors' contributions
All authors participated in the design and write-up of this study protocol. All authors contributed to, read and approved the final manuscript. TP is the principal investigator of the study, participated in all components of the study design and wrote the study protocol. TP, KW, MLee and MBB conceived the study idea, and contributed to the study design and protocol. TP, GL, RR, DM, and MLin participated in the design of the imaging protocol. CH and JSS participated in the design of the histopathology protocol.

Ethics approval and consent to participate
This study and associated patient information sheets have been approved by the South Western Sydney Local Health District Human Research and Ethics Committee (HREC). Reference HREC/13/LPOOL/158, local project number 13/097a, 13/097b, 13/097c, Sub-study Rectal Cancer. All patients provide written informed consent prior to any study-related procedures.

Consent for publication
All images have been de-identified. Written informed consent was obtained from all patients participating in this study for the publication of de-identified images and data.

Competing interests
The authors declare that they have no competing interests.

Author details
[1]Department of Radiation Oncology, Liverpool Cancer Therapy Centre, Liverpool Hospital, South Western Sydney Local Health District, Sydney, Australia. [2]Sydney West Radiation Oncology Network, Westmead, Blacktown and Nepean Hospitals, Sydney, Australia. [3]Faculty of Medicine, University of New South Wales, Sydney, Australia. [4]Ingham Institute for Applied Medical Research, Sydney, Australia. [5]Department of Radiology, Prince of Wales Hospital, Sydney, Australia. [6]Department of Anatomical Pathology, Liverpool Hospital, Sydney, Australia. [7]School of Medicine, Western Sydney University, Sydney, Australia. [8]Department of Nuclear Medicine, Liverpool Hospital, Sydney, Australia. [9]Faculty of Radiation and Medical Physics, University of Wollongong, Sydney, Australia.

Received: 22 January 2017 Accepted: 26 June 2017
Published online: 04 July 2017

References
1. Sauer R, Liersch T, Merkel S, Fietkau R, Hohenberger W, Hess C, Becker H, Raab HR, Villanueva MT, Witzigmann H, et al. Preoperative versus postoperative chemoradiotherapy for locally advanced rectal cancer: results of the German CAO/ARO/AIO-94 randomized phase III trial after a median follow-up of 11 years. J Clin Oncol. 2012;30(16):1926–33.
2. National Comprehensive Cancer Network (NNCN): NCCN Clinical Practice Guidelines in Oncology Rectal Cancer Version 3.2015. 2015.
3. National Institute for Health and Care Excellence (NICE): Colorectal cancer the diagnosis and management of colorectal cancer. *NICE clinical guideline 131* 2014.
4. Maas M, Nelemans PJ, Valentini V, Das P, Rödel C, Kuo L-J, Calvo FA, García-Aguilar J, Glynne-Jones R, Haustermans K, et al. Long-term outcome in patients with a pathological complete response after chemoradiation for rectal cancer: a pooled analysis of individual patient data. Lancet Oncol. 2010;11(9):835–44.
5. Valentini V, Coco C, Cellini N, Picciocchi A, Fares MC, Rosetto ME, Mantini G, Morganti AG, Barbaro B, Cogliandolo S, et al. Ten years of preoperative chemoradiation for extraperitoneal T3 rectal cancer: acute toxicity, tumor response, and sphincter preservation in three consecutive studies. Int J Radiat Oncol Biol Phys. 2001;51(2):371–83.
6. McCarthy K, Pearson K, Fulton R, Hewitt J. Pre-operative chemoradiation for non-metastatic locally advanced rectal cancer. The Cochrane database of systematic reviews. 2012;12:CD008368.
7. Renehan AG, Malcomson L, Emsley R, Gollins S, Maw A, Myint AS, Rooney PS, Susnerwala S, Blower A, Saunders MP, et al. Watch-and-wait approach versus surgical resection after chemoradiotherapy for patients with rectal cancer (the OnCoRe project): a propensity-score matched cohort analysis. Lancet Oncol.
8. Maas M, Beets-Tan RG, Lambregts DM, Lammering G, Nelemans PJ, Engelen SM, van Dam RM, Jansen RL, Sosef M, Leijtens JW, et al. Wait-and-see policy for clinical complete responders after chemoradiation for rectal cancer. J Clin Oncol. 2011;29(35):4633–40.
9. Habr-Gama A, Perez RO, São Julião GP, Proscurshim I, Gama-Rodrigues J. Nonoperative approaches to rectal cancer: a critical evaluation. Semin Radiat Oncol. 2011;21(3):234–9.
10. van der Paardt MP, Zagers MB, Beets-Tan RGH, Stoker J, Bipat S. Patients who undergo preoperative Chemoradiotherapy for locally advanced rectal cancer restaged by using diagnostic MR imaging: a systematic review and meta-analysis. Radiology. 2013;269(1):101–12.
11. Joye I, Deroose CM, Vandecaveye V, Haustermans K. The role of diffusion-weighted MRI and (18)F-FDG PET/CT in the prediction of pathologic complete response after radiochemotherapy for rectal cancer: a systematic review. Radiother Oncol. 2014;113(2):158–65.
12. Intven M, Reerink O, Philippens ME. Dynamic contrast enhanced MR imaging for rectal cancer response assessment after neo-adjuvant chemoradiation. J Magn Reson Imaging. 2015;41(6):1646–53.
13. George M, Dzik-Jurasz A, Padhani A, Brown G, Tait D, Eccles S, Swift R. Non-invasive methods of assessing angiogenesis and their value in predicting response to treatment in colorectal cancer. Br J Surg. 2001;88(12):1628–36.
14. Lim JS, Kim D, Baek SE, Myoung S, Choi J, Shin SJ, Kim MJ, Kim NK, Suh J, Kim KW, et al. Perfusion MRI for the prediction of treatment response after preoperative chemoradiotherapy in locally advanced rectal cancer. Eur Radiol. 2012;22(8):1693–700.
15. Ryan R, Gibbons D, Hyland J. Pathological response following long course neoadjuvant chemoradiotherapy for locally advanced rectal cancer. Histopathology. 2005;47:141–6.
16. Tofts PS, Brix G, Buckley DL, Evelhoch JL, Henderson E, Knopp MV, Larsson HB, Lee TY, Mayr NA, Parker GJ, et al. Estimating kinetic parameters from dynamic contrast-enhanced T(1)-weighted MRI of a diffusable tracer: standardized quantities and symbols. J Magn Reson Imaging. 1999;10(3):223–32.
17. Yankeelov T, Pickens D, Price R (eds.): Quantitative MRI in Cancer (Imaging in Medical Diagnosis and Therapy). Boca Raton, FL 33487–2742: CRC Press Taylor & Francis Group; 2012.
18. Liney GP, Holloway L, Harthi TMA, Sidhom M, Moses D, Juresic E, Rai R, Manton DJ. Quantitative evaluation of diffusion-weighted imaging techniques for the purposes of radiotherapy planning in the prostate. Br J Radiol. 2015;88(1049):20150034.

Chapter 4 Results and discussion (clinical study): Multi-parametric MRI for radiotherapy response prediction in locally advanced rectal cancer

4.1 Patients

A total of 39 patients were recruited to this study. The baseline characteristics are shown in Table 4.1. Of 39 patients, 6 had Stage IIA, 1 had Stage IIIA, 25 had Stage IIIB, and 7 patients had Stage IIIC disease at diagnosis. All patients completed neoadjuvant chemoradiotherapy (CRT). Two patients did not proceed to surgery due to patient refusal; of these patients 1 was lost to follow-up and excluded from analysis. All 39 patients had MRI before CRT, 37 patients had MRI during CRT, and 32 patients had MRI after CRT (before surgery). Of the 39 patients, 2 patients underwent DWI-MRI only and were unable to undergo DCE-MRI due to renal impairment and contraindication to gadolinium-based MRI contrast. Three DCE-MRIs at a single time-point had poor image quality due to incorrect timing of administration of gadolinium contrast (n = 1), marked rectal peristalsis (n = 1) or unanalysable images (n = 1) and were excluded from analysis. Five patients had mucinous histopathology and were analysed separately, leaving 33 patients for the main analysis.

Table 4.1 Patient baseline characteristics

Characteristic		Number (%)
Age	30 - 39	1 (2.6%)
	40 – 49	1 (2.6%)
	50 – 59	15 (38%)
	60 – 69	11 (28%)
	70 – 79	7 (17.9%)
	80 – 89	4 (10%)
Sex	Male	32 (82%)
	Female	7 (18%)
Clinical T Stage	T2	3 (7%)
	T3	32 (82%)
	T4	4 (10%)
Clinical N Stage	N0	6 (15.4%)
	N1	13 (33.3%)
	N2	20 (51.3%)
Stage	IIA	6 (15.4%)
	IIIA	1 (2.6%)
	IIIB	25 (64.1%)
	IIIC	7 (17.9%)
Total patients		39

4.2 Histopathology

Thirty-three patients with non-mucinous adenocarcinoma were included in this analysis. Three patients had a pathologic complete response (pCR) tumour regression grade (TRG) 0 (7.7%), 12 had TRG 1 (30.8%), 14 had TRG 2 (35.9%), and 3 had TRG 3 (7.7%). One patient (2.6%) who refused surgery had a clinical complete response on colonoscopy and biopsy performed at 18 months, which was considered as a surrogate endpoint for pCR and therefore classified as TRG 0. Sixteen patients were classified as responders (TRG 0 – 1), and 17 patients were classified as non-responders (TRG 2 – 3). Five patients with mucinous adenocarcinoma were analysed separately; of these 2 had TRG 1, 2 had TRG 2, and 1 had TRG 3.

One patient (2.6%) who refused surgery and was lost to follow-up did not have response status information, and was excluded from analysis. Further details on histopathology results for the 37 patients who underwent surgery are shown in Table 4.2.

Table 4.2 Histopathology results for patients who had surgery (n=37)

Histopathology characteristic		Number
Tumour regression grade	TRG 0	3
	TRG 1	14
	TRG 2	16
	TRG 3	4
Histologic subtype	Adenocarcinoma	26
	Not assessable due to pCR (adenocarcinoma confirmed on biopsy)	4
	Other	3
	Mucinous adenocarcinoma	5
Pathologic tumour stage	ypT0	4
	ypT1	2
	ypT2	7
	ypT3	22
	ypT4	2
Pathologic nodal stage	ypN0	28
	ypN1	9
	ypN2	1
Tumour grade	Low	30
	High	2
	Not assessable (including pCR)	5
Surgery type	APR	10
	Low / ultra-low anterior resection	27
Tumour in bowel wall at line of resection	No	37
	Yes	0

Histopathology characteristic		Number
Tumour at circumferential line of resection	No	33
	Yes	4
Vascular invasion	No	31
	Mural	1
	Extramural	5
Perineural invasion	No	33
	Yes	4

4.3 Optimisation of MRI protocol

A comprehensive protocol and analysis strategy using quantitative DWI-MRI and DCE-MRI in combination for multi-parametric, voxel-wise prediction of response to CRT in rectal cancer was developed. This protocol allowed for 3-dimensional characterisation of functional changes in tumour in response to CRT. The protocol was optimised based on review of image quality for the initial patients on the study.

A number of patient factors were found to affect the quality of MR images, and therefore accuracy of results. Rectal peristalsis and patient motion between sequences were found to affect the accuracy of the T1 map and DCE signal intensity – time relationship for each pixel. One of the initial patient DCE-MRI datasets had to be excluded from analysis due to marked rectal peristalsis during the dynamic scan (Figure 4.1). The optimised MRI protocol included the administration of butylscopolamine (Buscopan) 20mg intravenously prior to acquisition of functional MRI sequences. The administration of butylscopolamine was crucial in eliminating rectal motion and ensuring accurate signal intensity for each pixel over the 60 time-points in the dynamic imaging (Figure 4.2). In addition, patients were allowed to empty bladder and bowel immediately prior to the scan to ensure patient comfort and minimal motion during the scan. The 18 channel phase array coil was placed firmly around the pelvis and strapped to ensure good compression and reduction in abdominal movement with respiration.

For DCE analysis, rigid body registration of pre-contrast flip angle sequences to dynamic images was required for cases with minor patient motion. Deformable registration was not found to be useful in this regard. The registration ensured more accurate voxel-by-voxel calculation of K^{trans}, and had to be performed outside of commercial software owing to its limitations. This provided better results than using the available deformable registration Tissue 4D (Siemens). Images were pre-registered using commercial 3D visualisation software (Siemens) (Figure 4.3). Subsequently, the registered images were exported off-line and using in-house code were reassigned a full DICOM header to enable these images to be analysed in Tissue 4D (Siemens). Tissue 4D was used to produce K^{trans} maps by first pre-selecting an appropriate arterial input function, scaled

by dose, based on chi-squared goodness of fit, and using a two-compartment Tofts model (Figure 4.4) (43). The results showed a rapid wash-in of contrast into tumour, which was adequately sampled with the short temporal resolution of 5.28 seconds in the DCE TWIST technique. ADC and K^{trans} parameter maps were exported in DICOM format and registered to T2-weighted orthogonal images for multi-parametric analysis in OncoTreat (works-in-progress, Siemens).

Figure 4.1 Dynamic contrast enhanced MRI and rectal peristalsis.

Pre-contrast imaging (a), contrast-enhanced image at time-point 36 with ROI (b) used for pre-selection of an appropriate arterial input function, scaled by dose, based on chi-squared goodness of fit, and signal-intensity – time plot for ROI1 (c). This patient had marked rectal peristalsis during the dynamic contrast-enhanced examination. This resulted in an irregular signal intensity curve due to signal intensity plotting for incorrect pixels due to rectal movement.

(a) (b) (c)

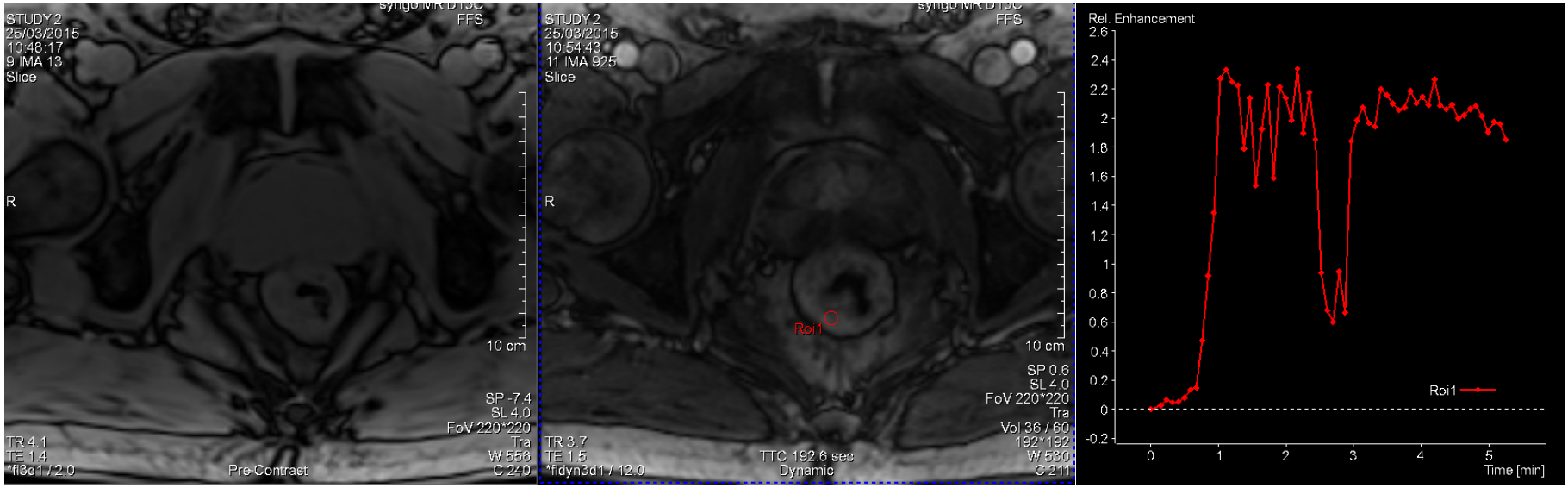

Figure 4.2 Dynamic contrast enhanced MRI with butylscopolamine.

Results of a patient who had butylscopolamine administered for the dynamic contrast-enhanced MRI. Pre-contrast imaging (a), contrast-enhanced image at time-point 35 with ROI used for pre-selection of an appropriate arterial input function, scaled by dose, based on chi-squared goodness of fit, and signal-intensity – time plot for ROI (c). Butylscopalamine resulted in a more accurate signal intensity – time plot and a better chi-squared goodness of fit as indicated in (c).

(a) (b) (c)

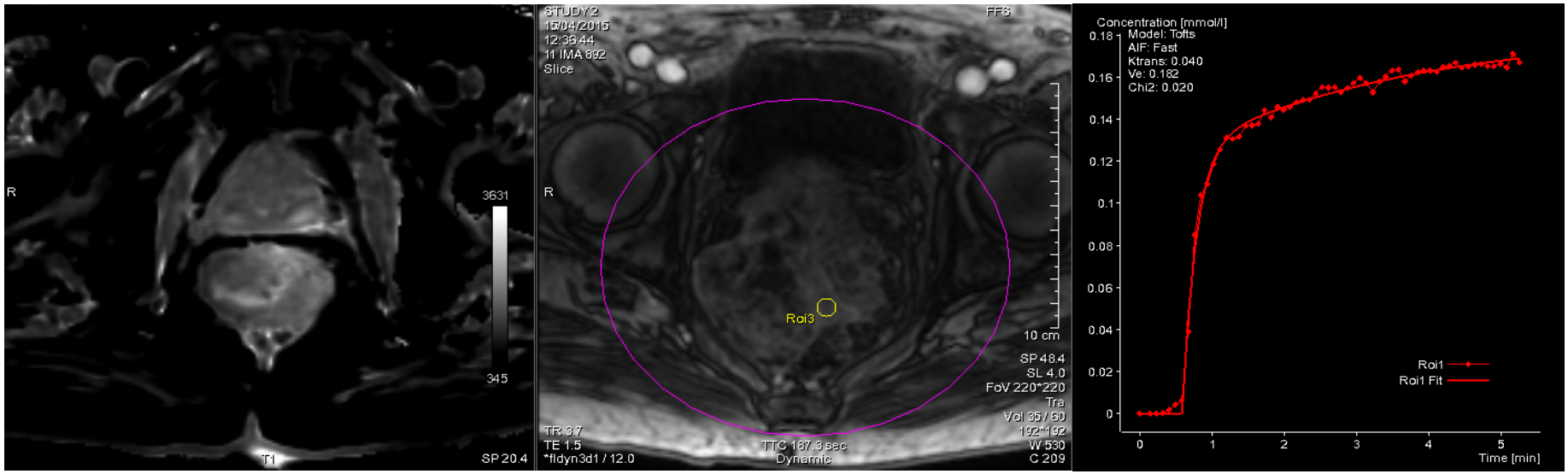

Figure 4.3 MRI registration

Registration was required in some cases due to patient motion between sequences. Rigid body registration of pre-contrast flip angle sequences to dynamic images was performed.

Unregistered **Registered**

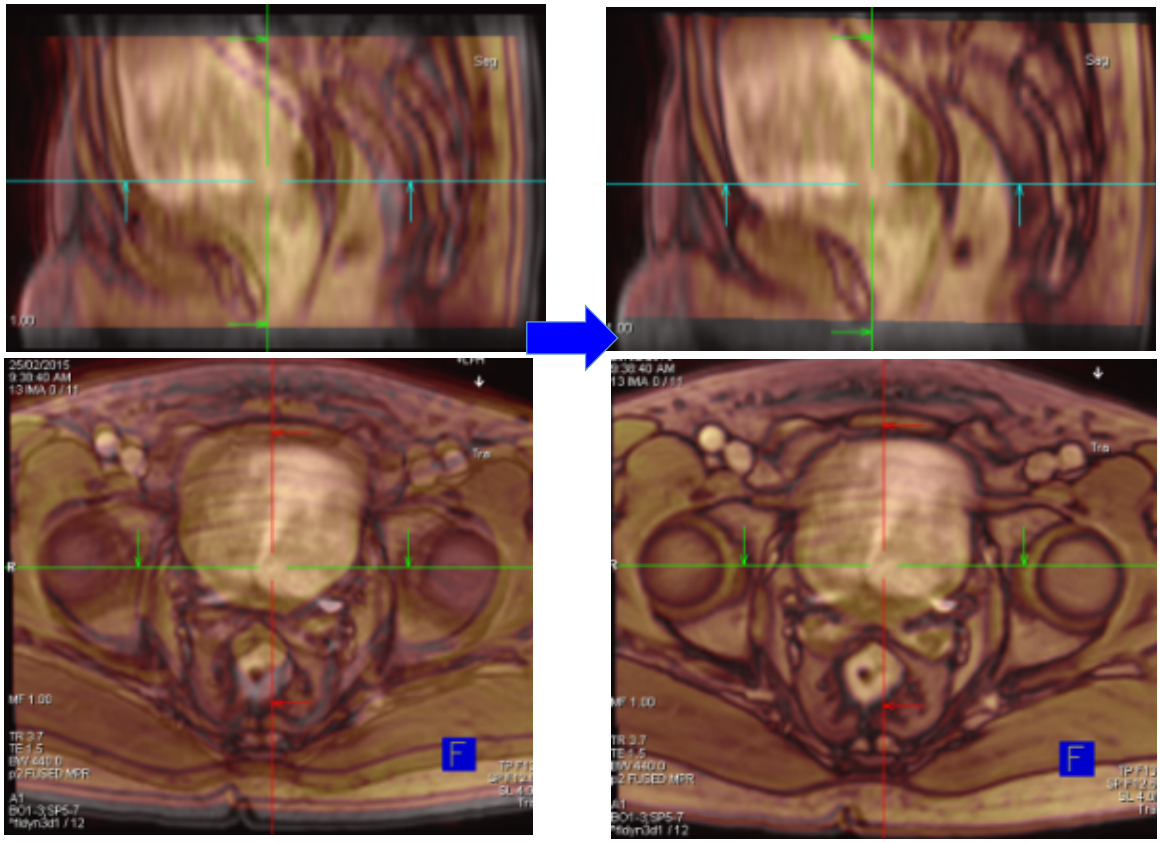

Figure 4.4 Dynamic contrast-enhanced MRI analysis strategy.

An example of one stage in the DCE-MRI analysis using Tissue 4D (Siemens).

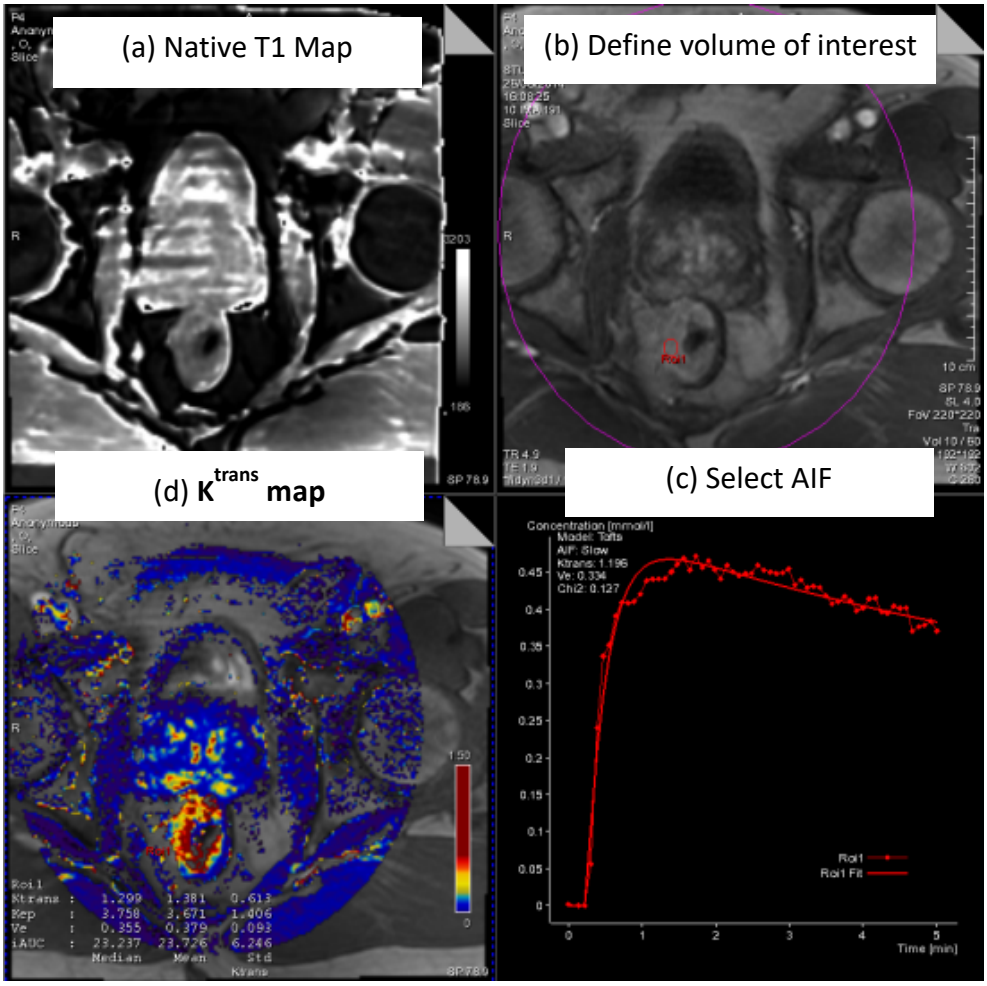

4.4 Representative multi-parametric MRI results produced in OncoTreat WIP for responders and non-responders to treatment

The two case examples described below demonstrate the robustness of the serial imaging datasets and feasibility of the multi-parametric quantitative analysis method developed in this study. Figure 4.5 shows the images of a patient with cT3N0M0 disease who had a pCR following CRT. In the T_2-weighted during CRT and after CRT images, tumour regression can be seen with a reduction in the size of tumour mass. However, it is difficult to distinguish residual tumour deposits within areas of radiation-induced necrosis and fibrosis on the T_2-weighted images alone. Tumour response to therapy was clearer in the DWI-RESOLVE images, with tumour signal enhancement decreasing over subsequent time-points. The calculated b = 1400 mm/s^2 images demonstrated increased signal intensity in tumour relative to surrounding normal tissues. Figure 4.6 and Figure 4.7 show the changes in ADC and K^{trans} histograms produced in OncoTreat (WIP, Siemens), respectively. The ADC histograms during CRT and after CRT demonstrated a shift in distribution of ADC of voxels to higher values. The K^{trans} histograms showed a shift in the distribution of K^{trans} to higher values during CRT, and a shift to lower values after CRT.

The MR images for a non-responder are shown in Figure 4.8. This patient had cT2N2M0 disease at diagnosis and histopathologic TRG 2. The changes in ADC and K^{trans} histograms produced in OncoTreat (WIP, Siemens) for this patient are shown in Figure 4.9 and Figure 4.10, respectively. The ADC histograms during CRT and after CRT also demonstrated a shift in distribution of ADC of voxels to higher values, however the magnitude of shift was not as great compared to the responder described above.

The corresponding multi-parametric scatterplots for each time-point for these patients are shown in Figure 4.11. The plots indicate the ADC and K^{trans} values for voxels within the whole segmented tumour. In the scatterplot after CRT for the responder, the majority of voxels had high ADC and low K^{trans} values. In contrast, in the scatterplots after CRT for the non-responder most voxels had medium ADC and high K^{trans}.

The histogram and scatterplots produced in OncoTreat (WIP, Siemens) contained erroneous data. In both ADC and K^{trans} voxel-wise data, some voxel values were erroneously repeated and these erroneous values were included in the OncoTreat histograms and scatterplots. For K^{trans} data, voxels with absent K^{trans} values were incorrectly assigned a value of 0 in OncoTreat WIP. The raw voxel-wise data was exported from OncoTreat WIP and cleaned for the analysis.

Figure 4.5 Multi-parametric MRI for a responder (pathologic complete response) (patient 31)

Multi-parametric MRI at 3 time-points for a patient with pCR AJCC TRG 0 to CRT (patient 31). The arrow indicates the rectal tumour.

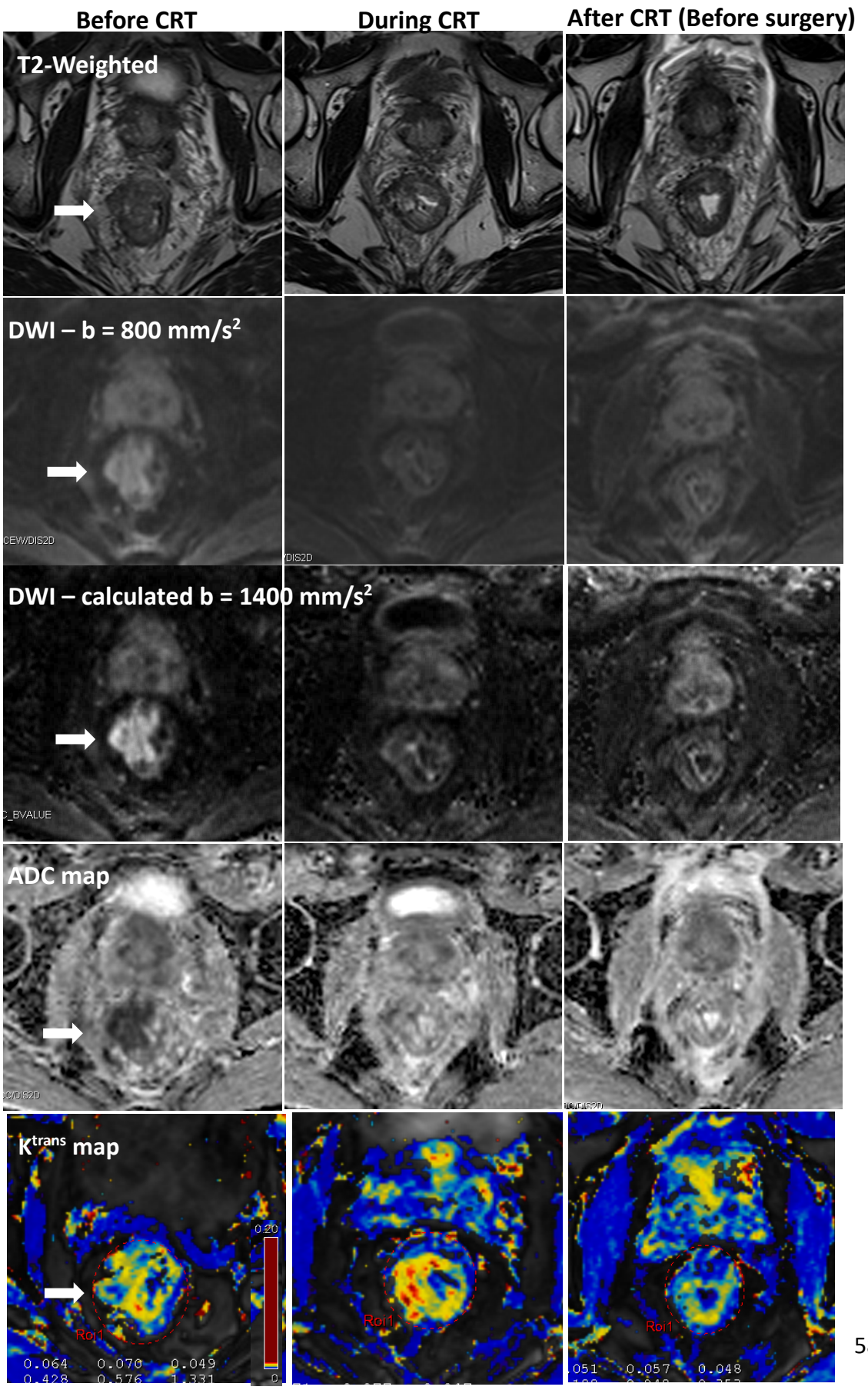

Figure 4.6 ADC colour-coded maps and voxel-by-voxel histograms for a responder (pathologic complete response) (Patient 31)

ADC maps and histograms for patient 31 (AJCC TRG 0) produced in OncoTreat WIP for the entire segmented region shown for before CRT (top panel), during CRT (middle panel) and after CRT (bottom panel). Blue voxels – ADC<1000x10^{-6} mm^2/s, green voxels – ADC 1000-1500x10^{-6} mm^2/s, red voxels – ADC >1500x10^{-6} mm^2/s.

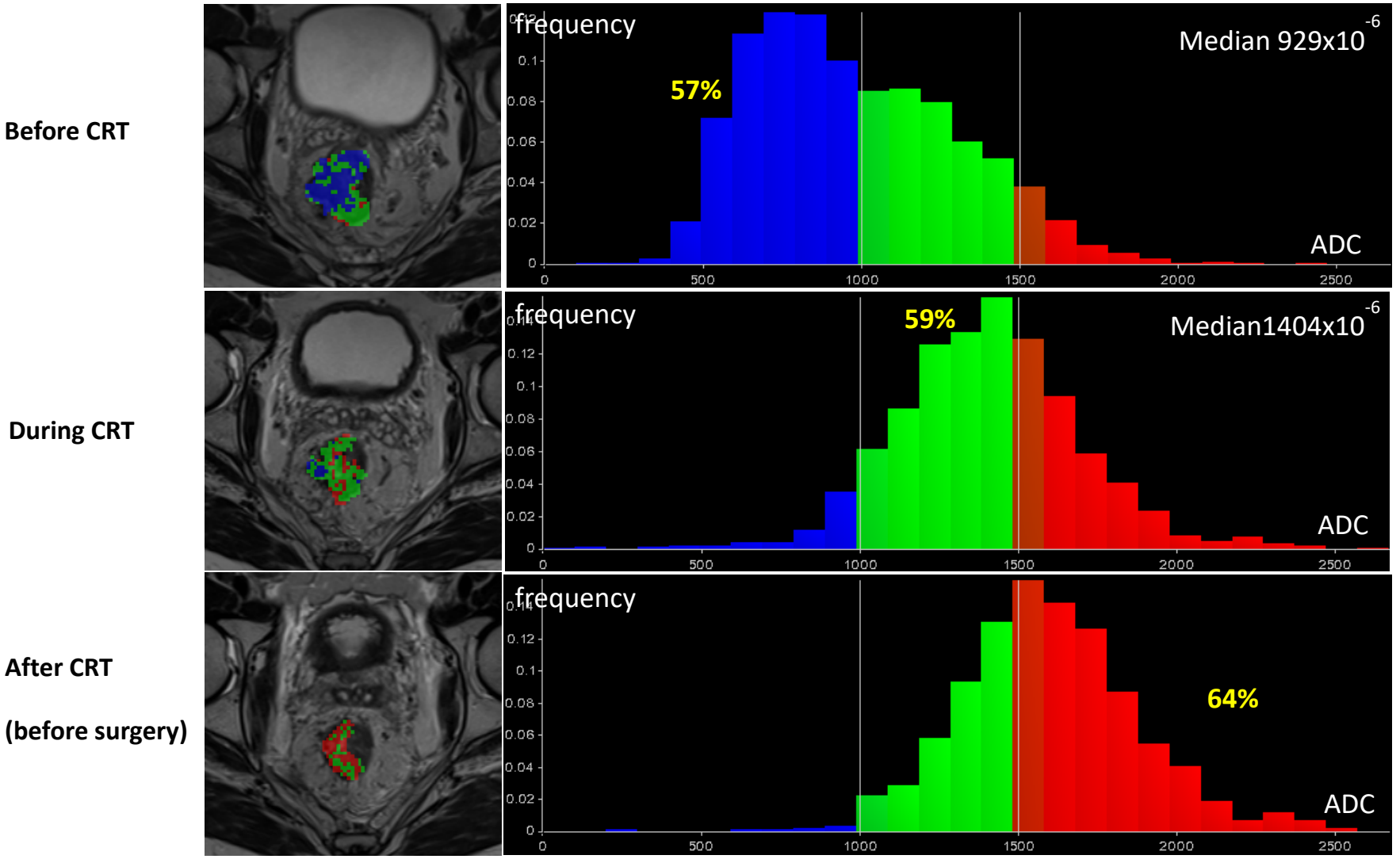

Figure 4.7 K^{trans} colour-coded maps and voxel-by-voxel histograms for a responder (pathologic complete response) (patient 31)

K^{trans} maps and histograms for patient 31 (AJCC TRG) produced in OncoTreat WIP for the entire segmented region shown for before CRT (top panel), during CRT (middle panel) and after CRT (bottom panel). Blue voxels – K^{trans} values < $100x10^{-3}$mL/g/min, green voxels K^{trans}100 - $500x10^{-3}$ mL/g/min.

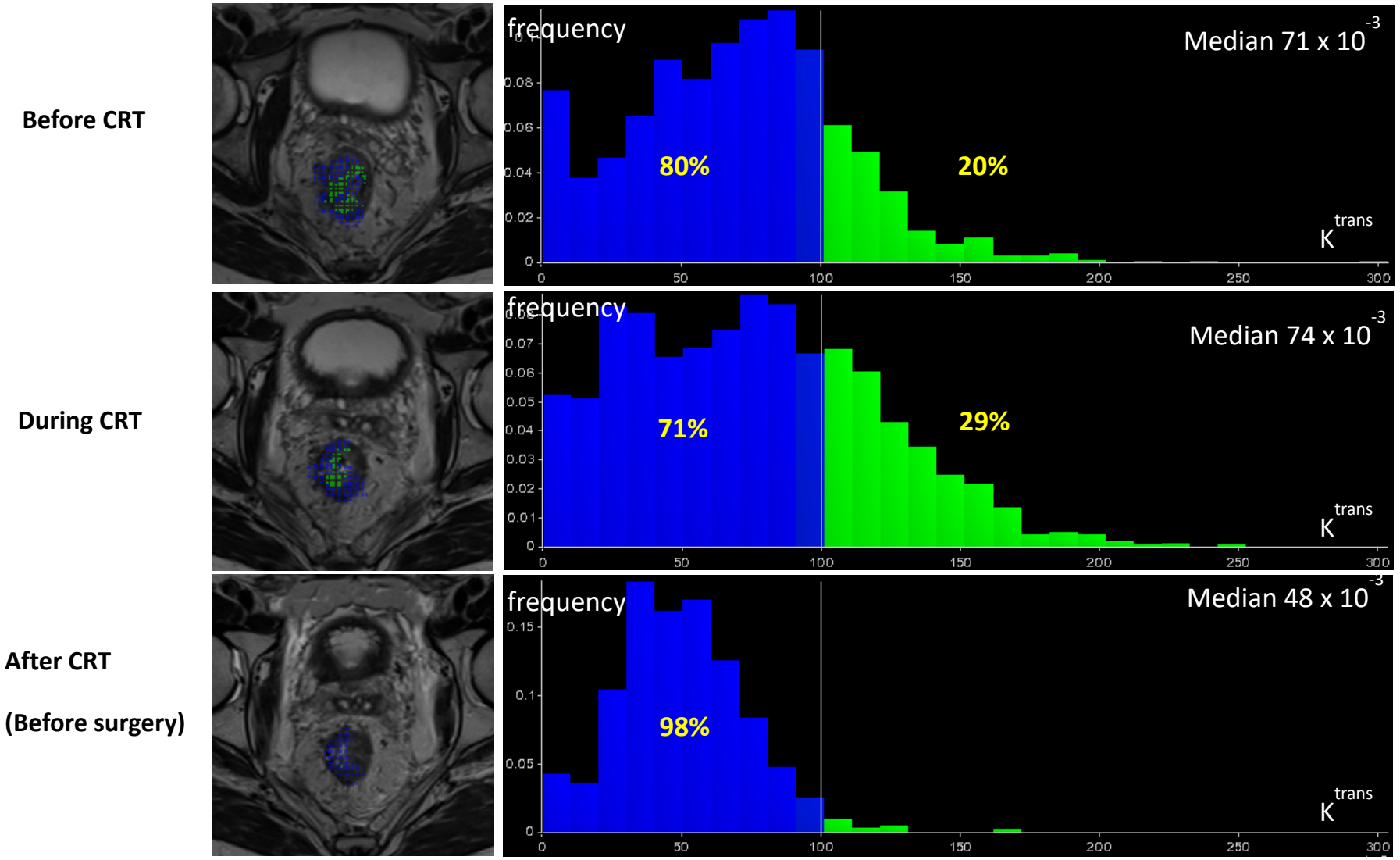

Figure 4.8 Multi-parametric MRI for a non-responder (patient 13)

MR images and functional parameter maps at 3 time-points for a non-responder (patient 13) to CRT with AJCC TRG 2. The rectal tumour is indicated by the arrow.

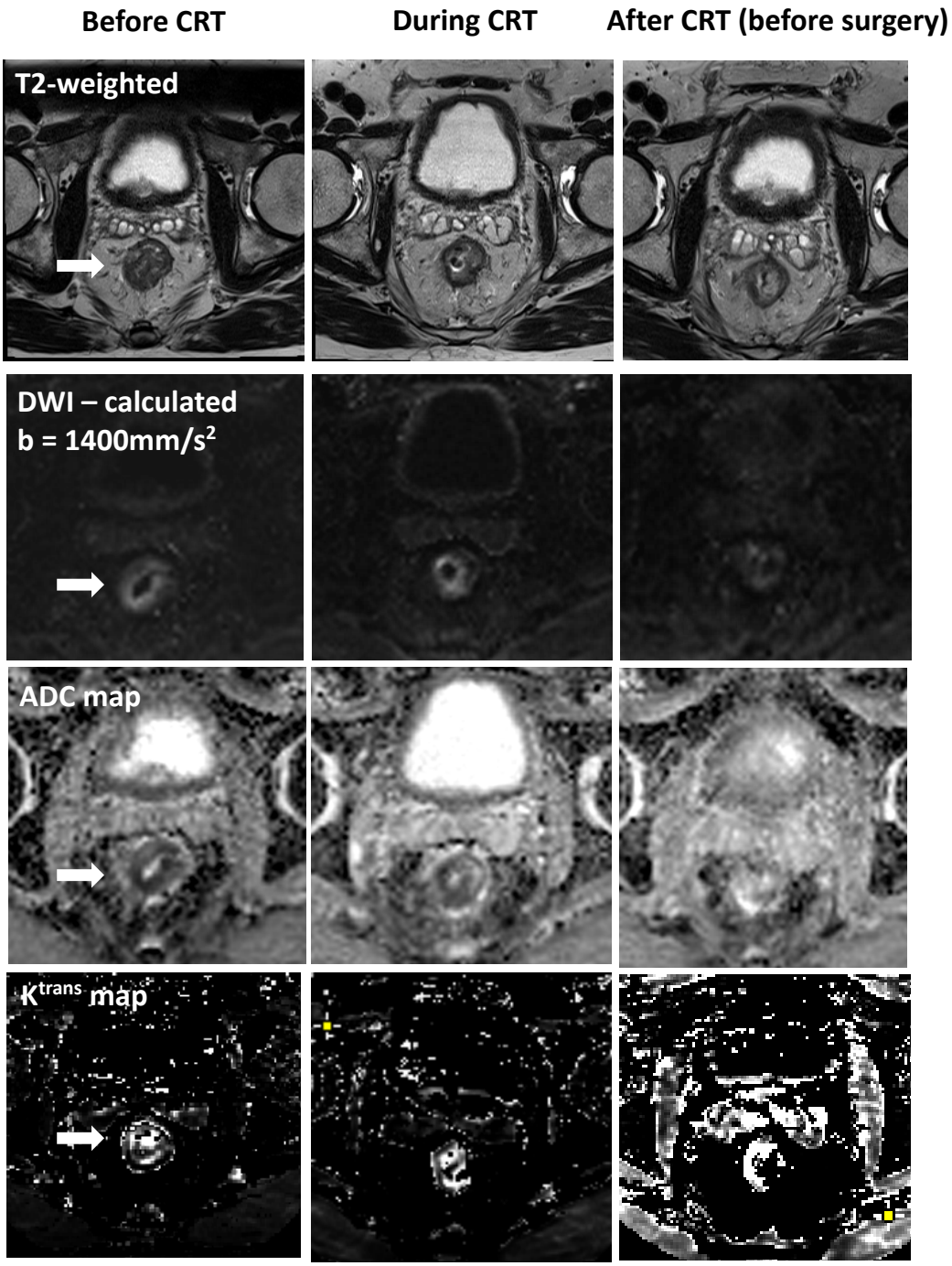

Figure 4.9 ADC colour-coded maps and voxel-by-voxel histograms for a non-responder (patient 13)

ADC maps and histograms for patient 13 (AJCC TRG 2) produced in OncoTreat WIP for the entire segmented region shown for before CRT (top panel), during CRT (middle panel) and after CRT (bottom panel). Blue voxels – ADC < $1000x10^{-6}$ mm^2/s, green voxels – ADC 1000 - $1500x10^{-6}$ mm^2/s, red voxels – ADC > $1500x10^{-6}$ mm^2/s

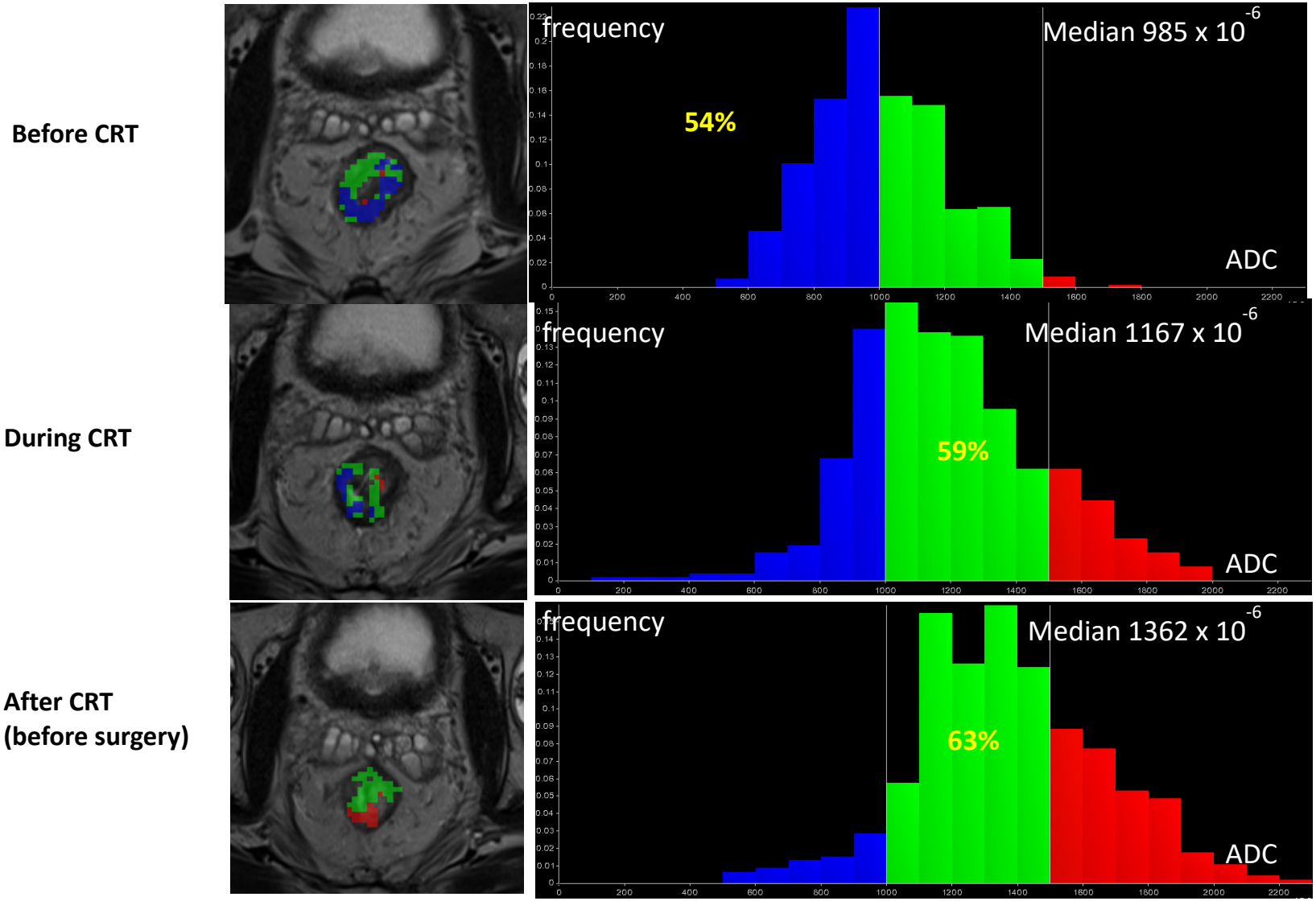

Figure 4.10 K^{trans} colour-coded maps and voxel-by-voxel histograms for a non- responder (patient 13)

K^{trans} maps and histograms for patient 13 (AJCC TRG 2) produced in OncoTreat WIP for the entire segmented region shown for before CRT (top panel), week 3 CRT (middle panel) and after CRT (bottom panel). Blue voxels – K^{trans} values < $100x10^{-3}$ mL/g/min, green voxels – K^{trans} 100 - $500x10^{-3}$ mL/g/min, red voxels – K^{trans} > $500x10^{-3}$ mL/g/min.

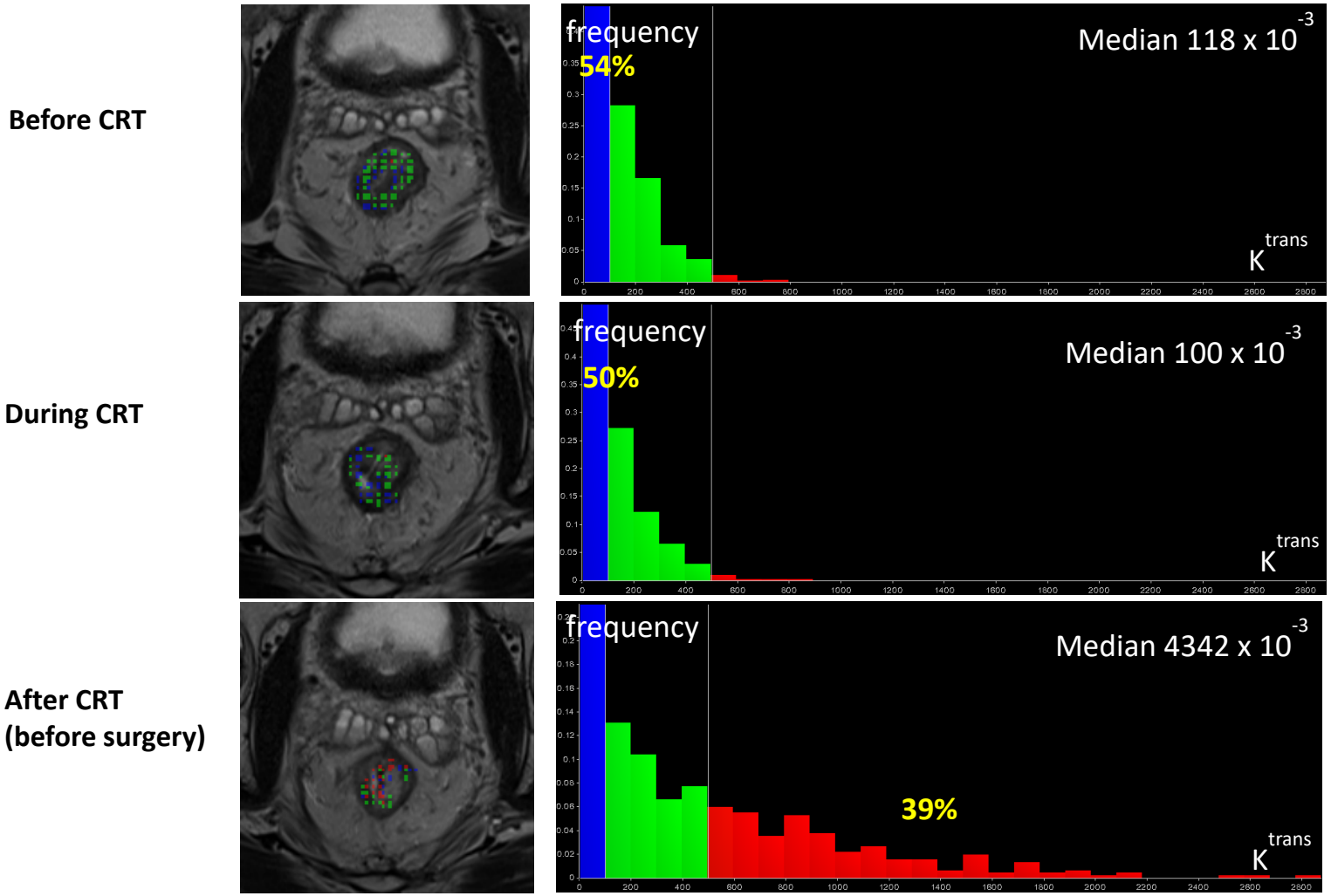

Figure 4.11 Multi-parametric scatterplots for a responder and non-responder produced in OncoTreat WIP

Top row – responder (pCR) (patient 31), bottom row – non-responder (patient 13)

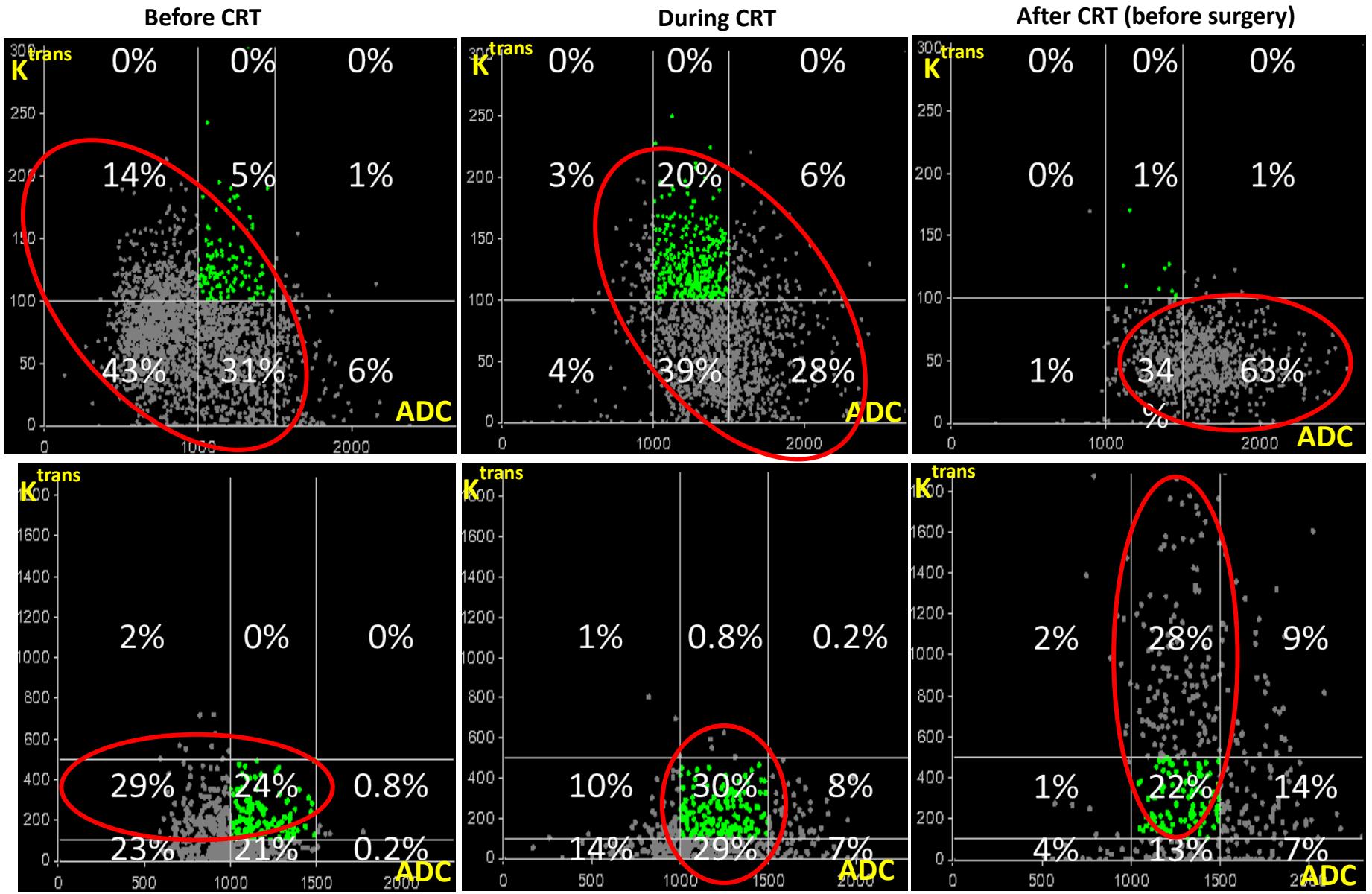

4.5 DWI and DCE-MRI histogram results for patients with non-mucinous adenocarcinoma

Histograms of ADC and K^{trans}

Histograms of the distribution ADC and K^{trans}, and combined ADC and K^{trans} scatterplots for each patient were produced. The cut-points for the distributions of ADC and K^{trans} were chosen from the 25^{th} (ADC 778 x 10^{-6}, K^{trans} 26 x 10^{-3}) and 75^{th} (ADC 1268 x 10^{-6}, K^{trans} 104 x 10^{-3}) percentiles from the overall results for all patients. The colours indicate the quartile cut-points (25^{th} and 75^{th}) for all patients; the blue bars indicate the lower quartile range, the green bars are range between the lower and upper quartile, and the red bars indicate the upper quartile range.

Representative MR images for a responder (patient 4) and non-responder (patient 26) are shown in Figure 4.12 and Figure 4.13 respectively, and the corresponding ADC and K^{trans} histograms, and multi-parametric scatterplots are shown in Figure 4.14 and Figure 4.15, respectively.

Figure 4.12 Multi-parametric MRI for a responder (patient 4 AJCC TRG 1)

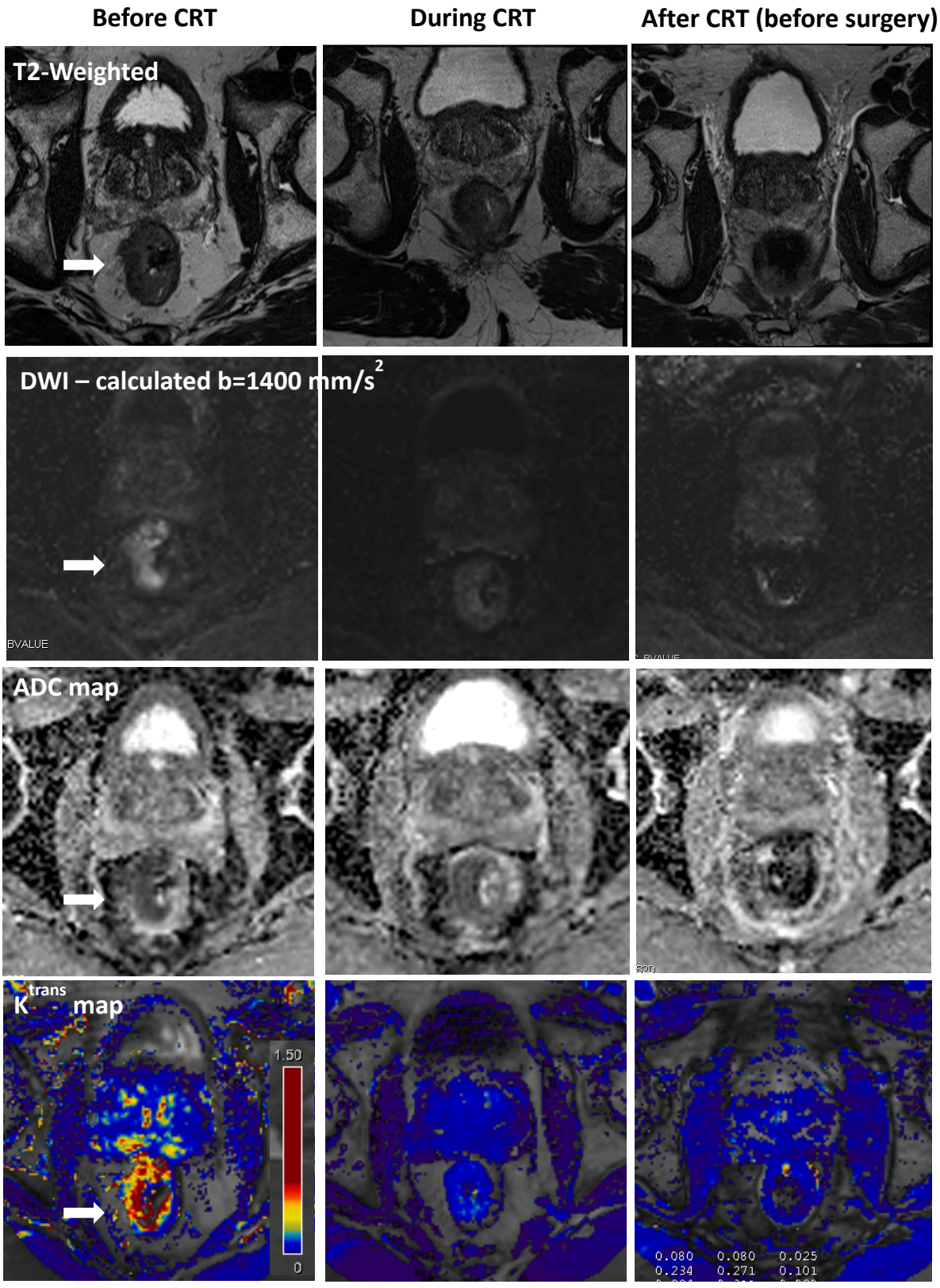

Figure 4.13 Multi-parametric MRI at 3 time-points for a non-responder (Patient 26 AJCC TRG 3)

The diffusion weighted images (row 2), and corresponding ADC maps (row 3) show persistent restricted diffusion during and after CRT. The K^{trans} map (row 4) shows an increase in tumour perfusion after CRT.

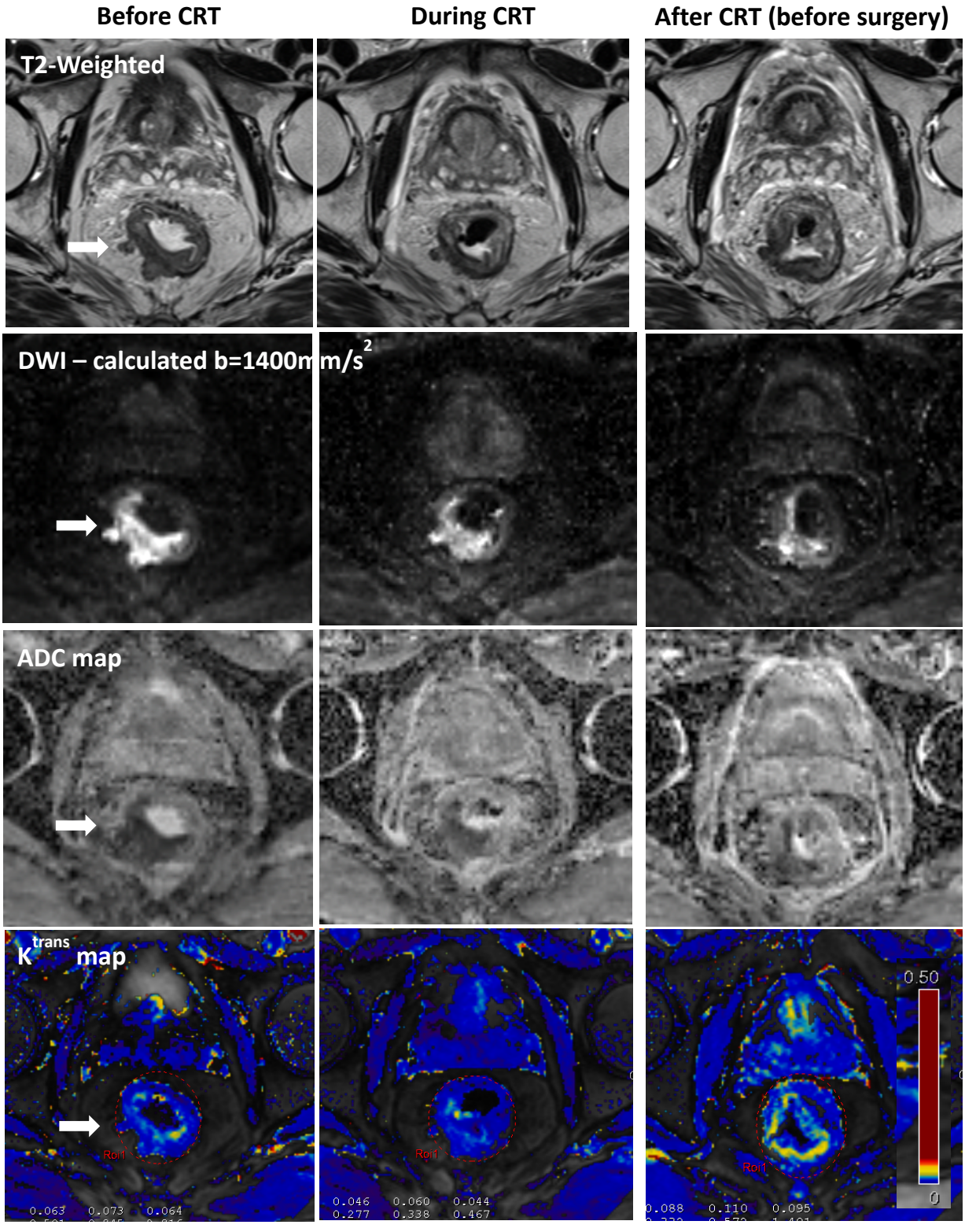

Figure 4.14 ADC and K^{trans} histograms for a responder (patient 4, AJCC TRG 1) a non-responder (patient 26 AJCC TRG 3)

The ADC histograms before CRT were more skewed to the right for the non-responder compared with the responder. This suggests freer diffusion before CRT for the non-responder which may be due to the presence of more necrotic tumour, a factor for radio-resistance, at baseline. The K^{trans} histograms after CRT were more skewed to the right for the non-responder compared to the responder, suggesting residual perfusion in the tumour bed for the non-responder.

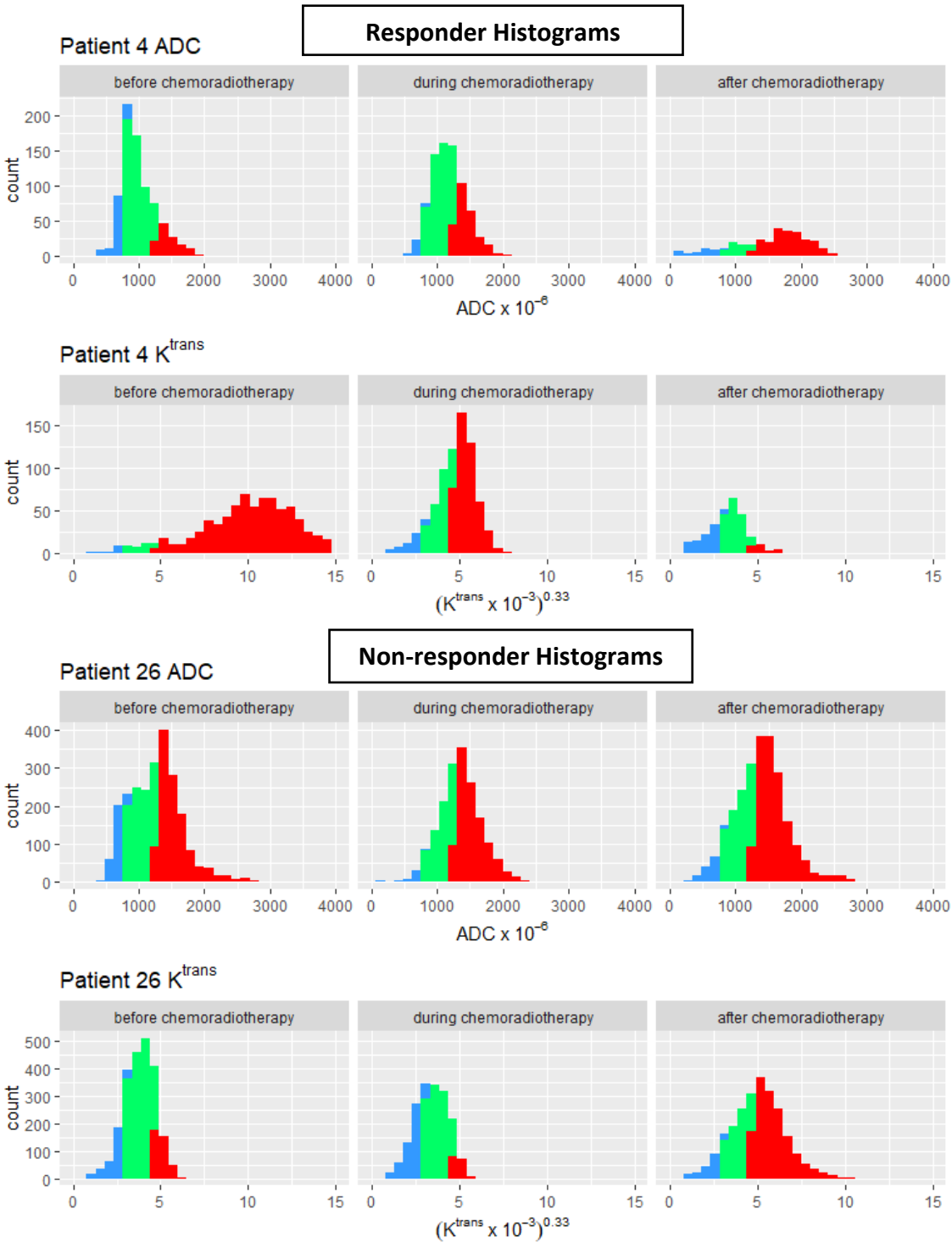

Figure 4.15 Multi-parametric scatterplots.

For the scatterplots combining ADC and K^{trans} for a responder and non-responder, red plots indicates before CRT, green indicates during CRT and blue indicates after CRT.

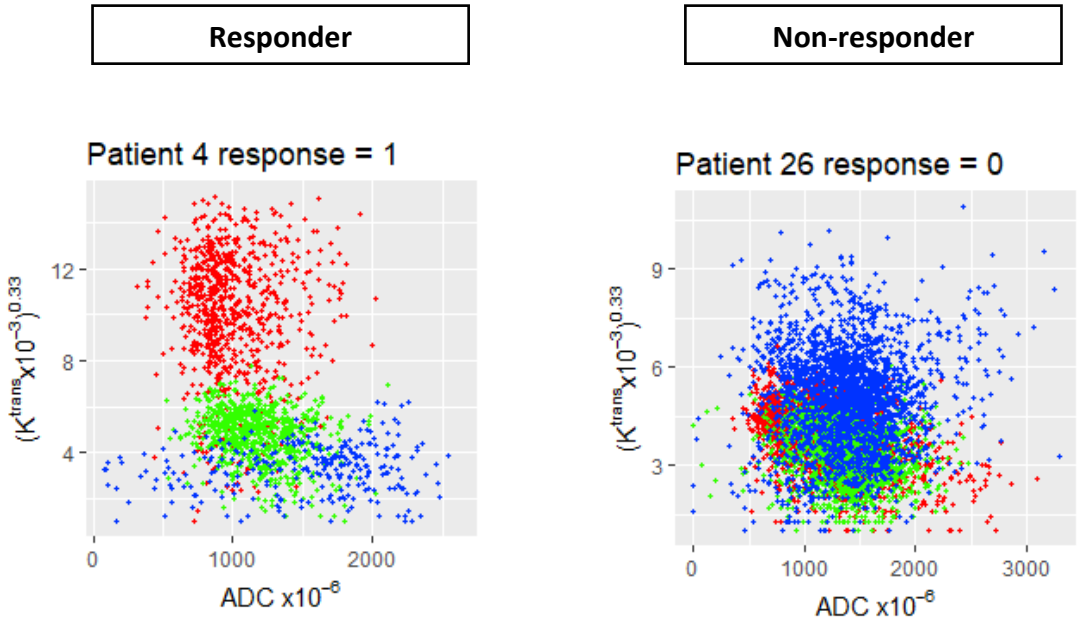

ADC and K^{trans} quantiles, kurtosis and skewness for all patients

The ADC quantile values by time-points for all patients are shown in Table 4.3. All ADC quantile values increased over the time-points in response to CRT. For all patients, there was a significant increase in ADC from before CRT to during CRT, and from before CRT to after CRT for the ADC 10^{th}, 25^{th}, 50^{th}, 75^{th}, and 90^{th} percentiles ($p < 0.001$). The K^{trans} quantile values by time-points for all patients are shown in Table 4.4. For all patients, the K^{trans} 10^{th}, 25th, 50^{th}, 75^{th} and 90^{th} quantiles increased from before CRT to during CRT, and from before CRT to after CRT, however this was not statistically significant ($p > 0.279$).

For all patients, the histograms showed the skewness of ADC was an approximately symmetric distribution that became more symmetric over time. For all patients, the change in skewness in ADC from before CRT to during CRT ($p=0.034$), and before CRT to after CRT ($p = 0.023$) were significant. K^{trans} had a highly skewed distribution at each time-point that decreased from before CRT to during CRT, and then remained stable after CRT. The change in K^{trans} skewness from before CRT to during CRT for all patients was statistically significant ($p = 0.041$).

ADC had small kurtosis, suggesting a distribution with shorter thinner tails, and a lower wider peak than a normal distribution. There were no significant changes in ADC kurtosis from baseline to during treatment, or from before CRT to after CRT. K^{trans} had substantial excess kurtosis implying a higher peak and much longer fatter tails than a normal distribution. K^{trans} kurtosis significantly decreased from baseline to during treatment for all patients (estimate -12.3, $p = 0.048$).

Table 4.3 Summary of ADC percentiles by time for all patients with non-mucinous adenocarcinoma

	10%	25%	50%	75%	90%	Skewness	Kurtosis
Before CRT	619 x 10^{-6}	778 x 10^{-6}	1000 x 10^{-6}	1268 x 10^{-6}	1513 x 10^{-6}	0.45	0.79
During CRT	824 x 10^{-6}	994 x 10^{-6}	1212 x 10^{-6}	1450 x 10^{-6}	1689 x 10^{-6}	0.36	0.78
After CRT	961 x 10^{-6}	1158 x 10^{-6}	1354 x 10^{-6}	1574 x 10^{-6}	1797 x 10^{-6}	0.08	1.1

Table 4.4 Summary of K^{trans} percentiles by time for all patients with non-mucinous adenocarcinoma

	10%	25%	50%	75%	90%	Skewness	Kurtosis
Before CRT	9 x 10^{-3}	26 x 10^{-3}	59 x 10^{-3}	104 x 10^{-3}	184 x 10^{-3}	6.3	53
During CRT	12 x 10^{-3}	30 x 10^{-3}	66 x 10^{-3}	130 x 10^{-3}	239 x 10^{-3}	5.5	36
After CRT	12 x 10^{-3}	33 x 10^{-3}	71 x 10^{-3}	143 x 10^{-3}	255 x 10^{-3}	5.5	49

4.6 Univariate Analysis

Correlation of ADC and K^{trans} quantiles, skewness and kurtosis with response status

Table 4.5 shows the summary of ADC quantiles by time-point and response status. Table 4.6 shows the summary of K^{trans} quantiles by time-point and response status.

ADC quantiles

The whole tumour ADC before CRT and during CRT 10^{th}, 25^{th}, 50^{th}, 75^{th} and 90^{th} and after CRT 10^{th}, 25^{th}, and 50^{th} percentiles were not statistically significantly different between responders and non-responders to CRT ($p > 0.080$) (Table 4.5). The ADC histograms after CRT (before surgery) 75^{th} (responders vs. non-responders $1620x10^{-6}$ vs. $1547x10^{-6}$, $p=0.036$) and 90^{th} percentiles (responders vs. non-responders $1859x10^{-6}$ vs $1753x10^{-6}$, $p=0.019$) were statistically significant for predicting response status.

K^{trans} quantiles

The before CRT, during CRT, and after CRT intra-tumour K^{trans} histogram 10^{th}, 25^{th}, 50^{th}, 75^{th} and 90^{th} percentiles (Table 4.6) were all lower in responders compared to non-responders, however this difference was not significant ($p > 0.103$).

Skewness and kurtosis

The skewness and kurtosis by time-point and responder status for ADC and K^{trans} are shown in Table 4.5 and Table 4.6. There was no statistically significant difference in ADC ($p > 0.141$) or K^{trans} ($p > 0.220$) skewness at any time-point between responders and non-responders. There was no significant difference in ADC ($p > 0.402$) or K^{trans} ($p > 0.504$) kurtosis between responders and non-responders at any time-point.

Table 4.5 Summary of ADC percentiles by time and response status for patients with non-mucinous adenocarcinoma

Time	Response status	10%	25%	50%	75%	90%	Skewness	Kurtosis
Before CRT	Responder	610×10^{-6}	758×10^{-6}	976×10^{-6}	1260×10^{-6}	1520×10^{-6}	0.57	0.692
	Non-responder	637×10^{-6}	810×10^{-6}	1035×10^{-6}	1278×10^{-6}	1504×10^{-6}	0.273	1.004
During CRT	Responder	816×10^{-6}	984×10^{-6}	1190×10^{-6}	1432×10^{-6}	1683×10^{-6}	0.489	1.052
	Non-responder	837×10^{-6}	1013×10^{-6}	1243×10^{-6}	1474×10^{-6}	1695×10^{-6}	0.159	0.391
After CRT	Responder	972×10^{-6}	1162×10^{-6}	1372×10^{-6}	1620×10^{-6}*	1859×10^{-6}*	0.023	1.004
	Non-responder	952×10^{-6}	1155×10^{-6}	1343×10^{-6}	1547×10^{-6}*	1753×10^{-6}*	0.095	1.156

*statistically significant $p < 0.05$

Table 4.6 Summary of K^{trans} percentiles by time and response status for patients with non-mucinous adenocarcinoma

Time	Response status	10%	25%	50%	75%	90%	Skewness	Kurtosis
Before CRT	Responder	7×10^{-3}	19×10^{-3}	45×10^{-3}	83×10^{-3}	124×10^{-3}	10.525	134.33
	Non-responder	17×10^{-3}	42×10^{-3}	82×10^{-3}	146×10^{-3}	376×10^{-3}	4.026	20.688
During CRT	Responder	8×10^{-3}	23×10^{-3}	47×10^{-3}	99×10^{-3}	168×10^{-3}	6.355	47.039
	Non-responder	21×10^{-3}	49×10^{-3}	98×10^{-3}	174×10^{-3}	326×10^{-3}	4.879	27.811
After CRT	Responder	9×10^{-3}	25×10^{-3}	55×10^{-3}	119×10^{-3}	250×10^{-3}	5.744	50.438
	Non-responder	15×10^{-3}	39×10^{-3}	81×10^{-3}	154×10^{-3}	258	5.342	46.433

4.7 Bivariate Analyses

ADC and K^{trans} of all intra-tumour voxels were combined in multi-parametric scatterplots for all patients. For the scatterplots, red plots indicates before CRT, green indicates during CRT and blue indicates after CRT. Example multi-parametric scatterplots combining ADC and K^{trans} for a responder and non-responder are shown in Figure 4.15.

The scatterplots showed that there was no bivariate pattern in change over time for responders and non-responders. Median ADC and K^{trans} were combined together at individual time-points in a multivariate logistic model for responders vs. non-responders; no significant difference by response status was found ($p > 0.225$). The change in median ADC and K^{trans} from before CRT to during CRT, and from before CRT to after CRT were also combined in a multivariate logistic model, and were found to be non-significant by response status ($p > 0.322$). There was no significant multivariate relationship between median ADCs and K^{trans}, and response status identified.

4.8 DWI and DCE histogram results for patients with mucinous adenocarcinoma

Patients

Five patients with histopathologic mucinous adenocarcinoma were analysed separately. Of these 5 patients, 2 had histopathology TRG 1, 2 had histopathology TRG 2, and 1 had TRG 3. Two patients were classified as responders, and 3 patients were classified as non-responders.

Multi-parametric MRI properties of mucinous adenocarcinoma

The MRI characteristics of mucinous adenocarcinomas were different to those of non-mucinous adenocarcinomas. These tumours overall exhibited higher signal intensity on the T2-weighted similar to that of water. On DWI, the tumours overall appeared brighter on the ADC maps, indicating freer diffusion due to the mucin. The DCE images showed that mucinous adenocarcinomas demonstrated intra-tumoural perfusion. Figure 4.16 shows the MRI properties of the different components of mucinous tumours.

The 3-D intra-tumour ADC histograms for responders with mucinous adenocarcinoma showed higher ADC values at baseline and a clear shift to the right in response to treatment (Figure 4.17). The ADC histograms for non-responders with mucinous adenocarcinoma also demonstrated a shift to the right in response to treatment, although this shift was not as marked as the responder (Figure 4.18).

Figure 4.16 Multi-parametric MRI mucinous adenocarcinoma for a responder (patient 17 AJCC TRG 1)

Multi-parametric MRI illustrating the different MRI properties for a patient with mucinous adenocarcinoma pre-treatment.

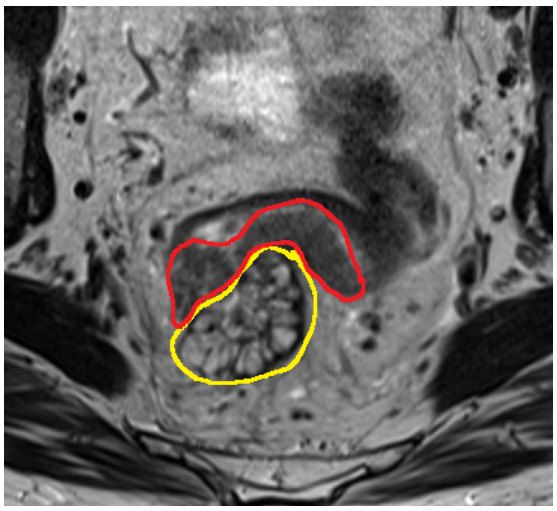

T2-weighted
Yellow annotation –mucinous component of tumour, Red annotation – solid component of tumour

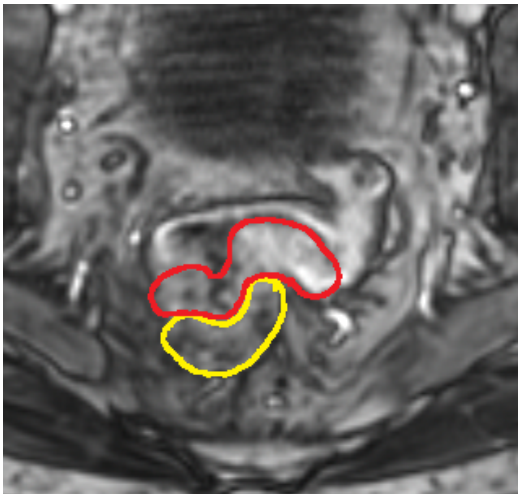

DCE
(Phase 16 image at 80 seconds)
Mucinous component of tumour (yellow) is non-enhancing on DCE
Solid component of tumour (red) enhances on DCE.

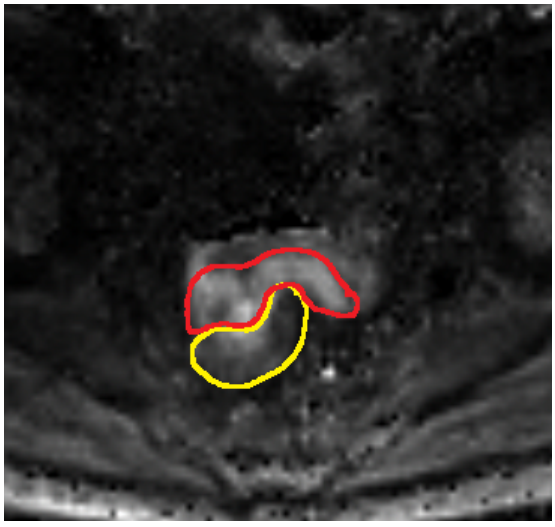

DWI - calculated b=1400mm/s^2
Mucinous component (yellow) of tumour has a lower signal intensity than the solid component of tumour

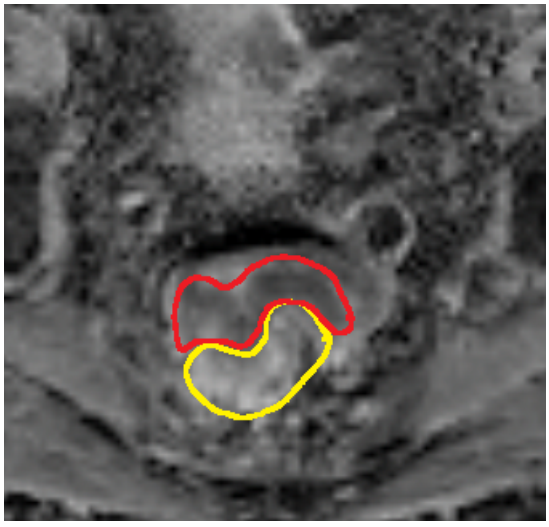

DWI – ADC map
Mucinous component of tumour shows free diffusion (bright) on the ADC map, whereas the solid component of tumour shows restricted diffusion (dark) on the ADC map.

Figure 4.17 ADC and K^{trans} histograms for mucinous adenocarcinoma responders (patients 17 and 36 AJCC, both AJCC TRG 1)

ADC histograms demonstrated a clear shift in values of ADC voxels to higher values during, and after CRT in the 2 responders.

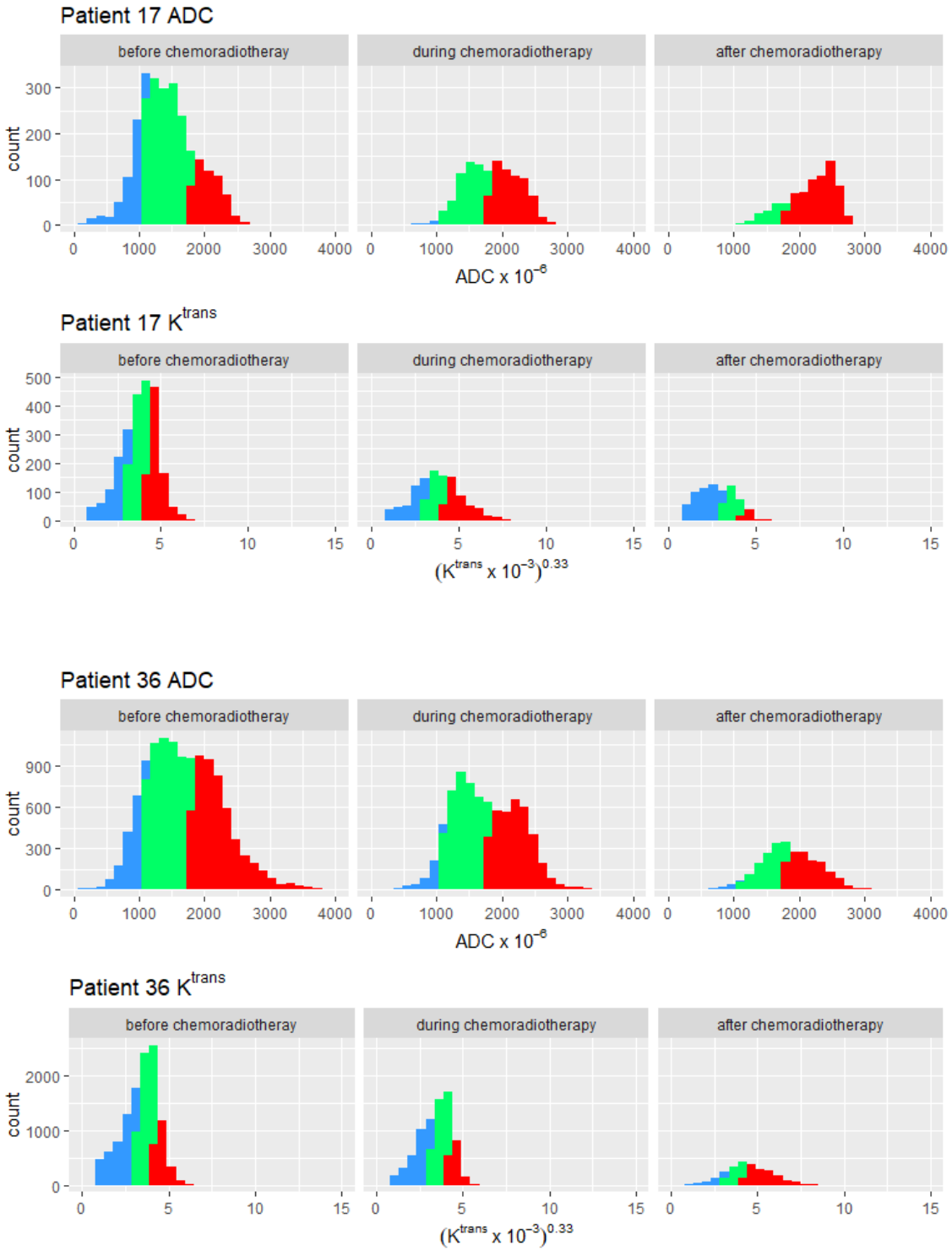

Figure 4.18 ADC and K^{trans} histograms for mucinous adenocarcinoma non-responders (patients 40 and 43, both AJCC TRG2)

The ADC histograms did not demonstrate a clear shift in response to CRT.

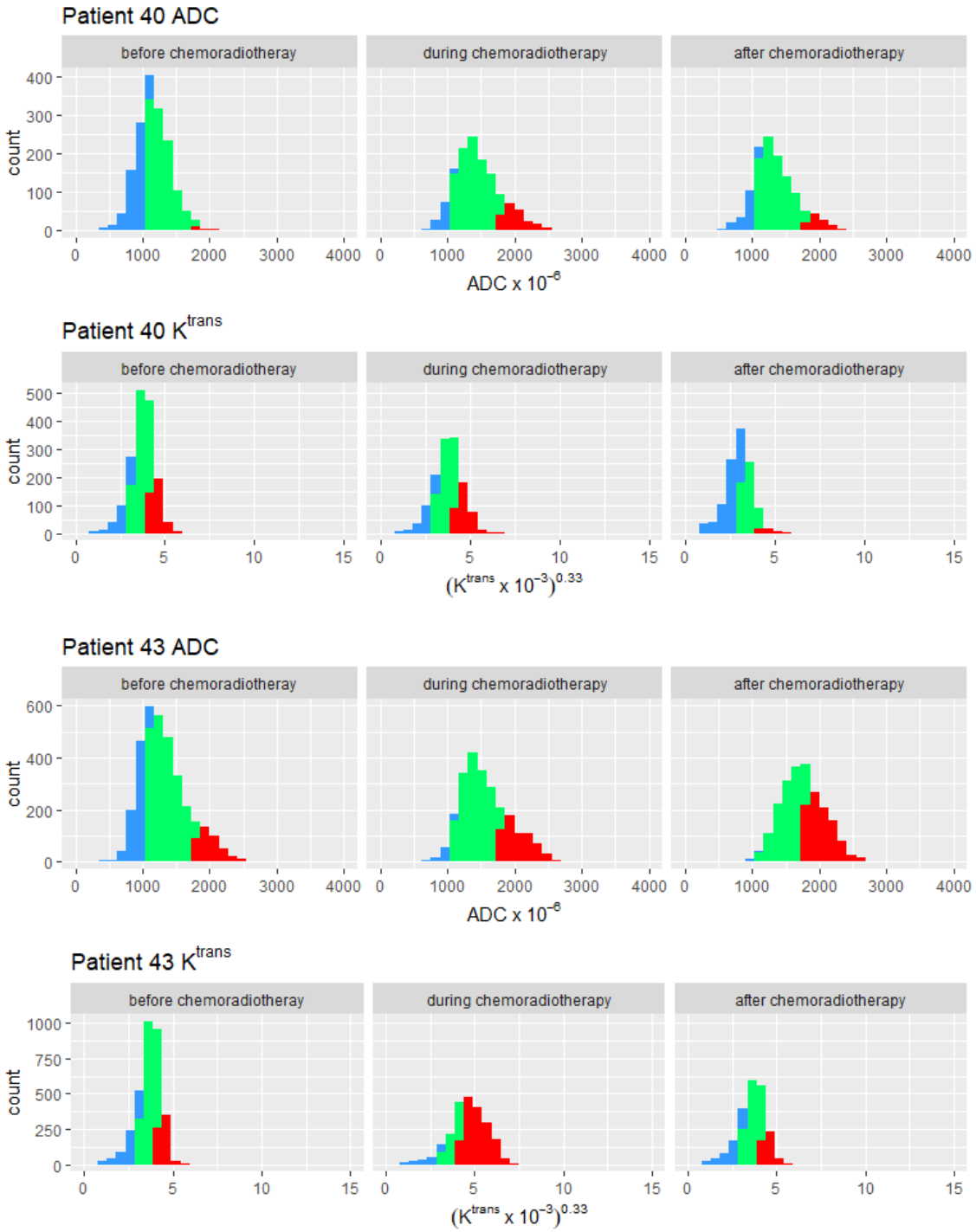

Figure 4.19 Multi-parametric scatterplots combining ADC and K^{trans} for patients with mucinous adenocarcinoma.

The red plots indicates before CRT, green indicates during CRT and blue indicates after CRT.

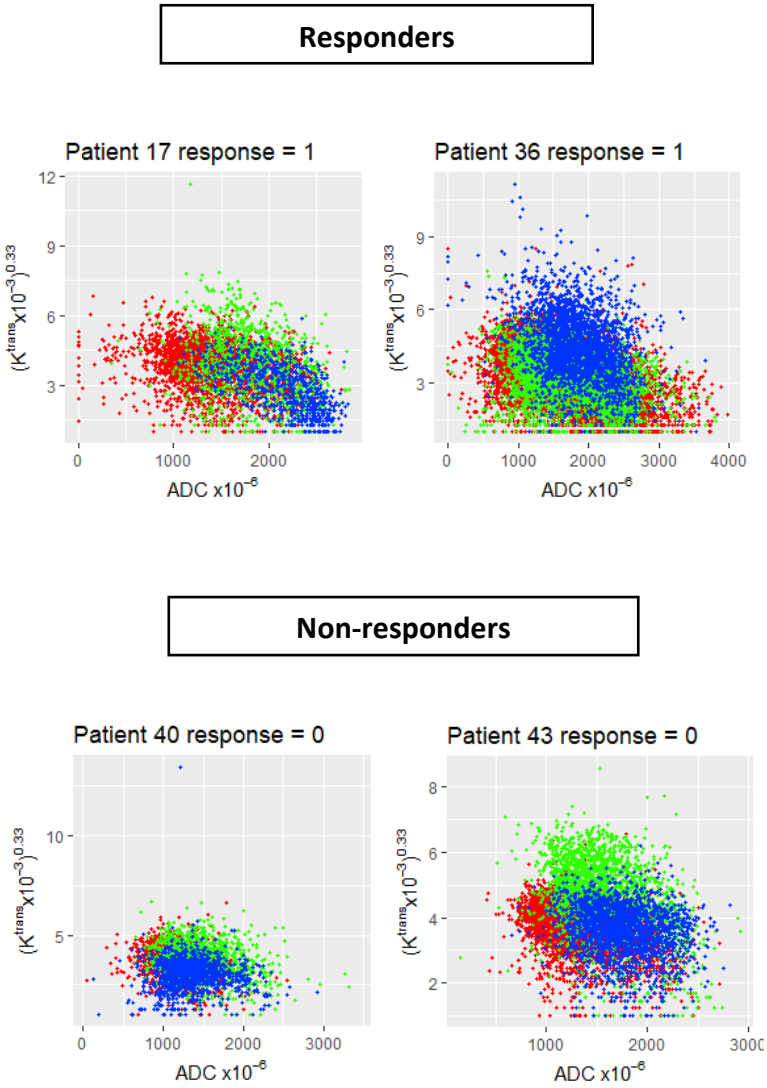

Summary of ADC and K^{trans} percentiles for all patients with mucinous adenocarcinoma

The ADC and K^{trans} quantiles for all patients with mucinous adenocarcinoma are shown in Table 4.7 and Table 4.8, respectively. All of the ADC quantiles were higher in mucinous adenocarcinoma than non-mucinous adenocarcinoma. This indicates freer diffusion in mucinous adenocarcinoma, which is likely due to the presence of >50% mucin which would be expected to have freer diffusion. All K^{trans} quantiles increased during CRT, then decreased after CRT. Due to the small number of patients with mucinous adenocarcinomas (n=5), statistical tests were not done to assess the difference in ADC or K^{trans} values between the time-points.

Table 4.7 Summary of ADC percentiles by time for all patients with mucinous adenocarcinoma

Time	10%	25%	50%	75%	90%
Before CRT	853×10^{-6}	1059×10^{-6}	1339×10^{-6}	1782×10^{-6}	2199×10^{-6}
During CRT	1069×10^{-6}	$12 \times 1059 \times 10^{-6}$	1524×10^{-6}	1946×10^{-6}	2299×10^{-6}
After CRT	1202×10^{-6}	1448×10^{-6}	1742×10^{-6}	2078×10^{-6}	2373×10^{-6}

Table 4.8 Summary of some K^{trans} percentiles by time for all patients with mucinous adenocarcinoma

Time	10%	25%	50%	75%	90%
Before CRT	12×10^{-3}	30×10^{-3}	54×10^{-3}	78×10^{-3}	101×10^{-3}
During CRT	14×10^{-3}	35×10^{-3}	69×10^{-3}	131×10^{-3}	479×10^{-3}
After CRT	12×10^{-3}	27×10^{-3}	51×10^{-3}	88×10^{-3}	164×10^{-3}

ADC and K^{trans} quantiles by time and responder status

All ADC quantiles for patients with mucinous adenocarcinomas were higher in responders than non-responders, at all time-points. Both responders and non-responders demonstrated a shift of ADC quantiles to higher values from before CRT to during CRT, and further after CRT.

K^{trans} quantiles during treatment was lower in mucinous responders than non-responders. Otherwise there was no obvious difference in K^{trans} quantiles between mucinous responders and non-responders.

Table 4.9 Summary of ADC percentiles by time and response status for mucinous adenocarcinoma

Time	Response status	0%	25%	50%	75%	100%
Before CRT	Responder	1390×10^{-6}	1454×10^{-6}	1518×10^{-6}	1583×10^{-6}	1647×10^{-6}
	Non-responder	1021×10^{-6}	1082×10^{-6}	1143×10^{-6}	1202×10^{-6}	1262×10^{-6}
During CRT	Responder	1714×10^{-6}	1744×10^{-6}	1774×10^{-6}	1804×10^{-6}	1834×10^{-6}
	Non-responder	1222×10^{-6}	1319×10^{-6}	1416×10^{-6}	1463×10^{-6}	1509×10^{-6}
After CRT	Responder	1827×10^{-6}	1932×10^{-6}	2036×10^{-6}	2141×10^{-6}	2246×10^{-6}
	Non-responder	1292×10^{-6}	1403×10^{-6}	1514×10^{-6}	1624×10^{-6}	1735×10^{-6}

Table 4.10 Summary of Ktrans percentiles by time and response status for mucinous adenocarcinoma

Time	Response status	0%	25%	50%	75%	100%
Before CRT	Responder	47×10^{-3}	50×10^{-3}	54×10^{-3}	57×10^{-3}	60×10^{-3}
	Non-responder	55×10^{-3}	56×10^{-3}	56×10^{-3}	60×10^{-3}	65×10^{-3}
During CRT	Responder	46×10^{-3}	49×10^{-3}	51×10^{-3}	54×10^{-3}	56×10^{-3}
	Non-responder	57×10^{-3}	82×10^{-3}	107×10^{-3}	304×10^{-3}	502×10^{-3}
After CRT	Responder	21×10^{-3}	38×10^{-3}	55×10^{-3}	72×10^{-3}	89×10^{-3}
	Non-responder	29×10^{-3}	35×10^{-3}	40×10^{-3}	46×10^{-3}	52×10^{-3}

4.9 Discussion

This study investigated the use of 3-D DWI and DCE MRI in combination for the prediction of CRT response in 39 patients with locally advanced rectal cancer. The study protocol allowed for voxel-wise 3-D characterisation of intra-tumour diffusion and perfusion, and its changes in response to CRT. To investigate intra-tumour heterogeneity, ADC and K^{trans} 10^{th}, 25^{th}, 50^{th}, 75^{th}, 90^{th} percentiles, skewness and kurtosis of whole tumour were examined. For all patients with non-mucinous adenocarcinoma, there was a significant increase in all ADC quantiles (10^{th}, 25^{th}, 50^{th}, 75^{th} and 90^{th}) from before to during CRT, and after CRT. After CRT (before surgery) ADC 75^{th} and 90^{th} percentiles were found to be the most promising parameters for predicting histological response to treatment. ADC histograms showed significantly higher ADC 75^{th} and 90^{th} percentile values in responders compared with non-responders. DCE-MRI showed higher K^{trans} quantile values (10^{th}, 25^{th}, 50^{th}, 75^{th} and 90^{th}) in non-responders than responders at all time-points suggesting increased angiogenesis in non-responders, although this was not statistically significant.

A strength in this study was the rigorous histopathology analysis method, with centralised consensus readings by 2 gastrointestinal pathologists. It was mandatory to embed the entire tumour bed for analysis. The pCR rate of 8% in this study was lower than in prior studies which demonstrate a pCR rate between 15 – 27% (8); this was likely due to careful histologic examination of the entire tumour bed leading to higher likelihood of finding viable tumour cells and therefore response being classified as TRG 1. A study comparing the 5 different TRG systems showed that the 4-tier AJCC system was most accurate in predicting recurrence and should be adopted as the standard (46). Patients with AJCC TRG 0 (pCR, no viable cancer cells) and TRG 1 (single cells or small groups of cancer cells) were classified as responders in this study; prediction of this category of response is clinically relevant as these patients could be eligible for organ conserving approaches such as ‘watch-and-wait’ or local excision, thereby avoiding or reducing surgical morbidity such as the need for a permanent colostomy.

This study demonstrated the limitation of using summary values to evaluate treatment response, and highlights the potential of intra-tumour heterogeneity analysis. There was no significant difference in the summary measure median ADC between responders and non-responders at any of the time-points in this study. However, on analysis of intra-tumour heterogeneity with the histograms of 3-D tumour ADC values, ADC 75^{th} and 90^{th} percentiles after CRT (before surgery) were higher in the responder group than the non-responder group. The higher ADC 75^{th} and 90^{th} percentile values after CRT in the responder group were likely due to treatment-induced cell lysis and necrotic cells in the tumour bed allowing increased diffusion of water, resulting in presence of a fraction of cells in the tumour bed having very high ADC values in responders after CRT (before surgery). This study suggests that ADC 75^{th} and 90^{th} percentiles after CRT could be useful for selection of responders (TRG 0 - 1) for an organ preservation approach with either 'watch-and-wait' or local excision.

The DCE-MRI showed that non-responders had higher K^{trans} values, suggesting increased angiogenesis as a mechanism for therapeutic resistance. This difference was not statistically significant. The study may have been underpowered due to small sample size, particularly for the DCE-MRI analysis as some patients were not able to have DCE-MRI due to renal impairment, and some of the acquired DCE datasets were unanalysable due to technical issues. Rectal peristalsis was minimized by butylscopolamine, and rigid pre-registration of flip angle to dynamic images, which had to be performed outside of commercial software, was done to correct for patient motion and ensure accurate voxel-wise analysis over 60 phases. Despite this, K^{trans} map produced had missing pixels in the ROI in some patients limiting interpretation of DCE-MRI results in the superimposed ROI segmented from DWI-MRI for voxel-wise whole tumour analysis. K^{trans} was selected for analysis in this study based on prior studies demonstrating K^{trans} to be promising in the prediction of CRT response (20, 47), although there are no studies comparing which semi(quantitative) parameter is best for analysis. A challenge in DCE-MRI interpretation is the number of (semi)quantitative parameters that can be analysed, making it difficult to compare studies. A study by Marten et al looking at multiple semi-quantitative

parameters suggested that only the before CRT late slope was able to predict CRT response (48).

A limitation in this study was the small number of patients, particularly after CRT where 32 of the enrolled 39 patients underwent MRI after CRT (before surgery). Despite this limitation, this study was able to demonstrate the usefulness of a whole tumour heterogeneity analysis of DWI-MRI performed after CRT (before surgery) for prediction of histological response. Another limitation was that multiple comparison adjustments were not employed. The findings would require validation in an external larger cohort. Currently, we are not aware of any other published combined DWI and DCE MRI prospective studies that assessed whole tumour heterogeneity for response prediction in patients with locally advanced rectal cancer undergoing CRT.

Scan reproducibility is a desirable characteristic to ensure stability of measured MRI biomarkers, however inclusion of a repeat baseline scan to assess reproducibility would have been more time intensive for patients and not done in this study. The current dataset is undergoing further testing in a subsequent study to assess the stability and reproducibility of MRI biomarkers across the different time-points. A "hop on hop off" study is also underway at this institution to test scan reproducibility by scanning patients twice in a single day time-point. The current study dataset could potentially be used in a future validation study if optimal MRI biomarkers cut-points become defined in other studies.

This study adds to the limited number of published studies combining DWI and DCE-MRI for CRT response prediction in rectal cancer and adds to the validation of promising imaging biomarkers in rectal cancer (Table 4.11) (49-51). Intven et al (49) assessed the combination of DWI and DCE-MRI at 2 time-points before CRT and after CRT (before surgery) for response assessment in rectal cancer in 55 patients and found that ADC was a promising tool for prediction of good response to CRT. However, the inclusion of K^{trans} did not increase the diagnostic accuracy for prediction of good response. Our study supports this finding; in a bi-variate analysis, K^{trans} did not add any value in the prediction

of CRT response. DeVries et al (50) examined DWI and DCE performed at a single time-point before CRT for assessing CRT response in rectal cancer in 34 patients. In this study, the DCE technique was different (16 acquisitions of T1-weighted FLASH images after gadolinium injection) and a different perfusion parameter used in older MRI protocols, perfusion index, was derived from DCE MRI. Non-responders had a higher perfusion index before CRT than responders. Our study had similar findings and found that K^{trans}, a parameter of tumour perfusion in modern MRI protocols, was higher in non-responders compared with responders at all time-points although this was not statistically significant. Tumours are characterised by leaky micro-vasculature; a possible hypothesis is that treatment-resistant rectal tumours are more likely to have greater angiogenesis, more aberrant microvasculature resulting in more leakage, perfusion and therefore higher K^{trans} than responding tumours. After CRT, the presence of high perfusion and K^{trans} in the tumour bed is suggestive of persistent abnormal vasculature and residual tumour.

Table 4.11 Prospective multi-parametric MRI studies combining DWI and DCE-MRI for prediction of CRT response

Study	N	MRI time points	MRI variables	Heterogeneity analysis	Results	Significance
Current study Pham et al 2019	33	Before CRT During CRT After CRT	ADC K^{trans}	Yes – whole tumour heterogeneity histogram 10^{th}, 25^{th}, 50^{th}, 75^{th}, 90^{th} quantiles, skewness and kurtosis	After CRT ADC 75^{th} higher in responders than non-responders After CRT ADC 90^{th} higher in responders than non-responders After ADC other quantiles K^{trans} all quantiles higher in non-responders than responders	p = 0.04 p = 0.02 p > 0.08 (ns) p > 0.10 (ns)
Intven et al, 2015 (33)	55	Before CRT after CRT	ΔADC ΔK^{trans}	No	ΔADC greater in responders ΔK^{trans} greater in non-responders Multiparametric analysis – addition of K^{trans} did not increase accuracy response prediction	p < 0.001 p < 0.001
DeVries et al, 2003 (50)	34	Before CRT	ADC mean Perfusion index (PI)	Yes Histogram heterogeneity obtained from a plane through tumour	Mean ADC ADC histogram – higher relative fraction of high ADCs in nonresponders than responders	p = ns p < 0.001 p < 0.001

Study	N	MRI time points	MRI variables	Heterogeneity analysis	Results	Significance
					PI mean – higher in non-responders PI cumulative fraction of pixels with PI > 12 mL/min/100mg	p < 0.001
De Cecco et al, 2016 (34)	12	Before CRT	ADC K^{trans} V_e K_{ep}	DWI – no DCE – yes highest 10^{th} and highest 25^{th} quantiles	ADC K^{trans} V_e lower in responders K_{ep} higher in responders	p = ns p = ns p = 0.04 p = 0.39

4.10 Conclusions

3-dimensional DWI ADC and DCE K^{trans} histograms demonstrated intra-tumour heterogeneity in response to CRT. DWI-MRI ADC 75^{th} and 90^{th} quantiles after CRT were the most promising parameters for prediction of CRT responder (TRG 0 -1) status prior to surgery in patients with locally advanced rectal cancer. This could aid in the selection of responders to CRT for an organ preservation approach with either 'watch-and-wait' or local excision. Due to the small number of patients in this study, this would need to be validated in a larger cohort. All DCE-MRI K^{trans} histogram quantiles were higher in non-responders than responders at all time-points, suggesting greater tumour perfusion and angiogenesis in non-responders, although this was not significant. Multi-parametric scatterplots and bi-variate analyses combining ADC and K^{trans} did not add value in predicting therapeutic response.

Chapter 5 Results and discussion (clinical study): Multi-parametric MRI for prediction of disease-free survival in locally advanced rectal cancer

5.1 Patients and disease-free survival

A total of 39 patients were recruited to this study. There were 33 patients with non-mucinous adenocarcinoma in the disease-free survival analysis; of these patients 33 had DWI and 31 had DCE-MRI before CRT, 31 had DWI and 29 had DCE-MRI during CRT, and 27 had DWI and 25 had DCE-MRI after CRT (before surgery). There were patient withdrawals from the study accounting for less patients during CRT (2 patients declined MRI) and after CRT (6 patients declined MRI). Two patients did not have DCE-MRI due to renal impairment and contra-indication to gadolinium contrast. Of the patients who had DCE-MRI, there were 2 datasets before CRT, and 1 dataset during CRT that were unanalysable due to technical issues (described in previous chapter). Five patients with mucinous adenocarcinoma were excluded from this analysis. One patient who did not undergo surgery and was lost to follow-up was excluded from this analysis.

The median follow-up time was 2.5 years (range 1.5 to 40 months). No patient had loco-regional relapse. Nine patients had distant metastases. Two patients died; 1 died of metastatic disease at 5 months and 1 died of other cause at 20 months. The 24 month disease-free survival probability for the whole cohort was 0.72 (CI 0.58 – 0.90).

5.2 DWI-MRI ADC and disease-free survival

The hazard ratios (HR) for time to relapse using a Cox proportional hazards model for before CRT, during CRT, and after CRT (before surgery) ADC values (10^{th}, 25^{th}, 50^{th}, 75^{th} and 90^{th} quantiles) were not statistically significant ($p > 0.06$). The HRs for change (Δ) in ADC values (10^{th}, 25^{th}, 50^{th}, 75^{th}, 90^{th} quantiles) from before CRT to during CRT, and from before CRT to after CRT were not statistically significant ($p > 0.09$).

5.3 DCE-MRI K^{trans} and disease-free survival

The HRs for time to relapse using a Cox proportional hazards model for before CRT and during CRT K^{trans} values (10^{th}, 25^{th}, 50^{th}, 75^{th} and 90^{th} quantiles) were not statistically significant ($p > 0.26$). The HRs for after CRT K^{trans} 10^{th} (HR = 1.04, 95% CI 1.004 -1.077, p = 0.03), 25^{th} (HR = 1.015, 95% CI 1 – 1.03, p = 0.04), 50^{th} (HR = 1.006, 95% CI 1 – 1.012, p = 0.04) and 75^{th} (HR = 1.003, 95% CI 1 – 1.006, p=0.04) quantile values were all statistically significant ($p < 0.05$). The HR for after CRT 90^{th} quantile (HR = 1.002, 95% CI 0.9999 – 1.004, p = 0.07) was not statistically significant. The HRs for ΔK^{trans} from before CRT to after CRT K^{trans} for 50^{th} (HR = 1.008, 95% CI 1.001 – 1.014, p = 0.03), 75^{th} (HR = 1.004, 95% CI 1.001 – 1.007, p = 0.02) and 90^{th} (HR 1.002, 95% CI 1.000 – 1.005, p = 0.03) quantiles were statistically significant. The HRs for K^{trans} percentile values, and ΔK^{trans} from before CRT to during and after CRT K^{trans} are shown in the forest plots in Figure 5.1 and Figure 5.2

The best after CRT K^{trans} cut-point for predicting relapse was 28×10^{-3} (the 10^{th} percentile value), with a higher K^{trans} value predicting for relapse (distant). The 24 month disease-free survival probability was 0.93 (95% CI 0.803 to 1.000) for patients with after CRT K^{trans} value $\leq 28 \times 10^{-3}$ versus 0.41 (95% CI 0.187 to 0.894) for patients with after CRT K^{trans} value $>28 \times 10^{-3}$. The Kaplan Meier disease-free survival curve using the K^{trans} cut-point of 28×10^{-3} is displayed in Figure 5.3, which shows that patients with a higher K^{trans} value after CRT (before surgery) had lower disease-free survival.

Figure 5.1 Forest plot of hazard ratios for K^{trans} for disease free survival

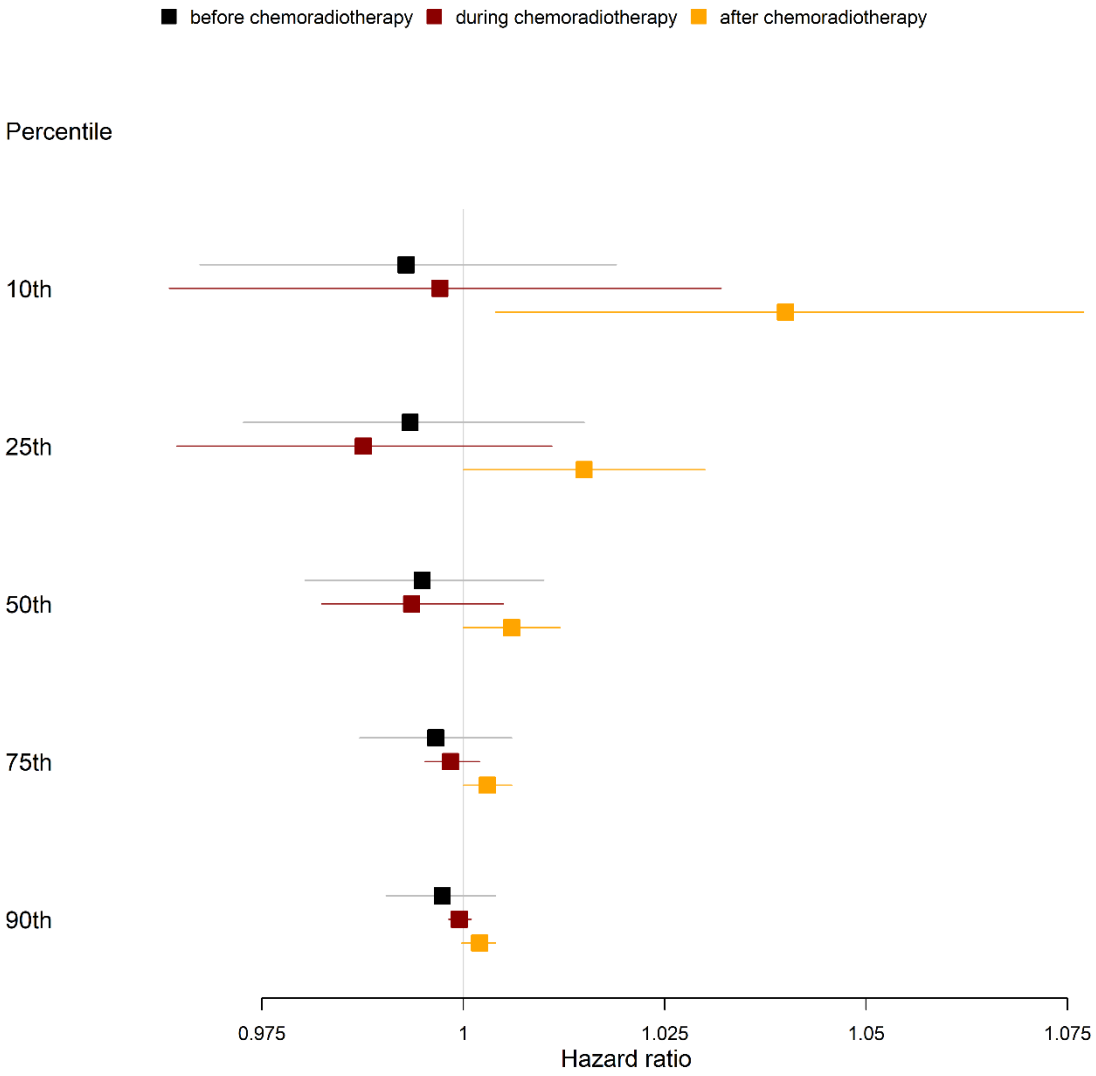

Figure 5.2 Forest plot of hazard ratios for ΔK^{trans} for disease free survival

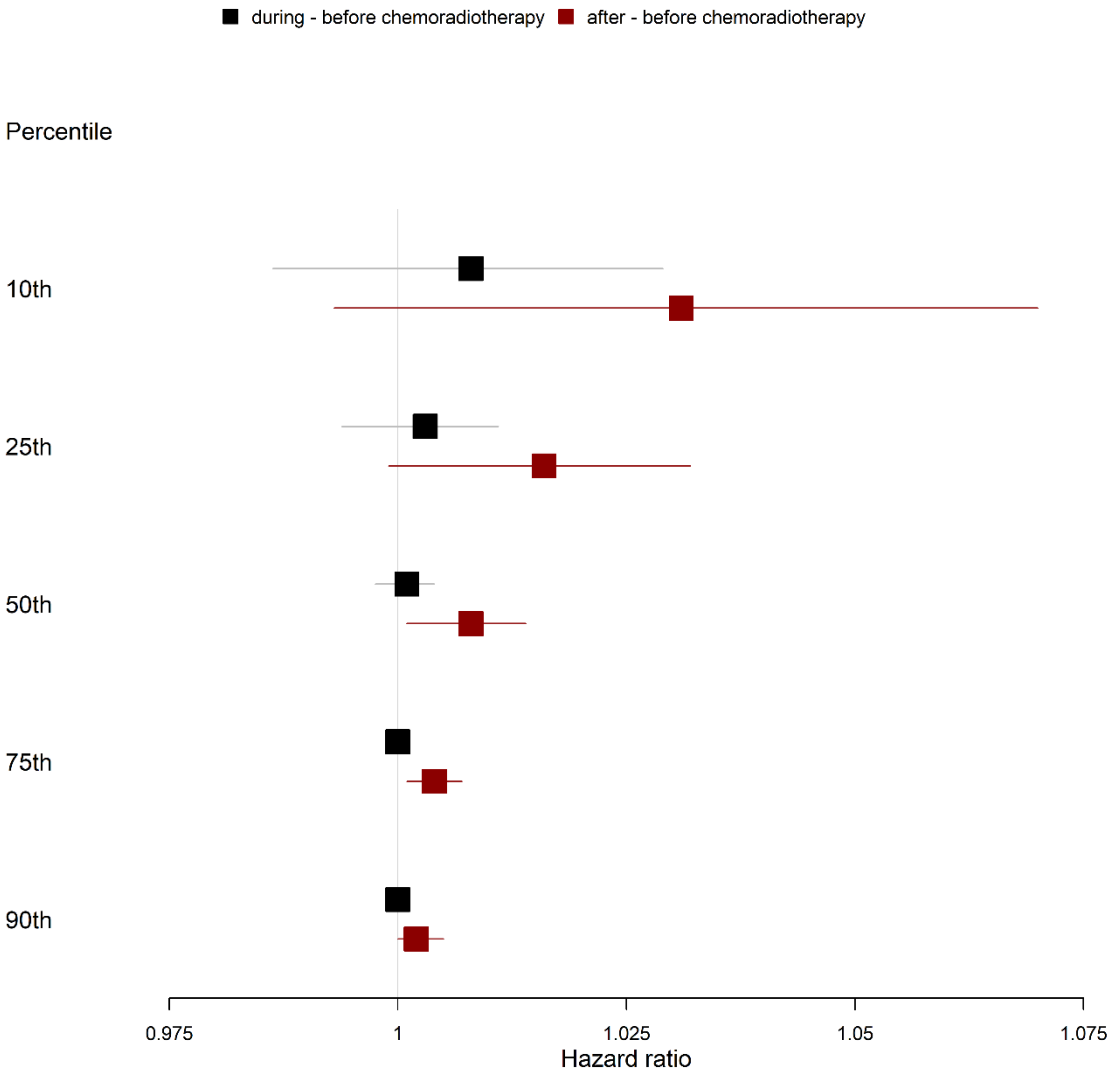

Figure 5.3 Kaplan Meier disease-free survival probability curve using after CRT (before surgery) K^{trans} cut-point value 28 x 10^{-3} (10^{th} percentile)

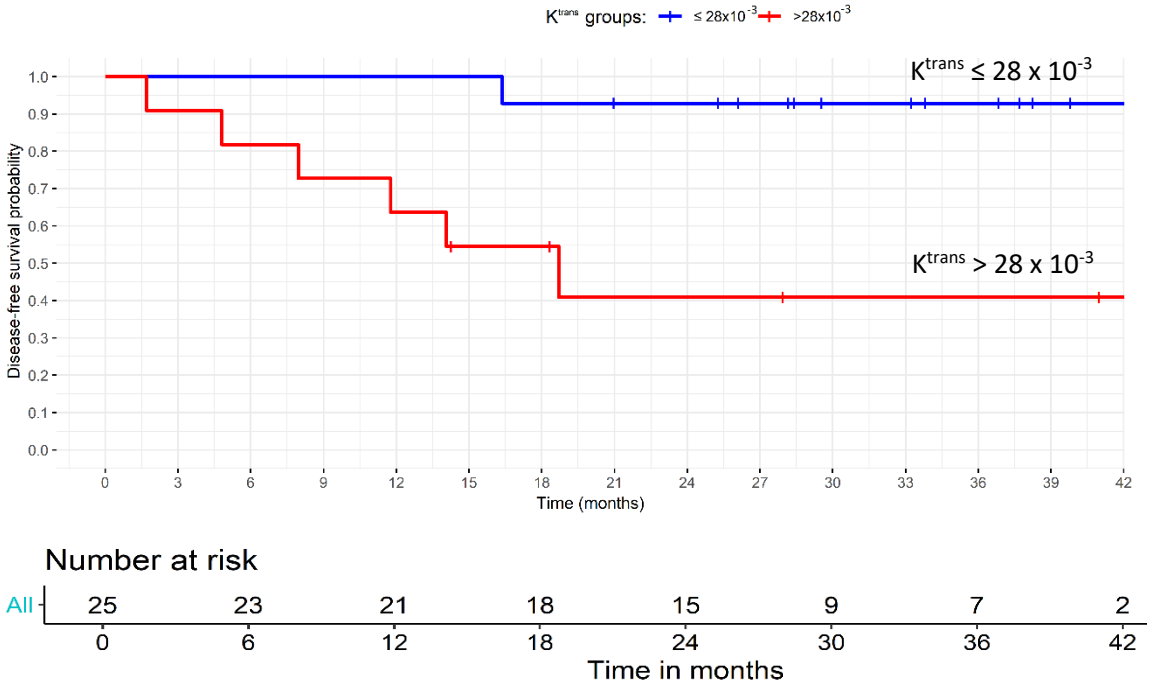

5.4 Discussion

This study showed that K^{trans} derived from DCE-MRI after CRT (before surgery) was a promising biomarker for the prediction of disease-free survival in patients with locally advanced rectal cancer undergoing neoadjuvant CRT followed by surgery. Patients with higher K^{trans} value after CRT (before surgery) had a significantly lower 2 year DFS. As all relapses in this study were distant, and there were no locoregional relapse, the higher K^{trans} value after CRT represents a higher probability of distant relapse. The 10^{th} percentile K^{trans} value of 28 x 10^{-3} was the best value for predicting 2 year DFS (HR of 1.04, p = 0.03); as this was analysed as a continuous variable, a HR of 1.04 indicates a 4% increased risk of distant relapse per every unit increase in K^{trans}. For the heterogeneity analysis, a significantly increased hazard of recurrence for higher K^{trans} values was also seen for the other K^{trans} quantiles (25^{th}, 50^{th} and 75^{th}) after CRT. In addition, ΔK^{trans} 50^{th}, 75^{th} and 90^{th} quantiles from before CRT to after CRT were also significant for 2 year DFS, with patients with a greater increase in K^{trans} values from before CRT to after CRT at greater risk of distant relapse. DWI-MRI was not able to predict disease-free survival at any time-point.

The higher K^{trans} after CRT indicates higher perfusion within the tumour bed. Our results showed that patients with higher K^{trans} value after CRT had significantly lower 2 year distant DFS. The higher K^{trans} value after CRT could represent greater vascular permeability and angiogenic activity within the tumour bed, providing a mechanism for haematogenous spread. In addition, a greater increase in K^{trans} value from before CRT to after CRT could indicate an increase in angiogenic activity and development of an aggressive tumour phenotype, leading to a greater risk of haematogenous spread. A previous study by DeVries et al in patients with locally advanced rectal cancer identified DCE-MRI perfusion index (PI), an older measure of tumour perfusion, as a predictive factor for DFS(52). Patients with higher PImean through one slice of tumour before CRT had decreased response to CRT and DFS, and the authors hypothesised that the higher PI parameter was a sign of more aggressive tumour resulting from high angiogenic activity. Although it has been shown that PI value is related to K^{trans}, PI is a measure from older MRI protocols. The Quantitative Imaging Biomarkers Alliance suggests K^{trans},

which takes into account arterial input function, as the most representative DCE-MRI vascular parameter for MRI protocols in contemporary oncology trials (53, 54). To the best of our knowledge, this is the first study assessing K^{trans} derived from DCE-MRI and disease-free survival in patients with locally advanced rectal cancer. In addition, our study incorporated a whole tumour, heterogeneity analysis method. There have been DCE-MRI studies in other tumour sites including breast cancer that have also shown higher tumour perfusion values before treatment predicted for a higher risk of metastases and lower DFS (55, 56).

ADC in this study was not useful for predicting DFS. ADC is an imaging biomarker of cellularity, and tumour cellularity may be less useful than tumour perfusion in the prediction of haematogenous spread.

This study has identified K^{trans} as a potential novel imaging biomarker predictive of disease-free survival and development of distant metastases in rectal cancer. This biomarker could be considered for stratification of patients for more intensive adjuvant systemic therapies in future studies. The rate of distant metastases in patients with locally advanced rectal cancer remains high, with a 5 year cumulative incidence of distant metastases of 30% shown in pooled data from European randomised control trials, despite multi-modality treatment strategies incorporating neoadjuvant CRT and total mesorectal excision surgery (10). Predictive biomarkers of distant metastases could help identify higher risk patients for more intensive systemic therapy following CRT and surgery.

A limitation of this study was the small numbers, particularly the number of patients undergoing MRI after CRT (before surgery) as some patients had declined MRI at this time-point prior to surgery. Only 25 patients (76%) had DCE-MRI after CRT. Despite the small sample size we found that DCE-MRI after CRT was statistically significant for predicting DFS. It is possible that the level of significance may be even higher with a larger cohort. The other limitation was the short median follow-up time of 2.5 years in this study. Validation of our study results in a larger study with longer follow-up duration

is required, prior to use to guide adjuvant treatment decisions. The K^{trans} results after CRT were significant across the multiple quantiles on the heterogeneity analysis, suggesting that there is likely a correlation between K^{trans} values after CRT and DFS worth further investigation.

5.5 Conclusions

In conclusion, this study showed that K^{trans} derived from DCE-MRI performed after CRT was predictive of 2 year DFS. Patients with higher K^{trans} value after CRT, or greater increase in K^{trans} from before CRT to after CRT had a significantly higher risk of distant metastases, and lower 2 year distant DFS. The higher K^{trans} value could indicate increased angiogenesis and an aggressive tumour phenotype. K^{trans} is a potential imaging biomarker that could assist in identification of patients at high risk of distant relapse, and guide stratification of patients for adjuvant systemic therapies in future studies. Validation is required in a larger cohort.

Chapter 6 Methods (ex vivo study): Ultra-high field MRI aided biomarker discovery in rectal cancer *ex vivo*

6.1 Introduction

Further MRI biomarkers in rectal cancer are required to enable individualisation of treatment based on more accurate assessment of tumour extent, heterogeneity, and radiotherapy response. In particular, MRI sequences are needed that allow for accurate differentiation between T1 and T2 rectal tumours (tumour invading muscularis propria). MRI sequences that enable differentiation between tumour and fibrosis would improve radiotherapy response prediction. There are many functional MRI biomarkers that have not yet been explored in rectal cancer. There have been no prior studies examining the potential of diffusion tensor imaging (DTI) MRI biomarkers in rectal cancer. Ultra-high field MRI (11.7 tesla) allows exploration of cancer at the microscopic level with imaging resolution of 100 – 200 μm and correlation with 'ground-truth' histopathology. A biomarker discovery pipeline linking ultra-high field MRI to clinical MRI (3.0 tesla) would allow for clinical translation of 'ground-truth' findings.

This exploratory study examined novel MRI derived biomarkers of rectal cancer stromal heterogeneity and tumour extent at ultra-high field. Specifically, the aims were to 1. Establish a framework for ultra-high field MRI analysis of Biobank cancer tissue *ex vivo* in order develop a pipeline for MRI biomarker discovery from ultra-high field to clinical field strengths and 2. Examine the microstructure of rectal cancer by ultra-high field DTI-MRI at 11.7 tesla *ex vivo* and correlate MRI findings with histopathology.

This project involved the use of the South Western Local Health District (SWSLHD) Centre for Oncology Education Research Translation (CONCERT) Biobank specimens from patients diagnosed with rectal cancer and undergoing surgery. A method of tissue preparation was developed for optimal MRI examination of rectal tissue *ex vivo* that allowed for preservation of tissue integrity, allowing for subsequent correlation with histopathology analysis. High field MRI (11.7 tesla) was used to examine the stromal

microstructure of malignant and normal rectal tissue *ex vivo*. MRI findings were co-registered and correlated with light microscopy examination of tissue specimens.

6.2 Type of study and patients

This was an exploratory study. The sample size was 5 patients. Patients with biopsy proven rectal cancer undergoing rectal surgery were eligible for this study. Suitable patients were flagged by the SWSLHD CONCERT Biobank for participation. All patients consented to Biobank tissue donation in accordance with the SWSLHD CONCERT Biobank standard consent processes. Fresh tissue was collected from the surgical specimens of suitable patients.

6.3 Patient clinical data

Clinical data for each patient were collected as part of standard CONCERT Biobank protocols. The following clinical data was accessed from the Biobank for this study: (i) patient characteristics – age at diagnosis, female / male, (ii) clinical staging (cTNM) (iii) pathologic staging (pTNM) (iv) histopathologic subtype (v) treatment details (type of rectal surgery, (neo)adjuvant chemotherapy, (neo)adjuvant radiotherapy (vi) Disease status at 12 months from diagnosis (Nil evidence of disease, or disease recurrence (loco-regional recurrence, distant metastases)).

6.4 Biobank tissue collection and preparation

Biobank tissue collection and handling techniques play a major role in obtaining reproducible and reliable results in *ex vivo* MRI (57). Tissue samples need to be prepared in a way that does not compromise MRI signal and image quality. Time in room temperature, delayed preservation, the freezing and thawing process and prolonged MR acquisition time can promote enzymatic activity and biochemical degradation in tissues (57). In addition, a high spinning rate can change the tissue morphology which can affect subsequent histologic analysis. Some standard Biobank tissue collection and storage processes are not suitable for certain MRI analysis methods. Frozen samples are not suitable for diffusion MRI analysis as the freezing process ruptures cell membranes and

releases para-magnetics which interfere with the MR images. In frozen samples, the water molecules reorientate very slowly that the spin – spin (ie. T2) relaxation time is too short resulting in signal decay before the end of the echo-based MRI pulse sequence, and no detectable MRI signal. Frozen samples may be suitable for MR spectroscopy methods. For MR spectroscopy, tissues have a high metabolic rate, samples should ideally be prepared on ice with a constant sample preparation time, and MR acquisition should also be carried out at a low temperature. Swanson et al found that metabolic degradation on prostate biopsies can be minimized by acquiring HR-MAS data at temperatures close to freezing (1ºC), and that over the first 2 hours, phosphocholine and glycerophosphocholine decreased by only 2.8%, whilst choline increased by 34.7% (58). However, the rate of biochemical degradation varies depending on tissue type, and it is unknown what time frame MR spectroscopy experiments on rectal tissue should be performed within, to avoid any observable biochemical alteration occurring *ex vivo.* Appropriate methods of tissue collection and preparation needs to be developed specifically for the MRI sequence of interest. Histopathology analysis of tissue provides a 'ground-truth' basis, however tissue sample orientation is of paramount importance for subsequent accurate correlation with MR images for analysis of correct tissue regions of interest, and this needs to be incorporated into MRI – histopathology correlation studies.

Standard SWSLHD CONCERT Biobanking procedures involves collection of tissue from the surgical specimen after the Pathologist has taken all tissue required for clinical purposes. Two samples are stored in the CONCERT Biobank; a snap frozen specimen and a formalin-fixed and paraffin embedded (FFPE) specimen (59). The existing snap-frozen and FFPE rectal tissue in the CONCERT Biobank were unsuitable DTI-MRI analysis in this study. Bespoke specimen collections were required for this study. Fresh rectal tissue specimens were collected and prepared by the CONCERT Biobank to the specifications of this study.

Rectal tissue specimens were obtained through the CONCERT Biobank in South Western Sydney Local Health District from patients diagnosed with rectal cancer undergoing

surgery. In accordance with the Biobank protocol, only tissue that was removed for the purposes of treatment and not required by the Pathologist for diagnostic purposes was collected. Two fresh tissue specimens were collected from each patient's surgical specimen: (i) full thickness (containing both mucosal and serosal surface) rectal cancer with peri-lesional adjacent normal rectum, and (ii) full thickness adjacent normal rectum tissue 5 – 10cm away from cancer. The specimens collected were up to 1.5 cm wide and 3 cm long, depending on the amount of tissue available for Biobank collection.

Collected specimens were immediately fixed in 10% Formalin for 24 – 48 hours. Tissue specimens were subsequently embedded in 1% agarose (1g agarose in 100ml distilled water) containing 2 mM gadopentetate dimeglumine (0.4ml of Bayer Magnevist 0.5M) for MR imaging. Agarose was chosen to embed tissue for number of reasons: (i) agarose has similar susceptibility to tissue (ii) to keep the tissue suspended in the MRI vial for imaging (iii) agarose stops the magnetic field from bending. Gadopentetate dimeglumine is a gadolinium based MRI contrast which reduces the T2 relaxation time. One gram of agarose was dissolved in distilled water at boiling point (100°C) in a glass flask. The agarose solution was allowed to cool and a thermometer was used to monitor the temperature of the solution. Magnevist 0.4 ml of 0.5M stock was added and mixed when the solution was 55°C. The agarose solution was poured in layers, starting with the base layer prior to laying the rectal tissue in the vial. Care had to be taken not to pour the solution on the specimen above 39°C, as this temperature would have degraded the tissue. The solution was poured onto the specimen when the solution was 37°C (body temperature) with the specimen held suspended in the middle of the vial by tweezers. The solution began setting at below 34°C. Air bubbles were not allowed in the set gel, as this would have led to bending of the magnetic signal. The specimen mucosal and serosal surface orientation in MRI vial were marked with lines labelled 'M' and 'S', respectively, on the MRI vial. Photos of gross specimens were taken to document specimen orientation and aid in subsequent MRI – histopathology correlation. Embedded tissue specimens were stored in the Biobank fridge at < 4°C for a minimum of 24 hours to allow the gel to set prior to MR analysis.

Animal bowel (porcine small bowel) from the butcher was used in a feasibility test to optimize the tissue preparation and MR DTI technique, prior to commencing the study on human Biobank specimens.

6.5 Ethics approval

The projects entitled 'Magnetic Resonance (MR) Aided Biomarker Discovery in Cancer' and 'Protocol Rectal Cancer' were approved by South Western Sydney Local Health District (SWSLHD) Human Research Ethics Committee on 15th September 2014. HREC reference: HREC/14/LPOOL/370. Local project number: 14/209. SSA references: SSA/14/LPOOL/371 and SSA/14/LPOOL/372. Western Sydney University HREC reference: H10843.

A detailed description of the following methods for this study are in chapter 7 in the published manuscript 'Correlation of ultra-high field MRI with histopathology for evaluation of rectal cancer heterogeneity'. Scientific Reports. 2019;9:9311

- MRI
- Histopathology examination
- MRI-histopathology correlation and co-registration
- MRI analysis
- Statistical analysis

Chapter 7 Results and discussion (*ex vivo* study): Ultra-high field MRI aided biomarker discovery in rectal cancer

The publication in this chapter contains methods (MRI, histopathology examination, MRI histopathology correlation and co-registration, MRI analysis, statistical analysis), results and discussion for the *ex vivo* ultra-high field study.

7.1 *Ex* vivo ultra-high field study Publication

Ultra-high field MRI at 11.7 tesla for evaluation of rectal cancer stromal heterogeneity ex vivo: correlation with histopathology. *Scientific Reports* 2019;9:9311. https://doi.org/10.1038/s41598-019-45450-2

Authors:

1. Trang T. Pham
2. Timothy Stait-Gardner
3. Cheok Soon Lee
4. Michael Barton
5. Petra L. Graham
6. Gary Liney
7. Karen Wong
8. William S. Price

SCIENTIFIC REPORTS

OPEN

Correlation of ultra-high field MRI with histopathology for evaluation of rectal cancer heterogeneity

Received: 9 April 2018
Accepted: 4 June 2019
Published online: 27 June 2019

Trang T. Pham[1,2,3], Timothy Stait-Gardner[4], Cheok Soon Lee[2,3,5,6], Michael Barton[1,2,3], Petra L. Graham[7], Gary Liney[1,2,3], Karen Wong[1,2,3] & William S. Price[1,4,5]

Current clinical MRI techniques in rectal cancer have limited ability to examine cancer stroma. The differentiation of tumour from desmoplasia or fibrous tissue remains a challenge. Standard MRI cannot differentiate stage T1 from T2 (invasion of muscularis propria) tumours. Diffusion tensor imaging (DTI) can probe tissue structure and organisation (anisotropy). The purpose of this study was to examine DTI-MRI derived imaging markers of rectal cancer stromal heterogeneity and tumour extent *ex vivo*. DTI-MRI at ultra-high magnetic field (11.7 tesla) was used to examine the stromal microstructure of malignant and normal rectal tissue *ex vivo*, and the findings were correlated with histopathology. Images obtained from DTI-MRI (A0, apparent diffusion coefficient and fractional anisotropy (FA)) were used to probe rectal cancer stromal heterogeneity. FA provided the best discrimination between cancer and desmoplasia, fibrous tissue and muscularis propria. Cancer had relatively isotropic diffusion (mean FA 0.14), whereas desmoplasia (FA 0.31) and fibrous tissue (FA 0.34) had anisotropic diffusion with significantly higher FA than cancer ($p < 0.001$). Tumour was distinguished from muscularis propria (FA 0.61) which was highly anisotropic with higher FA than cancer ($p < 0.001$). This study showed that DTI-MRI can assist in more accurately defining tumour extent in rectal cancer.

Standardised surgical technique with total mesorectal excision, and multimodality treatment strategies with neo-adjuvant chemoradiotherapy have led to improved survival in rectal cancer[1–3]. In selected patients with early rectal cancer, local excision may be an appropriate treatment option. Accurate pre-operative staging in rectal cancer is therefore of paramount importance in the selection of optimal surgical technique, and stratification of patients into those who can undergo surgery alone or those who would benefit from neoadjuvant chemoradiotherapy. Current clinical magnetic resonance imaging (MRI) techniques using T_2-weighted imaging have an established role in the primary staging of rectal cancer, however, there are limitations with their use. Firstly, T_2-weighted MRI is unable to accurately differentiate stage T1 (tumour invades submucosa) from stage T2 (tumour invades muscularis propria) tumours[4,5], and endoscopic ultrasound is currently the recommended imaging modality of choice by the European Society of Gastrointestinal and Abdominal Radiology (ESGAR) to differentiate between T1 and T2 tumours if local resection is being considered[4]. Secondly, T_2-weighted MRI has limited ability to examine the rectal cancer stromal microenvironment, and differentiation of tumour from desmoplastic reaction or fibrous tissue can be challenging. Stranding into the mesorectal fat is an equivocal sign that may indicate either a T2 tumour with desmoplasia or a T3 (tumour invades through the muscularis propria into perirectal tissue) tumour with tumoural strands[4]. Functional MRI has the capability to non-invasively characterise tumour heterogeneity and its role in more accurate staging of rectal cancer should be further explored.

Tumour stroma evolves during cancer progression and is associated with increased extracellular matrix. The increased deposition of extracellular matrix (fibrosis) in tumours is known as desmoplasia, and characteristic of many advanced cancers[6,7]. Histopathologic studies in colorectal cancer have identified changes in the tumour stroma, including increased collagen fibril stiffness and anisotropy, compared to normal healthy mucosa[8]. Fibril

[1]Department of Radiation Oncology, Liverpool Cancer Therapy Centre, Liverpool Hospital, Sydney, Australia. [2]South Western Sydney Clinical School, Faculty of Medicine, University of New South Wales, Sydney, Australia. [3]Ingham Institute for Applied Medical Research, Sydney, Australia. [4]Nanoscale Organisation and Dynamics Group, Western Sydney University, Sydney, Australia. [5]School of Medicine, Western Sydney University, Sydney, Australia. [6]Department of Anatomical Pathology, Liverpool Hospital, Sydney, Australia. [7]Centre for Economic Impacts of Genomic Medicine (GenIMPACT), Macquarie Business School, Macquarie University, Sydney, Australia. Correspondence and requests for materials should be addressed to T.T.P. (email: trang.pham@health.nsw.gov.au)

anisotropy (degree of organisation) may serve as a novel predictive stromal biomarker for cancer invasion and assist in more accurate staging in rectal cancer. Since the fibres cause anisotropic restriction of the diffusion of tissue water, diffusion tensor imaging (DTI) MRI may provide a non-invasive method for characterising such fibril anisotropy. DTI-MRI, which provides a rotationally invariant description of tissue diffusion for each voxel in the image, has the potential to supply additional information about the tumour stromal microenvironment. DTI-MRI can probe stromal microstructure and organisation (anisotropy). The apparent diffusion coefficient (ADC) and fractional anisotropy (FA) for each voxel can be calculated from the diffusion tensor measured for each voxel. Viable tumours restrict cellularity and water movement, resulting in a low ADC. FA may be useful for more accurate tumour delineation and detection of tumour invasion into tissues with highly structured organisation[9]. Most tumours typically exhibit relatively isotropic diffusion, whereas organised tissues exhibit anisotropic diffusion. To our knowledge, the potential clinical utility of DTI-MRI in rectal cancer has not yet been investigated in the *ex vivo* or clinical settings.

We hypothesise that DTI-MRI can assess stromal heterogeneity in rectal cancer, thereby allowing for more accurate delineation of rectal cancer extent and staging. This paper examines the potential of DTI-MRI to characterise fibril anisotropy as a probe of the stromal microenvironment and tumour extent. This proof of principle study was performed on an ultra-high field MRI at 11.7 tesla. The advantage of ultra-high field MRI is that the microscopic spatial (i.e., voxel) resolution (200 µm) can be used to reveal cancer microstructure *ex vivo*. This allows for direct correlation with 'ground-truth' histopathology analysis of the same tissue specimen.

The purpose of this exploratory study was to examine DTI-MRI derived imaging markers of rectal cancer stromal heterogeneity and tumour extent, *ex vivo*. Specifically, the stromal ultrastructure of rectal cancer and adjacent normal rectum was examined by high field strength DTI-MRI at 11.7 tesla *ex vivo*, and the MRI findings were correlated with histopathology.

Methods

Patients and biobank tissue collection. Patients with biopsy proven rectal cancer undergoing rectal surgery alone were eligible for this study. All patients who participated in this study provided written informed consent. All study protocols were approved by the institutional ethics committee South Western Sydney Local Health District (SWSLHD) Human Research Ethics Committee (HREC) (Approval numbers: HREC/14/LPOOL/152, HREC/14/LPOOL/370, Local Project Number 14/209, SSA/14/LPOOL/371, SSA/14/LPOOL/372, H10843). All study methods were carried out in accordance with SWSLHD HREC approved study protocols and SWSLHD Centre for Oncology Education Research Translation (CONCERT) Biobank procedures[10].

Tissue was collected from the surgical specimens of rectal cancer patients. Two fresh tissue specimens were collected from each patient's surgical specimen: (i) full thickness (containing both mucosal and serosal surface) rectal cancer with peri-lesional adjacent normal rectum, and (ii) full thickness adjacent normal rectum tissue 5–10 cm away from cancer. The specimens collected were up to 1.5 cm wide and 3 cm long, depending on the amount of tissue available for Biobank collection. Collected specimens were immediately fixed in 10% formalin for 24–48 hours. Tissue specimens were subsequently embedded in 1% agarose (1 g agarose in 100 ml distilled water) containing 2 mM gadopentetate dimeglumine (0.4 ml of Bayer Magnevist 0.5 M) for MR imaging. Care was taken to avoid tissue folding within the agarose gel. The orientation of mucosal and serosal surface in the MRI vial was marked. Photos were taken of gross specimens to document specimen orientation and aid in subsequent MRI – histopathology correlation.

Magnetic resonance imaging. All rectal cancer and normal rectum tissue specimens were scanned on the Bruker Avance II 500 MHz (11.7 tesla) wide bore MRI spectrometer at the Western Sydney University Biomedical Magnetic Resonance Facility. The MRI vials were placed in the MRI bore with the specimen mucosal surface orientated to the left, and serosal surface orientated to the right of the MRI bore. An initial 3-dimensional MRI with 100 µm voxels (using Bruker's TurboRARE-3D method with RARE factor 2, repetition time 300 ms, echo time 10.34 ms, 90° excitation pulse and 4 averages) was acquired for some specimens to facilitate anatomical registration of MR images with histopathology until it was determined that the A0 data from the DTI scan was equally suitable for this task. Three-dimensional spin-echo DTI were acquired with isotropic voxel resolution of 200 µm with b-values 200, 800, and 3200 s/mm^2. The FOV was 27 × 27 mm in the axial plane and typically between 12 and 16 mm longitudinally depending on the length of the specimen. The echo time was 26 ms and repetition time was 900 ms. Eight diffusion directions were acquired with 3 diffusion experiments per direction. One A0 (i.e., $b = 0$) image was acquired. The diffusion gradient separation was 15 ms, and diffusion gradient duration was 5 ms. No image acceleration such as echo-planar imaging (EPI) was used leading to relatively long experimental times between 41 and 67 hours.

Histopathology examination. Following *ex vivo* MR imaging, the rectal cancer and normal rectum tissue specimens were histologically examined by light microscopy. Specimens were sectioned axially from mucosal surface to serosal surface, as per conventional histopathology sectioning for diagnostic purposes. The slice thickness was 90 µm. Sections were mounted onto slides and stained with haematoxylin and eosin (H&E) stain, masson trichome stain and elastic Van Gieson (eVG) stain. Unmarked histopathology slides were scanned with an Aperio ScanScope Model CS digital scanner at 40× resolution. Histopathology slides could be viewed at any resolution up to a maximum resolution of 40× (0.25 µm/pixel) using the zoom window.

H&E stains were used to assess cancer and normal rectum ultrastructure. The masson trichome and eVG stains were used to analyse the extracellular matrix ultrastructure, and identify regions of desmoplasia and fibrosis. Histopathology assessment was undertaken by a pathologist with sub-specialisation in gastrointestinal pathology. Regions of interest were annotated on the digital histopathology images, viewed via Aperio ImageScope (version 12.3.2.9013). The following regions of interest were annotated on rectal cancer digital histopathology

images: (a) cancer (b) cancer-associated desmoplasia (c) fibrous tissue and (d) non-malignant rectum (if present). The histologic sub-type and depth of carcinoma invasion into the rectal wall was also assessed. The following regions of interest were annotated on normal rectum digital histology images: (a) mucosa (b) submucosa (c) muscularis propria and (d) serosa. Any additional regions of interest that were identified in the histopathology specimen, such as granulation tissue, were also annotated.

MRI - Histopathology correlation and co-registration. A pathologist sub-specialising in lower gastrointestinal malignancy, and a radiation oncologist with MRI expertise sub-specialising in lower gastrointestinal malignancy worked together to match the MRI with histopathology. Either the 3-dimensional MRI TurboRARE sequence or the A0 data from the DTI scan was used to select the MRI slice that visually matched with histopathology. As the MRI voxels acquired were isotropic, the MRI data could, through software processing, be visualised along arbitrary axes to ensure a good match with histopathology. The documented orientation of mucosal and serosal surfaces in the MRI vial, gross specimen images, and histopathology slicing direction (axial from mucosal to serosal surface) were used to indicate virtual slicing direction on MRI TurboRARE images to match the histopathology slice. The MRI TurboRARE dataset was aligned with the DTI-MRI dataset, allowing for automatic translation of the selected MRI TurboRARE slice to the corresponding DTI-MRI slice for analysis. Anatomic landmarks that were identifiable on both the MRI TurboRARE sequence and H&E slides were used to correlate MRI with histopathology. These landmarks included the specimen contour along the outer and inner rectal wall (including peaks and curvatures along the edges), mucosal surface, muscularis propria, serosal surface, and blood. A minimum of 7 landmarks were identified for MRI – histopathology correlation. Tissue regions, including tumour, fibrous tissue, desmoplasia, and rectal wall layers, identifiable on both modalities were contoured on corresponding DTI-MRI and histopathology images for subsequent evaluation of co-registration.

The DTI-MRI slice for analysis and annotated histopathology image were then co-registered to validate the visual match. A rigid co-registration method developed by Reynolds *et al.*[11] was used to fuse the DTI-MRI slice with annotated histopathology using the MATLAB Image Processing Toolbox software R2018a version 16.4 (MathWorks, Natick, United States). This co-registration method was previously quantitatively validated by Reynolds *et al.* and found to have a mean distance of 0.57 mm between control points after registration[11]. To initialise the registration between annotated histopathology and DTI-MRI, multiple control points were placed on the MR image and histopathology image. The pathologist and radiation oncologist worked in conjunction to select a minimum of 7 control points based on histopathology landmarks described above. The co-registration method used the co-ordinates of the control points to compute a similarity transformation, by minimising the Euclidean distance between the selected control points.

The *ex vivo* MRI – histopathology co-registration results were then qualitatively validated by the pathologist and radiation oncologist working in conjunction. This involved visual assessment of alignment on co-registered *ex vivo* MRI – histopathology of (i) anatomic landmarks used to drive registration, (ii) additional tissue regions of interest contours, including tumour, desmoplasia, fibrous tissue and rectal wall layers, independent of those used to drive registration, and (iii) geometry of the tissue specimen.

MRI analysis. Histopathology was the standard reference for analysis. Regions of interest for analysis on annotated histopathology slides were identified on the matching DTI slice by visual inspection. MR image and quantitative measurements of DTI were performed in Amira 6 (FEI Visualization Sciences Group, Mérignac Cedex, France). The rectal tissue specimen was contoured on the selected DTI slice for analysis to provide a rectal mask. For MRI analysis, regions of interest were placed on cancer, desmoplasia, fibrous tissue, mucosa, submucosa, and muscularis propria. All voxels within regions of interest were included for analysis. The A0, ADC and FA maps were generated from the DTI-MRI dataset and used to probe rectal cancer stromal heterogeneity. To completely determine the diffusion tensor, diffusion measurements along at least six non-collinear directions are required. A0 and ADC can both be acquired from a subset of directions but FA requires determination of the full diffusion tensor.

The signal intensity from the A0 images were obtained. ADC values were calculated using the formula $ADC = (D_{xx} + D_{yy} + D_{zz})/3$ where D_{xx}, D_{yy} and D_{zz} are the diagonal elements of the diffusion tensor. The FA values were calculated using the formula

$$FA = \sqrt{\frac{3}{2}} \frac{\sqrt{(\lambda_1 - \langle\lambda\rangle)^2 + (\lambda_2 - \langle\lambda\rangle)^2 + (\lambda_3 - \langle\lambda\rangle)^2}}{\sqrt{(\lambda_1^2 + \lambda_2^2 + \lambda_3^2)}}$$

where the λ_1, λ_2, λ_3, and $\langle\lambda\rangle$ are the diffusion eigenvalues in three orthogonal directions and their average value, respectively[12]. FA maps were generated on a voxel-by-voxel basis with FA = 0 indicating isotropic diffusion (disorganised) and FA = 1 indicating anisotropic diffusion (organised) and provide a greyscale image of variations in fractional anisotropy. Direction encoded colour FA maps that show anisotropy in different colours according to the direction of the major axis were also produced; the colours green, blue and red were assigned to three orthogonal orientations.

Statistical analysis. A linear mixed-effects model using a random intercept to control for repeated measures on the same individual was used to explore the relationship between estimated mean A0, ADC, and FA and tissue regions of interest. Following determination that the mean A0, ADC, and FA for at least one pair of tissue regions differed significantly, Dunnett's multiple comparisons[13] with control (cancer) methods were used to determine which tissue regions (if any) differed compared to cancer. A 5% significance level was used throughout the paper. The fold difference in A0, ADC and FA between cancer and other tissue regions was calculated using the ratio of mean values. Fold difference provides a useful unitless interpretation of the differences allowing comparison

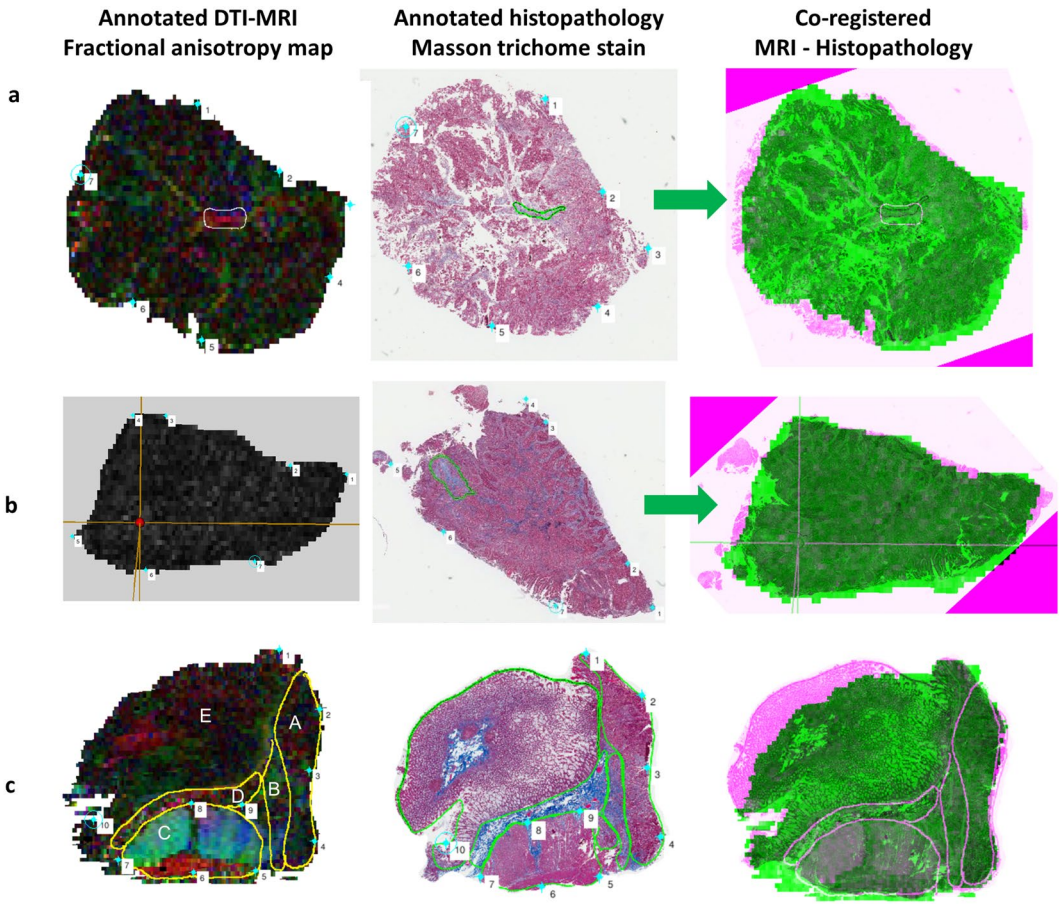

Figure 1. MRI – Histopathology co-registration process. Images for co-registration process performed using a co-registration method developed by Reynolds *et al.*[11]. The diffusion tensor imaging fractional anisotropy (FA) map (first column) was fused with the annotated histopathology (middle column). The MRI-histopathology co-registration image in shown in the last column. **(a)** A region of fibrous tissue was contoured on FA map and histopathology. Evaluation of the co-registration results showed good correlation between MRI and histopathology. **(b)** A region of demosplasia annotated on the FA map (cross-hairs) and histopathology matched well on the MRI-histopathology image. There was a small triangular area of tissue fragmentation that occurred during histopathology slicing and mounting onto the slide. **(c)** The contoured regions of interest on FA map and histopathology match well on the co-registered image. Annotated regions were A cancer, B desmoplasia, C muscularis propria, D fibrous tissue and E mucosa. Mucosa was flattened on histopathology mounting, resulting in some co-registration discrepancy in this region. The results show the value of MRI in assessing the true geometry of the tissue, within minimal distortion, allowing for MRI-histopathology correlation.

between the MRI measurements. A number of packages within R version 3.5.1 (R Core Team 2018, Vienna, Austria) statistical software were used for all analyses.

Results

Patients. A total of 10 rectal tissue specimens were collected by the SWSLHD CONCERT Biobank for this study from 5 patients with a diagnosis of rectal adenocarcinoma undergoing surgery. Three patients were male, two were female. The age range was 56–89 years. All patients had upper rectal tumours. All patients underwent primary surgery; 4 patients had an anterior resection and 1 had a pelvic exenteration. No patients had neoadjuvant radiotherapy or chemotherapy. Nine rectal tissue specimens were analysed at 11.7 tesla. One normal rectal specimen which was analysed at 14 tesla was excluded.

MRI – Histopathology co-registration. MR images and histopathology analysis showed that the tissue preparation method used in this study was able to maintain tissue integrity between MR scanning and histopathology. The MRI – histopathology co-registration results shown in Fig. 1 confirmed good correlation between annotated MRI and histopathology. Qualitative assessment of the co-registration results demonstrated good alignment of anatomic landmarks used to drive registration, additional annotated regions of interest and tissue geometry between *ex vivo* MRI and histopathology (Fig. 1). The results demonstrated good geometric preservation of the rectal specimens from MR analysis to histopathology analysis. The suspension of rectal specimens within the agarose gel allowed prevention of tissue folding during MR imaging. Our co-registration results showed there was a minimal amount of tissue fragmentation, which occurred at the step of histopathology slicing

and mounting onto slides. The results show the value of MRI in being able to assess the true geometry of the specimen and avoid fragmentation and distortion, thereby allowing for direct correlation with histopathology analysis of the same tissue sample after MR imaging.

Diffusion tensor imaging evaluation of rectal cancer stroma and adjacent normal rectum. Ultra-high resolution DTI-MRI was able to depict stromal heterogeneity in rectal cancer. Of the A0 images, ADC maps and diffusion encoded colour FA maps, the diffusion encoded colour FA maps provided the best contrast for depicting the different tissue regions of interest. The A0 images showed that cancer had a higher signal intensity compared to fibrous tissue (Fig. 2a). However, the differences between cancer and other tissue regions of interest were less obvious on qualitative evaluation of the A0 images. On the ADC maps it was difficult to differentiate the different tissue regions of interest on qualitative evaluation. The direction encoded colour FA maps exhibited relatively low signal intensity in regions of cancer, indicating relatively isotropic diffusion (Fig. 3). DTI-MRI allowed heterogeneity within the cancer stroma to be visualised, with regions of relatively high signal intensity corresponding to desmoplasia (Figs 2 and 4) or normal fibrous tissue (Figs 2 and 3) on direction encoded colour FA maps. Cancer invasion into muscularis propria (stage T2) was identifiable in the direction encoded colour FA map (Fig. 2). Muscularis propria was clearly distinguished from tumour, with muscularis propria having high signal intensity with highly anisotropic FA maps (Figs 2, 4 and 5). Muscularis propria, and its different muscular fibre orientations of the inner circular and outer longitudinal layers were able to be visualised on the direction encoded colour FA maps, and corresponded well with histopathology. Amongst the A0 images, ADC maps and direction encoded colour FA maps, muscularis propria was most clearly distinguished from cancer on the direction encoded colour FA maps.

A0, ADC and FA values of rectal cancer and adjacent normal rectum. The DTI-MRI derived A0, ADC and FA mean estimate and standard error for rectal cancer and other tissue regions of interest are tabulated in Table 1. The A0 mean of cancer was significantly higher than all other tissue regions of interest ($p < 0.001$). The A0 image was most useful in discriminating between cancer and fibrous tissue ($\times$ 0.37 fold difference compared with cancer). The ADC mean of cancer was significantly lower than desmoplasia ($p = 0.046$), fibrous tissue ($p = 0.026$), mucosa ($p < 0.001$) and submucosa ($p < 0.001$), and significantly higher than muscularis propria ($p < 0.001$). The ADC mean was useful in discriminating between cancer and submucosa ($\times$ 1.82 fold increase compared with cancer). However, the fold differences in ADC for cancer and other tissue regions were very small ($\times$ 0.93–1.09). The FA mean of cancer was significantly lower than desmoplasia, fibrous tissue, submucosa and muscularis propria ($p < 0.001$). The FA mean of cancer was low (0.14) indicating near-isotropic diffusion and lack of stromal organisation. Desmoplasia and fibrous tissue had moderate mean FA values (0.31, and 0.34, respectively), indicating some degree of tissue organisation. Muscularis propria had high mean FA value (0.61), indicating highly organised and anisotropic diffusion. FA was most useful in discriminating between cancer and desmoplasia ($\times$ 2.15 fold increase compared with cancer), fibrous tissue ($\times$ 2.37 fold increase compared with cancer), and muscularis propria ($\times$ 4.25 fold increase compared with cancer).

Figure 6 shows A0, ADC and FA box plots summaries for each tissue region of interest. The box plots summarise the upper and lower quartiles, and median values. Of the A0, ADC and FA box plots, FA had the greatest separation of median values and interquartile ranges between cancer and desmoplasia, fibrous tissue and muscularis propria. The box plots show that FA discriminates the most between cancer and desmoplasia, fibrous tissue, or muscularis propria.

Discussion

This exploratory MRI – histopathology correlative study demonstrated the ability of DTI-MRI to assess rectal cancer stromal heterogeneity and tumour extent *ex vivo*. The DTI-MRI derived A0, ADC and FA values were able to differentiate between cancer and other tissue regions (desmoplasia, fibrous tissue, mucosa, submucosa and muscularis propria). The A0 images were useful in discriminating between cancer and fibrous tissue. The differences in ADC values between cancer and other tissue regions were very small. The direction encoded colour FA maps and FA values provided the best discrimination between cancer and regions of desmoplasia, fibrous tissue and muscularis propria. DTI revealed that tumour is disorganised and consequently has relatively isotropic diffusion (low FA). In contrast, desmoplasia and normal fibrous tissue have moderate stromal organisation and significantly higher FA than cancer. DTI was also useful in assessing the depth of tumour invasion into the rectal wall. DTI enabled clear differentiation of tumour from muscularis propria which was highly organised and anisotropic, allowing for detection of tumour infiltration into muscularis propria. This finding could be particularly useful in the differentiation between stage T1 and T2 tumours. This study has shown that FA constitutes a potential novel MRI biomarker of rectal cancer stromal organisation and infiltration *ex vivo*.

For each of the specimens three derived images were obtained from the DTI experiments, these being the A0, FA and ADC. Of these, the ADC and FA are derived from the diffusion tensor and are theoretically instrumentation independent. The A0 image is the intensity image when the diffusion gradients are zero. Its voxels are weighted by T_1, T_2 and proton density and its contrast is more dependent on the instrument and parameters. Thus the ADC and FA results are more suited to clinical translation as the contrast between tissue types should remain similar across instrumentation.

Our MRI – histopathology co-registration results demonstrated good correlation between MRI and histopathology. This study demonstrated the value of MRI in assessing the true geometry of tissue with little deformation. Tissue preparation and MRI scanning in this study resulted in no tissue destruction between imaging and histopathology, allowing for direct correlation with 'ground-truth' histopathology for analysis. The method of tissue fixation and suspension in agarose gel ensured preservation of tissue geometry and orientation from MR imaging to histopathology slicing resulting in a good match between MRI and histopathology. This study

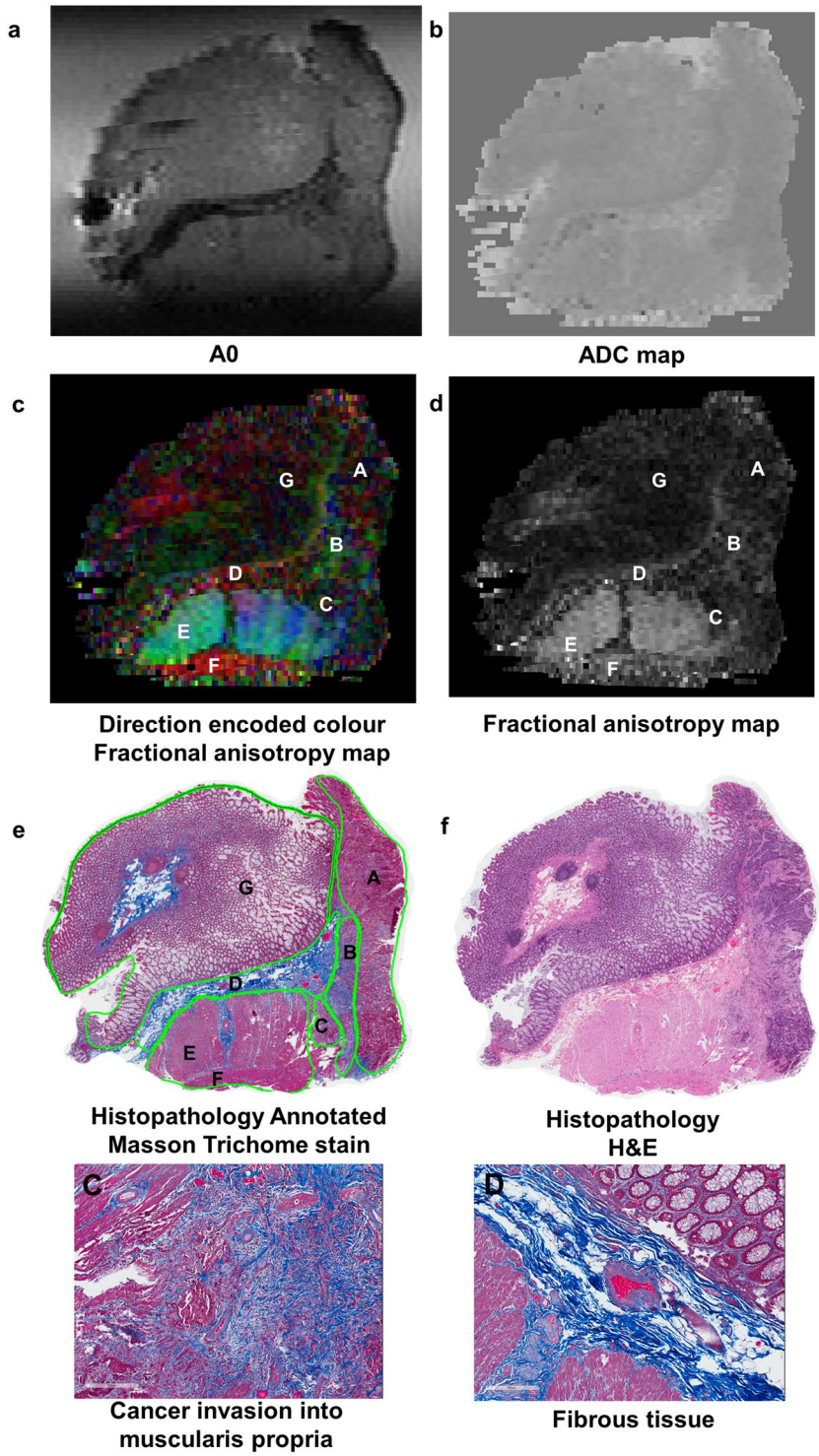

Figure 2. High field DTI-MRI and histopathology correlation results for rectal cancer tissue specimen 1. The DTI-MRI images shown are **(a)** A0, **(b)** ADC map, **(c)** direction encoded colour fractional anisotropy (FA) map, and **(d)** FA map. The corresponding histopathology is shown in **(e)** and **(f)**. The annotated regions on the diffusion tensor image and histopathology (including zoomed images) are: A cancer B desmoplasia C cancer invasion into muscularis propria D fibrous tissue E muscularis propria inner circular layer F muscularis propria outer circular layer and G mucosa. The A0 image was able to identify the band of fibrous tissue which had lower signal intensity. Cancer appeared hypointense on the ADC map, indicating restricted diffusion in cancer. The direction encoded colour FA map was the best MRI image for distinguishing the different tissue regions of interest; cancer and muscularis propria were most clearly distinguished on this image.

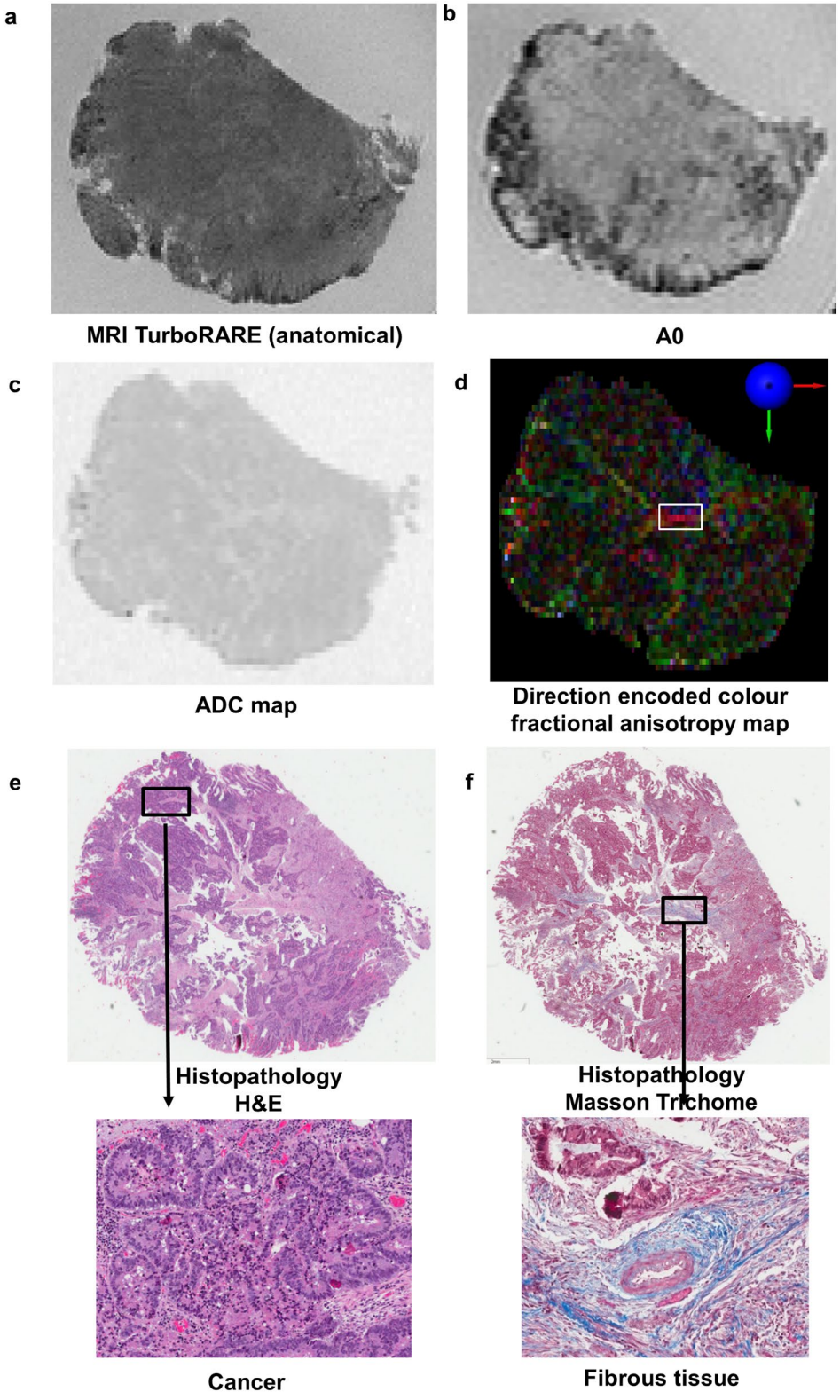

Figure 3. High field DTI-MRI and histopathology correlation results for rectal cancer tissue specimen 2. **(a)** An MRI TurboRARE image was used as the reference image to obtain the same slice on the DTI-MRI dataset as histopathology for analysis. The DTI-MRI images shown are **(b)** A0, **(c)** ADC map, and **(d)** direction encoded colour fractional anisotropy map. **(e)** Histopathology haematoxylin and eosin (H&E) stain with a region of cancer zoomed in. **(f)** Histopathology masson trichome stain with a region of mature fibrous tissue zoomed in. The direction encoded colour fractional anisotropy map was the best DTI-MRI derived image to identify fibrous tissue within the cancer specimen; fibrous tissue had brighter signal intensity and higher fractional anisotropy value than cancer.

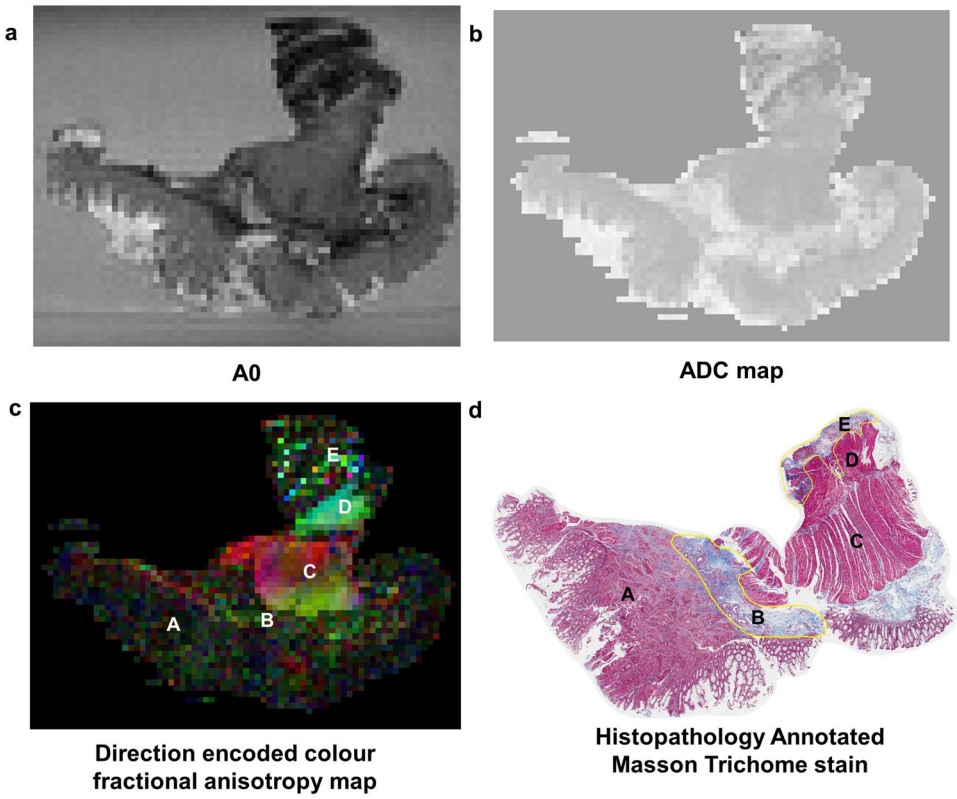

Figure 4. High field MRI and histopathology correlation results for rectal cancer tissue specimen 3. The MRI images shown are **(a)** A0, **(b)** ADC map, and **(c)** direction encoded colour fractional anisotropy (FA) map. The annotated regions are diffusion tensor image and histopathology are: A cancer B desmoplasia C muscularis propria inner circular layer D muscularis propria outer longitudinal layer and E heterogeneous regions of granulation tissue and inflammation. The direction encoded colour FA map was the best image to distinguish the different tissue regions of interest; muscularis propria was clearly distinguished from cancer on this image.

used an *ex vivo* MRI – histopathology co-registration framework developed and validated by Reynolds *et al.*[11]. The quantitative validation of the co-registration method by Reynolds *et al.* demonstrated a mean distance of 0.57 mm (range 0.06–1.99 mm) between the control points after registration. Various other MRI – histopathology correlation methods have been used in previous studies. Yamada *et al.* examined oesophageal and gastric cancer tissue *ex vivo* using DTI-MRI at 7 tesla[14,15]. They performed a qualitative visual correlation between MRI and histopathology, without formal co-registration, in their analysis. A technique for co-registration of *in vivo* MRI with histopathology in rectal cancer has been developed by Antunes *et al.*[16]. Antunes *et al.* imaged *in vivo* at 3 tesla. For *in vivo* imaging and histopathology co-registration, there are additional factors leading to tissue deformation that need to be considered. Rectal peristalsis *in vivo*, surgical removal of rectum and tissue fixation can lead to tissue deformation, shrinkage and distortion of tissue geometry between *in vivo* imaging and histopathology. A deformable registration process was used by Antunes *et al.* to overcome this. The spatial alignment strategies used in this study were similar to that used by Antunes *et al.*, with both studies visually identifying landmarks on histopathology corresponding to edges or curvatures along the rectal wall to drive the MRI – histopathology co-registration procedure. Antunes *et al.* quantitatively validated their co-registration results by using additional independent landmarks. Their quantitative validation demonstrated excellent co-registration with overall deviation of 1.50+/−0.63 mm between *in vivo* MRI and histopathology. The present study performed a qualitative validation of the co-registration. A quantitative validation of the co-registration results was not performed, as the co-registration method had previously been validated. The present study was performed at ultra-high field (11.7 tesla). A huge advantage of ultra-high field imaging is that the high resolution images allows excellent visualisation of tissue regions such as rectal wall layers and fibrous tissue, otherwise not seen at low field, to then validate co-registration results. Ultimately, the 'microscopic' resolution of images at ultra-high field allows visual confirmation of the co-registration results.

MRI plays an important role in the primary staging of rectal cancer, and is the staging imaging of choice. Despite the important role of conventional MRI for staging rectal cancer, there are some limitations. Conventional high spatial resolution T_2-weighted MRI has moderate reproducible accuracy in the prediction of tumour stage of rectal cancer, with accuracy of 67% and 83% by 2 independent observers in a study by Beets-Tan *et al.*[17] A study by Brown *et al.* found that the majority of disagreements between thin-slice T_2-weighted MRI and histopathology were between T1 and T2 tumours, and between T2 and T3 tumours[18]. Conventional MRI is poor at separating stage T1 from stage T2 rectal tumours, making it inadequate in the selection of patients for local excision[4,5,18,19]. A desmoplastic reaction in rectal cancer can also pose challenges in accurate staging of rectal

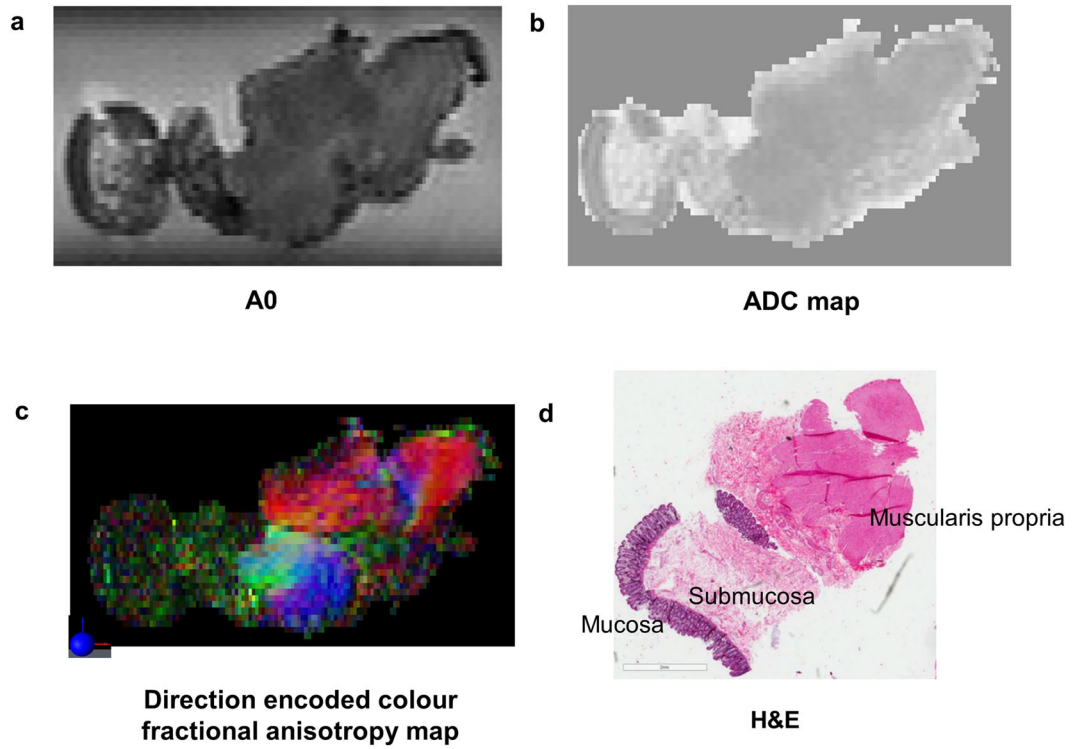

Figure 5. High field MRI and histopathology correlation for adjacent normal rectum tissue. The muscularis propria layer was most clearly identified on the direction encoded colour FA map.

Tissue region of interest	A0		ADC		FA	
	Mean (SE) and p-value for comparison with cancer	Fold difference compared with cancer	Mean (SE) and p-value for comparison with cancer	Fold difference compared with cancer	Mean (SE) and p-value for comparison with cancer	Fold difference compared with cancer
Cancer	12405 (693)		0.002508 (0.00018)		0.1441 (0.011)	
Desmoplasia	8346 (766) $p < 0.001$	× 0.67	0.002736 (0.00019) $p = 0.046$	× 1.09	0.3096 (0.016) $p < 0.001$	× 2.15
Fibrous tissue	4646 (723) $p < 0.001$	× 0.37	0.002680 (0.00019) $p = 0.026$	× 1.07	0.3413 (0.013) $p < 0.001$	× 2.37
Mucosa	10543 (708) $p < 0.001$	× 0.85	0.002751 (0.00018) $p < 0.001$	× 1.09	0.1389 (0.012) $p = 0.956$	× 0.96
Submucosa	9612 (712) $p < 0.001$	× 0.77	0.004567 (0.00018) $p < 0.001$	× 1.82	0.1849 (0.012) $p < 0.001$	× 1.28
Muscularis propria	9896 (692) $p < 0.001$	× 0.80	0.002329 (0.00018) $p < 0.001$	× 0.93	0.6127 (0.011) $p < 0.0001$	× 4.25

Table 1. Estimated A0, apparent diffusion co-efficient (ADC), and fractional anisotropy (FA) means and standard errors (SE) (from the linear mixed effects model) for each tissue region of interest with p-values from Dunnett's multiple comparison with cancer, and fold difference compared with cancer.

cancer, as desmoplastic stranding can appear similar to tumour on MRI, resulting in overestimation of tumour extent. The presence of fibrous tissue can also lead to staging difficulty as this has similar appearance to tumour on conventional T_2-weighted MRI[20]. This study has shown that DTI-MRI was clearly able to differentiate cancer from muscularis propria. DTI-MRI was able to visualise tumour invasion into muscularis propria, with disruption of the muscularis propria at the invasive tumour front. In addition, DTI-MRI was able to assess cancer stromal heterogeneity and was able to distinguish desmoplasia or normal fibrous tissue, with these regions having significantly higher FA than cancer. FA was able to characterise fibril anisotropy as a probe of stromal microenvironment.

This study has also shown the power of quantitative analysis of DTI-MRI in detecting differences in A0, ADC and FA between cancer and other tissue regions that were not obvious on qualitative review of the images. The FA value for cancer was significantly different compared with all other tissue regions, except mucosa. DTI-MRI may add value in more accurately defining tumour extent in rectal cancer which would assist with surgical planning and warrants further investigation. Yamada *et al.* have examined DTI-MRI at 7 tesla in oesophageal and gastric

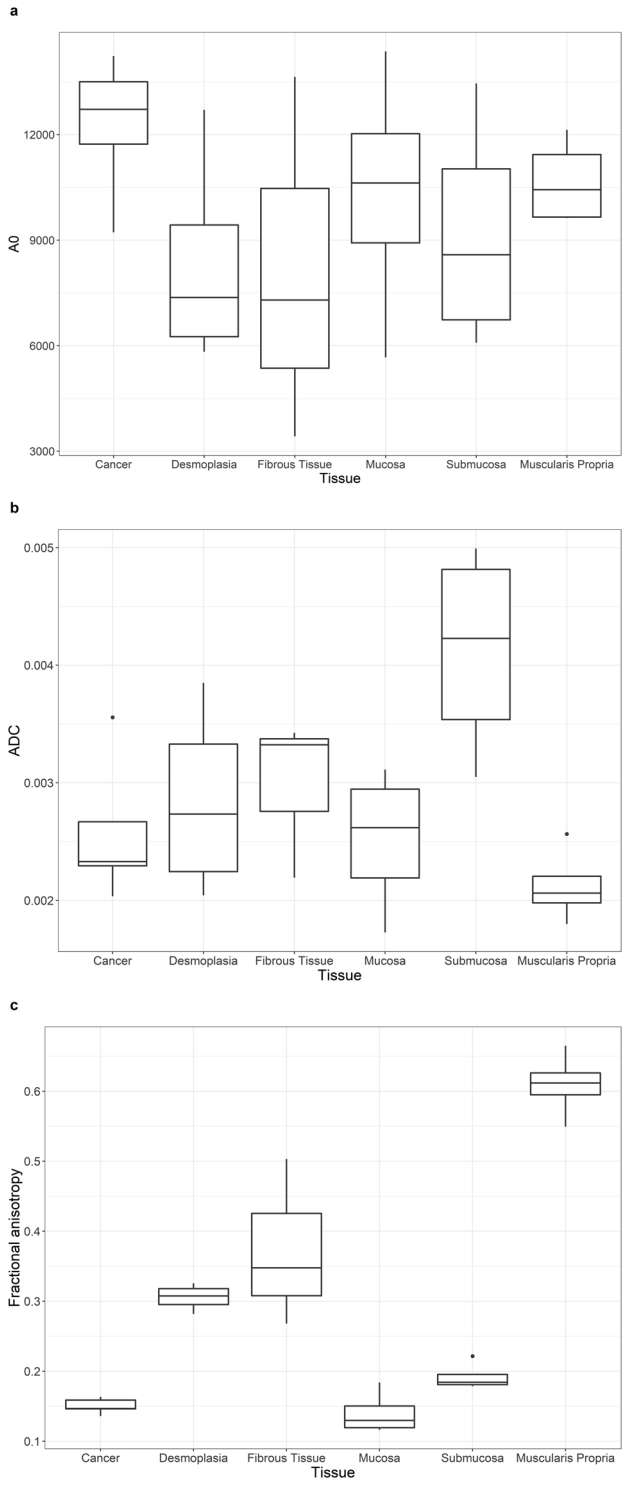

Figure 6. Box plots of (**a**) A0, (**b**) apparent diffusion co-efficient (ADC) and (**c**) fractional anisotropy (FA) values for each tissue region of interest for all patients. The boxes represent the 25th to 75th percentile (interquartile range), the lines within the box represent the median values and the whiskers show the range of values. The dots are outliers. The box plots showed that FA had the clearest contrast between cancer and desmoplasia, fibrous tissue and muscularis propria.

cancers *ex vivo* and found that DTI was a feasible means of evaluating mural depth of invasion[14,15,21]. To the best of our knowledge, there are no other published studies examining the role of DTI-MRI in rectal cancer.

This study was performed on an ultra-high field 11.7 tesla MRI, with a magnet bore size of 89 mm. An advantage of higher field is the approximately linear increase in signal, resulting in the potential to acquire data with

improved spatial resolution. An increase in signal-to-noise ratio is also important for functional imaging techniques. Most clinical MRI systems are now available at both 1.5 and 3 tesla, and it is anticipated that over the next decade the market share of clinical MRI systems will change toward higher field strengths[22]. Human MRI scanners at 7 tesla have been installed in recent years[23,24]. Preliminary results from human brain MRI studies at 9.4 tesla have indicated that safe and successful human imaging is feasible at even higher field strengths[25]. Ongoing work into increasing the field strengths of clinical MRI scanners and the adoption of clinical 7 tesla MRI scanners, should facilitate the translation of this DTI-MRI protocol to clinical usage.

This study focused on the potential of DTI-MRI in the differentiation of stromal heterogeneity and primary staging of rectal cancer. Our results demonstrated the feasibility of DTI-MRI in distinguishing fibrosis from tumour. We propose that this finding could be useful in the assessment of chemoradiotherapy response and should be investigated in this setting. In patients who have received neoadjuvant chemoradiotherapy, the role of diffusion weighted imaging (DWI) in the clinical assessment of response is emerging[26–32]. However, the differentiation of radiotherapy-induced fibrosis from residual tumour on T_2-weighted and DWI-MRI remains a challenge[33]. Radiotherapy-induced fibrosis can result in restricted diffusion that is detectable in DWI, mimicking the appearance of residual tumour and making it difficult to correctly identify pathologic complete responders to chemoradiotherapy. Jang *et al*. found that 42% of patients with pathologic complete response had restricted diffusion on DWI-MRI, and that radiotherapy-induced fibrosis was a significant predictor of diffusion restriction. The potential of DTI-MRI has not yet been investigated in patients who have received neoadjuvant radiotherapy; whether DTI-MRI can add value to current clinical MRI techniques in distinguishing residual tumour from fibrosis and contribute to radiotherapy response assessment should be investigated.

There were a number of limitations in this study. Firstly, the sample size in this study was small due to the limited number of rectal cancer patients participating in CONCERT Biobank. Secondly, this study did not compare DTI-MRI with standard T_2-weighted MRI. A future study with a larger sample size would enable assessment of the accuracy (sensitivity and specificity) of DTI-MRI in defining tumour extent in rectal cancer compared with conventional T_2-weighted MRI. Thirdly, the scan time was considerably long. Reducing the number of *b*-values and utilising image acceleration would substantially reduce the scan time. We are currently working on further DTI-MRI experiments at 7 and 9.4 tesla fields to facilitate clinical translation of our findings.

In conclusion, this exploratory MRI-histopathology correlative study demonstrated the ability of DTI-MRI to examine rectal cancer stromal heterogeneity and tumour extent at high field *ex vivo*. DTI-MRI derived A0, ADC and FA values made it possible to probe rectal cancer stromal heterogeneity. FA provided the best discrimination between cancer and desmoplasia, fibrous tissue and muscularis propria. This study has shown that FA is a potential novel biomarker of rectal cancer stromal organisation and tumour infiltration, *ex vivo*. DTI-MRI at 11.7 tesla was able to differentiate tumour regions from desmoplasia or fibrous tissue *ex vivo*; cancer had relatively isotropic diffusion, whereas regions of desmoplasia or fibrous tissue had anisotropic diffusion with higher FA than cancer. DTI-MRI was also useful in assessing extent of tumour infiltration into the rectal wall. DTI was able to identify cancer invasion into muscularis propria, which was highly anisotropic and clearly able to be distinguished from tumour. Thus, DTI-MRI may provide clear characterisation of tumour stromal heterogeneity and accurate delineation of tumour extent in rectal cancer and warrants further investigation.

References

1. Heald, R. J. Total mesorectal excision is optimal surgery for rectal cancer: a Scandinavian consensus. *Br J Surg* **82**, 1297–1299 (1995).
2. Valentini, V. *et al*. Nomograms for predicting local recurrence, distant metastases, and overall survival for patients with locally advanced rectal cancer on the basis of European randomized clinical trials. *J Clin Oncol* **29**, 3163–3172 (2011).
3. Zeestraten, E. C., Kuppen, P. J., van de Velde, C. J. & Marijnen, C. A. Prediction in rectal cancer. *Semin Radiat Oncol* **22**, 175–183 (2012).
4. Beets-tan, R. G. *et al*. Magnetic resonance imaging for the clinical management of rectal cancer patients: recommendations from the 2012 European Society of Gastrointestinal and Abdominal Radiology (ESGAR) consensus meeting. *Eur Radiol* **23**, 2522–2531 (2013).
5. Brown, G. *et al*. Effectiveness of preoperative staging in rectal cancer: digital rectal examination, endoluminal ultrasound or magnetic resonance imaging? *Br J Radiol* **91**, 23–29 (2004).
6. Kalluri, R. & Zeisberg, M. Fibroblasts in cancer. *Nat Rev Cancer* **6**, 392–401 (2006).
7. Hanahan, D. & Weinberg, R. A. Hallmarks of cancer: the next generation. *Cell* **144**, 646–674 (2011).
8. Nebuloni, M. *et al*. Insight on colorectal carcinoma infiltration by studying perilesional extracellular matrix. *Sci Rep* **6**, 22522 (2016).
9. Yankeelov, T., Pickens, D. & Price, R. In Imaging in Medical Diagnosis and Therapy (ed. Henee, W.) (CRC Press Taylor & Francis Group, Boca Raton, F. L. 33487–2742, 2012).
10. Caixeiro, N., Aghmesheh, M., de Souza, P. & Lee, C. S. The Centre for Oncology Education and Research Translation (CONCERT) Biobank. *Open J Bioresourc* **2**, e3 (2015).
11. Reynolds, H. M. *et al*. Development of a registration framework to validate MRI with histology for prostate focal therapy. *Med Phys* **42**, 7078–7089 (2015).
12. Basser, P. J. & Pierpaoli, C. Microstructural and physiological features of tissues elucidated by quantitative-diffusion-tensor MRI. *J Magn Reson B* **111**, 209–219 (1996).
13. Hsu, J. C. Multiple comparisons: theory and methods. *Chapman and Hall UK* (1996).
14. Yamada, I. *et al*. Ultra-high-resolution MR imaging of esophageal carcinoma at ultra-high field strength (7.0T) *ex vivo*: correlation with histopathologic findings. *Magn Reson Imaging* **33**, 413–419 (2015).
15. Yamada, I. *et al*. Gastric carcinoma: Evaluation with diffusion-tensor MR imaging and tractography *ex vivo*. *Magn Reson Imaging* **34**, 144–151 (2016).
16. Antunes, J. *et al*. Coregistration of preoperative MRI with *ex vivo* mesorectal pathology specimens to spatially map post-treatment changes in rectal cancer onto *in vivo* imaging: preliminary findings. *Acad Radiol* **25**, 833–841 (2018).
17. Beets-Tan, R. G. H. *et al*. Accuracy of magnetic resonance imaging in prediction of tumour-free resection margin in rectal cancer surgery. *The Lancet* **357**, 497–504 (2001).
18. Brown, G. *et al*. Preoperative assessment of prognostic factors in rectal cancer using high-resolution magnetic resonance imaging. *Br J Surg* **90**, 355–364 (2003).
19. Stollfuss, J. C. *et al*. Rectal carcinoma: high-spatial-resolution MR imaging and T2 quantification in rectal cancer specimens. *Radiology* **241**, 132–141 (2006).

20. Beets-Tan, R. G. & Beets, G. L. Rectal cancer: review with emphasis on MR imaging. *Radiology* **232**, 335–346 (2004).
21. Yamada, I. *et al*. Gastric carcinoma: *ex vivo* MR imaging at 7.0 T–correlation with histopathologic findings. *Radiology* **275**, 841–848 (2015).
22. Liney, G. P. & Moerland, M. A. Magnetic resonance imaging acquisition techniques for radiotherapy planning. *Semin Radiat Oncol* **24**, 160–168 (2014).
23. Jin, J. *et al*. An open 8-channel parallel transmission coil for static and dynamic 7T MRI of the knee and ankle joints at multiple postures. *Magn Reson Med* **79**, 1804–1816 (2018).
24. U.S. Food and Drug Administration. FDA clears first 7T magnetic resonance imaging device, https://www.fda.gov/NewsEvents/Newsroom/PressAnnouncements/ucm580154.htm (2017).
25. Vaughan, T. *et al*. 9.4T Human MRI: Preliminary Results. *Magn Reson Med* **56**, 1274–1282 (2006).
26. Barbaro, B. *et al*. Diffusion-weighted magnetic resonance imaging in monitoring rectal cancer response to neoadjuvant chemoradiotherapy. *Int J Radiat Oncol Biol Phys* **83**, 594–599 (2012).
27. Intven, M., Reerink, O. & Philippens, M. Diffusion-weighted MRI in locally advanced rectal cancer. *Strahlenther Onkol* **189**, 117–122 (2013).
28. Monguzzi, L. *et al*. Locally advanced rectal cancer: value of ADC mapping in prediction of tumor response to radiochemotherapy. *Eur J Radiol* **82**, 234–240 (2013).
29. Cai, G. *et al*. Diffusion-weighted magnetic resonance imaging for predicting the response of rectal cancer to neoadjuvant concurrent chemoradiation. *World J Gastroenterol* **19**, 5520–5527 (2013).
30. Musio, D. *et al*. Diffusion-weighted magnetic resonance application in response prediction before, during, and after neoadjuvant radiochemotherapy in primary rectal cancer carcinoma. *BioMed Res Int* **2013**, 740195 (2013).
31. Carbone, S. F. *et al*. Diffusion-weighted MR volumetry for assessing the response of rectal cancer to combined radiation therapy with chemotherapy. *Radiology* **263**, 311 (2012).
32. Pham, T. T., Liney, G. P., Wong, K. & Barton, M. B. Functional MRI for quantitative treatment response prediction in locally advanced rectal cancer. *Br J Radiol* **90**, 20151078 (2017).
33. Jang, K. M. *et al*. Pathological correlation with diffusion restriction on diffusion-weighted imaging in patients with pathological complete response after neoadjuvant chemoradiation therapy for locally advanced rectal cancer: preliminary results. *Br J Radiol* **85**, e566–572 (2012).

Acknowledgements

We gratefully acknowledge the facilities and the scientific and technical assistance of the Australian National Imaging Facility, Western Sydney University Node (WSU Biomedical Magnetic Resonance Facility). The authors would like to thank Dr Hayley Reynolds for providing us with the MRI-histopathology co-registration code they developed. The authors would like to acknowledge the SWSLHD CONCERT Biobank, Mr Wayne Ng and Dr Nicole Caixeiro for assistance with collection and preparation of Biobank tissue specimens for MRI analysis, and Professor Hedley Coleman for assistance with digital scanning of histopathology slides. The authors would like to thank Professor Malcolm Hudson from the NHMRC Clinical Trials Centre for his review of the statistical analysis in this study.

Author Contributions

T.P., T.S.G., C.S.L., M.B., P.G., G.L., K.W. and W.S.P. designed the study protocol. T.P., T.S.G., C.S.L and W.S.P. performed experiments. T.P., T.S.G., C.S.L., M.B., P.G., G.L., K.W. and W.S.P. performed analysis, data interpretation and manuscript writing.

Additional Information

Competing Interests: The authors declare no competing interests.

Publisher's note: Springer Nature remains neutral with regard to jurisdictional claims in published maps and institutional affiliations.

Chapter 8 Future Directions in Rectal Cancer MRI

8.1 Introduction

This PhD work has investigated clinical functional diffusion (DWI) and perfusion (DCE) MRI biomarkers at 3.0 tesla in the assessment of tumour heterogeneity and prediction of radiotherapy response in patients with advanced stage rectal cancer. In addition, exploratory work was performed at ultra-high field 11.7 tesla on biobank rectal cancer tissue *ex vivo* to assess novel diffusion (DTI) biomarkers that could further assist in the quantification of rectal cancer heterogeneity, extent and prediction of radiotherapy response. Future work should investigate the application of radiomics and deep learning in improving the assessment of tumour heterogeneity and prediction of treatment response. In addition, new MRI strategies should focus efforts on accurate MRI selection of patients for organ-preservation treatment strategies. In early stage rectal cancer, this would involve the investigation of MRI to accurately select patients for local organ-sparing options such as local resection or contact X-ray therapy. In advanced stage rectal cancer, this would involve identifying MRI sequences to select patients with complete response to CRT for a 'watch-and-wait' pathway, and those with residual disease after CRT for an early contact X-ray therapy boost to attempt to improve response for a 'watch-and-wait' pathway. Ultra-high field MRI correlated with histopathology could be used as a 'ground-truth' to explore new MRI functional biomarkers that could assist with assessment of tumour extent and treatment response. Ultimately, a MRI virtual whole tumour 'biopsy' of tumour extent and treatment response could be used for real-time tracking, adaption and targeting of tumour function on the MRI-Linac. Early work on the Australian MRI-Linac is described in this chapter.

8.2 Radiomics and deep learning for assessment of tumour heterogeneity

This PhD work used a simple manual 2 parameter voxelised histogram analysis method in the MRI assessment of tumour heterogeneity. This is a simple method of assessing tumour heterogeneity for prediction of CRT response and may be faster to translate to

the clinic. There are likely to be other tumour heterogeneity features, such as textural and spatial heterogeneity, on functional imaging that are be difficult for the clinician to visually detect and segment. Extraction of other heterogeneity features on functional MRI may improve the accuracy of response prediction.

Radiomics and deep learning are emerging as strategies to analyse intra-tumoural heterogeneity. Radiomics is computational, high-throughput analysis of medical images that can extract hundreds to thousands of quantitative imaging parameters to characterise tumour phenotypes. Deep learning is a subset of machine learning and artificial intelligence that used to analyse radiomics data, together with clinical parameters to build clinical prediction models for use in personalised medicine. In locally advanced rectal cancer, Nie et al (51), and Liu et al (60), have used radiomics assessment of MRI for prediction of CRT response. Nie et al extracted 103 imaging features, including texture and histogram features, from baseline multi-parametric MRI (DWI and DCE) of 48 patients undergoing CRT in rectal cancer (51). They also compared a conventional volume-averaged analysis with a voxelised heterogeneity analysis method, and found that the latter had better prediction accuracy. Liu et al extracted 2252 radiomics features from T2-weighted and DWI MRI pre- and after CRT in 222 patients (60). They developed and validated a radiomics model comprising of 30 selected features for prediction of pCR response to CRT. A study by Bibault et al combined deep learning and radiomics to predict pCR in rectal cancer patients undergoing CRT (61). They extracted 1683 radiomics features from 95 patients and created a deep neural network to predict response. The deep neural network predicted pCR with 80% accuracy.

There are challenges for the clinical translation of radiomics and deep learning models to support clinical decision making. These include the complex computing workflows that are challenging to reproduce, high false-positive rates from extraction of a huge amount of imaging parameters from limited number of patients, and reporting of overly optimistic results, all of which affect generalisability of radiomics models from studies (62). The clinical relevance of new deep learning models will need to be tested in prospective patient cohorts in future studies. Standardisation of MRI biomarker

collection and reporting is a major challenge in quantitative MRI analysis. Work in this area is required for collation of big data for radiomics, reproducibility and validation. The Image Biomarker Standardisation Initiative (IBSI) is an international collaboration that addresses this challenge through the standardisation of MRI biomarker definitions and image processing steps, and provision of reporting guidelines (63).

8.3 New MRI and treatment strategies for early stage rectal cancer

More accurate staging of early stage rectal cancers would enable appropriate selection of patients for individualised, organ-sparing treatment options. Standard MRI techniques using T2-weighted imaging is unable to accurately differentiate between T1 and T2 tumours, and endoscopic ultrasound is currently the recommended imaging modality of choice by the European Society of Gastrointestinal and Abdominal Radiology (ESGAR). Multiple organ-sparing options for patients with localized early stage rectal cancer are emerging. Local resection techniques such as transanal excision are now options for patients with superficial T1 rectal cancers (64). Another organ-sparing technique for patients with small T1 rectal tumours (<3cm) is contact X-ray brachytherapy (also called 'Papillon' technique) (65). Accurate tumour staging is of paramount importance for the appropriate selection of patients for these treatment strategies. The SPECC (significant polyps and early colorectal cancer) initiative has identified the need for greater precision in preoperative assessment of early rectal cancer (66). The UK MINSTREL trial assessed the performance of high-resolution MRI in assessment of early rectal cancer. High resolution T2-weighted MRI parameters were defined as 3mm slice thickness, no inteslice gap and a matrix of 256 x 256 (0.6 mm x 0.6 mm x 3 mm resolution), acquired using a standard surface phased array coil at 1.5 T. High resolution MRI was able to assess depth of cancer invasion into rectal wall with an accuracy of 89% compared with gold standard histopathology (67). High resolution MRI allowed clearer visualisation of the rectal wall anatomy, and this MRI technique is now being prospectively evaluated for the selection of early rectal cancer for organ preservation through transanal excision.

This PhD work has shown the value of functional MRI techniques, specifically DTI, in addition to anatomic techniques, in defining early rectal cancer lesions *ex vivo*. DTI-MRI could be investigated, in addition to high resolution anatomic MRI, in the assessment of early rectal cancer in the clinical setting in future studies. This could result in improved selection of early stage rectal cancer patients for local treatment techniques such as local excision or contact X-ray brachytherapy.

8.4 New MRI and treatment strategies for advanced stage rectal cancer

In advanced stage rectal cancer, two management pathways are emerging as ways of avoiding surgical morbidity, depending on individual neoadjuvant CRT response. For patients who are responders to CRT, "watch-and-wait" is an option for patients to avoid surgery, and results from multiple cohorts have been reported (68-70). In these cohort studies, at least two-thirds of patients are able to avoid surgery, without development of local re-growth. Up to a third of patients on a "watch-and-wait" program develop tumour regrowth and the long term outcomes are uncertain. The UK OnCoRe study reported a local tumour regrowth rate of 34% after a median follow-up of 33 months, even though 88% of these recurrences were successfully salvaged. MRI assessment of CRT response was not standardised in these studies. Improvement of MRI for CRT response prediction is crucial for proper selection of patients before the "watch-and-wait" pathway can become standard care. For patients with incomplete response after completion of CRT, brachytherapy either with contact X-ray brachytherapy or HDR endoluminal or interstitial brachytherapy, is a treatment option to boost residual disease as a way of increasing the proportion of patients achieving a clinical complete response and allowing them to avoid surgery (71-72). The selection of appropriate brachytherapy boost modality depends on the size, depth, and endoluminal circumference of residual disease. Improvements in MRI prediction of CRT response would be required to appropriately select patients and boost modality, and also accurately target brachytherapy to residual disease.

New MRI strategies to better differentiate fibrosis and tumour would assist in improving the prediction and assessment of neoadjuvant radiotherapy response in patients with

locally advanced rectal cancer. Radiotherapy-induced fibrosis is seen on pathological examination of responders to radiotherapy. Currently, the imaging differentiation of radiotherapy-induced fibrosis from residual tumour remains a challenge on T2-weighted and DWI MRI. Radiotherapy-induced fibrosis mimics the appearance of tumour on DWI, with both showing restricted diffusion. This PhD work explored the use of DTI-MRI analysis of rectal tissue from patients with early rectal cancer and showed that FA was able to differentiate fibrosis from tumour. In addition, DTI derived A0 (morphologic) was found to be able to differentiate fibrosis from tumour. These findings could have relevance in the setting of advanced stage rectal cancer. A recent study showed that high resolution T2-weighted MRI allowed for clearer visualisation of rectal wall anatomy (66). A multi-parametric approach combining high resolution MRI and DTI could be explored in the setting of advanced stage rectal cancer to determine whether this could improve imaging prediction of radiotherapy response.

8.5 Clinical translation pipeline between pre-clinical (ultra-high field) and clinical field MRI

This PhD work has set up a part of an MRI biomarker discovery pipeline for screening biobank rectal cancer tissue at high field for new MRI biomarkers of tumour extent and radiotherapy response. An established MRI-Histopathology co-registration framework was used to allow direct correlation of MRI findings with 'ground-truth' histopathology. A huge advantage of high field MRI is that the ultra-high resolution images produced allow 'microscopic' visualisation of tissue details approaching the resolution seen on histopathology. This allows for investigation of new MRI sequences to search for 'ground-truth' histopathology features on high field MRI.

A link between ultra-high field MRI (11.7 – 14.0 tesla) and clinically relevant field MRI (0.5 to 3.0 tesla) needs to be established for translating 'ground-truth' findings at ultra-high field to clinical field strengths for clinical use. The immediate challenge is the lower signal to noise ratio and lower resolution images at clinical field strengths make it difficult for the clinician to visually identify 'ground-truth' features on the corresponding clinical field images. In addition, the thicker cut slices on lower field MRI make it difficult

to match the MRI accurately with histopathology. Single image super-resolution through deep learning is a method of obtaining high resolution output from a low resolution image (73). This has been mainly explored in applications outside of medical imaging. Deep learning-based super-resolution has been shown to be feasible in 2D photographic images (74) and histopathology coherent imaging systems (75). Single image super-resolution could provide a way to recover higher resolution information from clinical MR images obtained at clinical fields (0.5 – 3.0 tesla). Early studies have investigated deep learning based super-resolution in clinical musculoskeletal (76) and brain MRI (77) and found deep learning based super-resolution to outperform simplistic methods of interpolation of low resolution images into high resolution. These studies used high resolution (thin-slice) MRI at clinical fields as the 'ground truth' to train a deep learning algorithm to recover high resolution thin-slice images from lower resolution images.

Ultra-high field MRI correlated with histopathology would provide a truer 'ground-truth' image than a clinical field MRI to train a deep learning algorithm to create a super-resolution image from an MRI at clinical field. However there are no published MRI studies that have incorporated ultra-high MRI into the deep learning process. Deep learning could be explored as a method to recognise patterns on higher field MR images and extract these same patterns on corresponding clinical field images. This would require deep learning application training datasets to develop an algorithm, and subsequent validation of the deep learning models on validation datasets. Deep learning could be explored to detect 'ground-truth' ultra-high field MRI findings on the corresponding low field MR images, and could potentially provide the link between ultra-high and clinical field MRI for clinical translation.

A proposed MRI biomarker discovery and clinical translation pipeline is shown in Figure 8.1. This shows a workflow for discovery of MRI biomarkers of tumour extent and treatment response at ultra-high field 'microscopic' resolutions, and clinical translation of these findings for a clinical MRI virtual whole tumour 'biopsy' and use in targeted patient treatment. This PhD work has established a method for MRI functional biomarker map correlation with histopathology at 11.7 tesla shown in Figure 8.1 (a).

The MR biomarker maps at 11.7 tesla and 3.0 tesla in Figure 8.1 are from this PhD work. In Figure 8.1(a), an 11.7 tesla DTI-MRI direction encoded colour FA functional biomarker map of a rectal cancer tissue sample is shown, with the corresponding histopathology. These ultra-high field images were on the first rectal cancer tissue specimen obtained from the CONCERT Biobank as part of the PhD manuscript entitled 'Correlation of ultra-high field MRI with histopathology for evaluation of rectal cancer heterogeneity'. In Figure 8.1(b), the corresponding DTI-MRI FA and direction encoded FA biomarker maps of the same Biobank tissue sample at 3.0 tesla are shown. The vial containing the tissue sample was placed in a custom gel phantom for scanning on the radiotherapy dedicated 3.0 T MRI-Simulator. DTI MRI was acquired using the head and neck surface coil with b values 0 and 1200, bandwidth 1040 Hz / Px, in-plane resolution 0.57mm x 0.57mm, slice thickness 1.30 mm, 1 average, repetition time 8000 ms, echo time 105 ms. The 3.0 tesla images shown in Figure 8.1 (b) are un-orientated and difficult to assess visually due to the lower resolution.

Future work will be directed at developing the clinical translational pipeline shown in Figure 8.1. This will incorporate deep learning super-resolution methods for the translation of ultra-high field findings to clinically relevant fields. The complete MRI biomarker discovery pipeline loop would include *in vivo* patient imaging, patient tissue biobanking for evaluation of the patient's cancer tissue at ultra-high and clinical field strengths, with *in vivo* and *ex vivo* MRI results correlated with the patient's histopathology and oncology outcomes.

Figure 8.1 MRI – Biobank cancer biomarker discovery and clinical translation pipeline

11.7 T NMR
Ex vivo analysis of biobank tissue

3 T MRI
Ex vivo analysis of biobank tissue
Deep learning

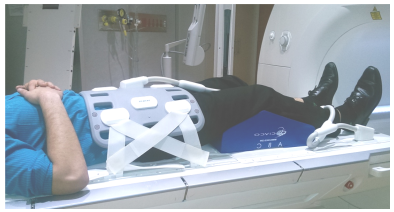

3 T MRI
In vivo imaging
Single image super resolution (SISR)

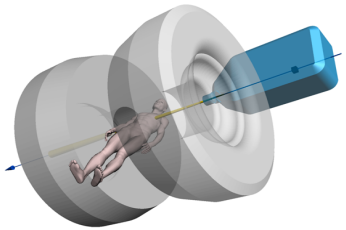

Diagnostic MRI and MRI-Linac
Individualised treatment
Functional targeting on MRI-Linac

(a) MRI functional biomarker map Histopathology 'ground-truth'
Explore novel MRI biomarkers of tumour extent and treatment response at 'microsopic' resolution and correlate with histopathology 'ground-truth'

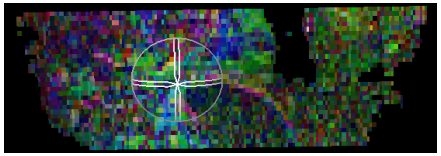

(b) Translation of high field findings to lower clinically relevant field
Deep learning training and validation for detection of higher field MRI 'ground-truth' features on clinical field MRI

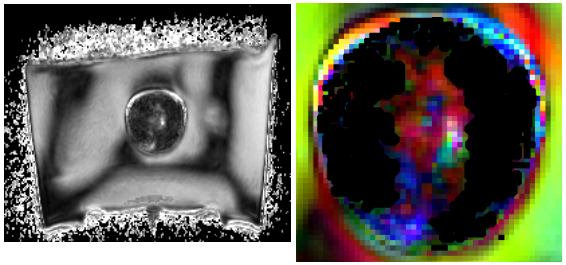

(c) Clinical testing of deep learning models Tissue biobanking
Clinical image used to produce SISR to detect MRI biomarkers of tumour extent and treatment response

(d) MRI virtual whole tumour 'biopsy' of extent and function Tissue biobanking
Patient outcomes to inform future MRI-Biobank studies

(e) MRI – Biobank studies
Collaboration for high field MRI atlas
Multiple tumour subsite studies

8.6 MRI-Linac guided radiotherapy and human rectal Images on the Australian MRI-Linac

MRI-Linacs are a new generation of radiotherapy machines with MRI replacing plain X-rays and CT as the image guidance strategy. An MRI-Linac combines a radiotherapy linear accelerator with an MRI scanner. It allows for exquisite soft tissue imaging facilitating improved anatomical targeting of cancer. The ability to obtain daily MR images during radiotherapy without additional ionising radiation dose will enable improved real-time guidance and adaption of radiotherapy to tumour. In addition, the development of functional capabilities on the MRI-Linac platforms opens up the possibility of targeting of tumour physiology. The Australian MRI-Linac is currently one of four prototypes around the world (78). It combines a 1.0 tesla MRI in an inline configuration, where the radiation beam is aligned with the magnetic field (B0). The first human images have been acquired on the Australian MRI-Linac (79). The first successful live imaging and radiotherapy delivery on the Australian MRI-Linac was performed on a rat with injected glioma cells (80). T2-weighted and T1-weighted images were acquired after administration of a gadolinium nanoparticle contrast agent to verify the brain target and confirm the presence of a brain tumour and uptake of gadolinium nanoparticle contrast agent in tumour. Dynamic fast gradient-echo sequence was acquired during radiotherapy delivery to provide real-time assessment of animal respiration and intra-fraction motion. A clinical trial to treat the first patients on this radiotherapy device is underway for 2020.

In rectal cancer, the exquisite soft tissue images on an MRI-Linac allows for real time anatomical image guidance superior to the cone-beam CT images currently acquired on standard radiotherapy linacs. On a rectal cone-beam CT, it is difficult to visualise tumour definition, and surrounding normal structures such as anal sphinctor. A healthy male volunteer was scanned on the Australian MRI-Linac on the **'Magnetic Resonance Imaging in healthy volunteers'** study (ethics approval numbers HREC/15/LPOOL/506, SSA/16/LPOOL/3, project number 15/270). The MRI-Linac integrated body coil was used. T2-weighted turbo spin echo images were acquired with TR 10260 ms, TE 86 ms, in plane resolution of 2 mm x 2 mm, slice thickness 3.5 mm, 4 averages, 1 concatenation,

bandwidth 202 Hz / Px, and with offline 3D distortion correction. The acquisition time was 6.08 minutes. Figure 8.2 shows the MR images acquired on the healthy volunteer. The results show excellent soft tissue definition of relevant rectal cancer treatment targets such as rectum and meso-rectum, and the surrounding normal structures such prostate, levator ani and anal sphinctor achieved on images acquired on the Australian MRI-Linac. Important considerations for future improvement of MRI-Linac anatomical imaging for rectal cancer include faster sequences to allow for faster daily imaging and minimising patient time on treatment bed. Diffusion images were not acquired on this volunteer as the Australian MRI-Linac does not yet have this capability due to limitations from the gradient coils.

Functional imaging is being implemented on MRI-Linac platforms and this could provide additional physiologic information on rectal cancer, which could be acquired at multiple time-points during treatment, enabling identification and targeting of biologically relevant tumour sub-volumes. In rectal cancer, relevant biological targets would include tumour cellularity and perfusion. DWI could identify sub-regions of tumour necrosis at the beginning of radiotherapy that are more likely to be radio-resistant, for consideration of early treatment intensification with a radiotherapy boost. DCE could identify sub-regions of increased tumour perfusion, representing areas of increased angiogenesis and tumour aggressiveness for early boosting. Tumour biology is dynamic and functional imaging on an MRI-Linac could allow daily adaption to changes in tumour function. For example, temporal and spatial heterogeneity in tumour hypoxia exists (81), and functional imaging on an MRI-Linac could allow for daily assessment and radiotherapy adaption to changes in tumour perfusion and hypoxia. At present, DCE imaging can be performed on the Australian MRI-Linac. However, the Australian MRI-Linac is unable to perform other functional imaging (diffusion). Fusion of functional images from a diagnostic MRI scanner, or radiotherapy dedicated MRI-Simulator, with the planning MRI could allow targeting of tumour biologic sub-regions present at time of radiotherapy simulation and treatment planning. However, for adaption to functional changes during the course of treatment, more development of functional imaging on the MRI-Linac platforms is required.

Another possibility on the MRI-Linac in rectal cancer is the use of functional images acquired on the MRI-Linac for treatment response prediction and individualisation of patient treatment. For patients with locally advanced rectal cancer, patients identified as responders to CRT could be placed on a 'watch-and-wait' pathway, allowing them to avoid the morbidity of surgery and in the case of patients with low rectal cancer, a permanent colostomy. Patients with residual tumour after completion of CRT could have treatment intensification with a radiotherapy boost using contact x-ray brachytherapy directed to radiotherapy resistant sub-regions identified on functional MRI to attempt to improve the tumour response and also avoid morbidity of surgery.

Figure 8.2 Healthy volunteer pelvic images acquired on the Australian MRI-Linac

a – j are axial slices through the mid to lower rectum of a healthy male volunteer acquired with distortion correction at 1.0 tesla. The images below show the excellent soft tissue definition of relevant radiotherapy targets and organs at risk.

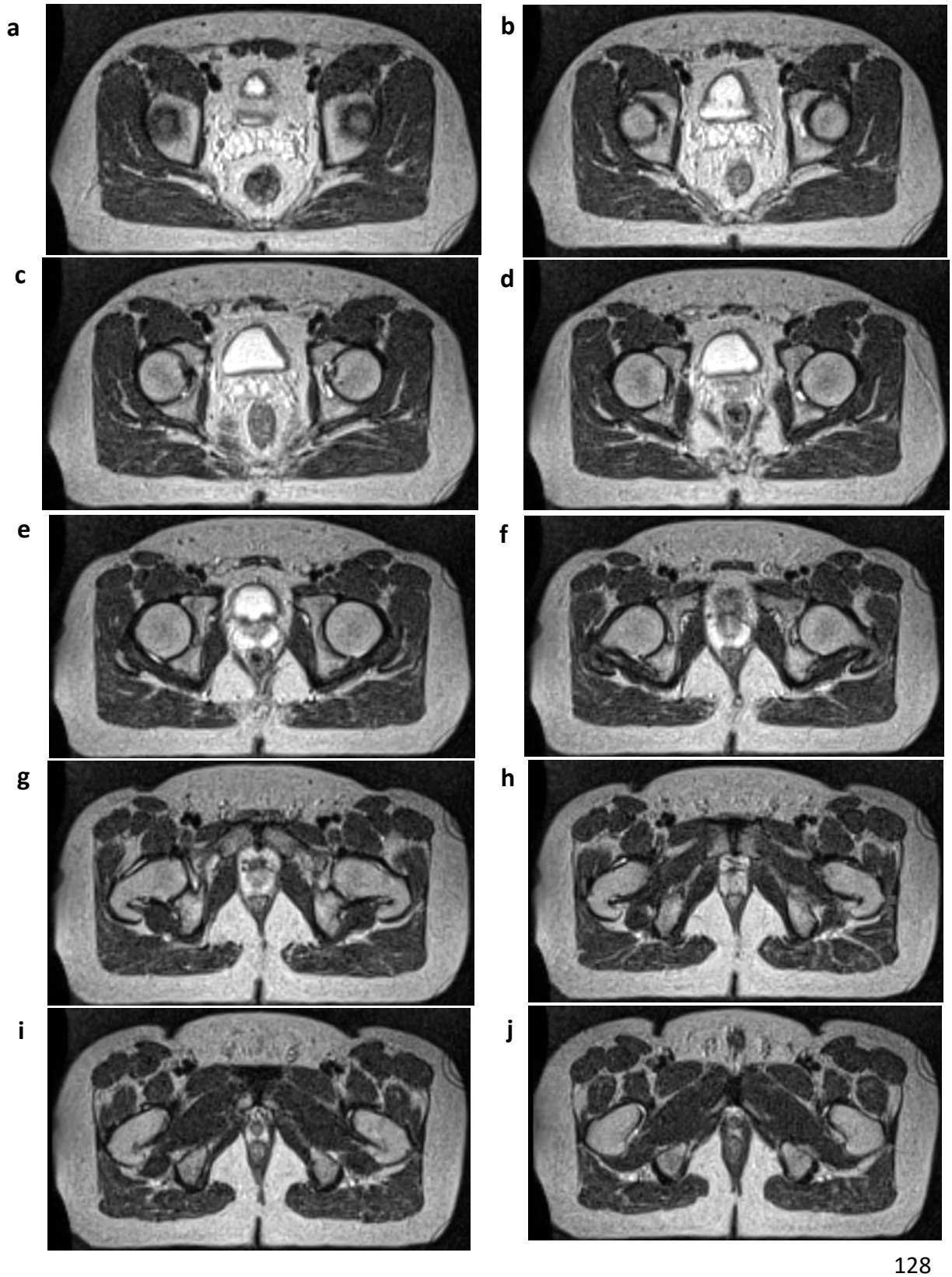

Chapter 9 Conclusions

This PhD work has demonstrated the ability of functional MRI for evaluation of tumour heterogeneity, extent, and prediction of response of rectal cancer to radiotherapy. This work encompassed clinical *in vivo* MRI at 3.0 tesla on patients undergoing CRT through to exploratory *ex vivo* ultra-high field MRI at 11.7 tesla on Biobank tissue specimens. MRI findings were correlated with 'ground-truth' histopathology.

1. Multi-parametric MRI tumour heterogeneity analysis for therapeutic response prediction in rectal cancer (3.0 tesla)

This is the first prospective multi-parametric MRI study, combining DWI and DCE, to incorporate a whole tumour heterogeneity analysis for prediction of CRT response. DWI-MRI incorporating a voxelised histogram analysis of whole tumour heterogeneity was able to predict CRT response in patients with locally advanced rectal cancer. Responders to CRT had significantly higher DWI-MRI derived ADC 75^{th} and 90^{th} percentile values after CRT (before surgery) than non-responders, despite there being no significant difference in median ADC values. This work highlights the value of incorporating a 3-D histogram assessment of tumour heterogeneity, rather than using volume averaged analysis. Thus, whole tumour ADC heterogeneity analysis after CRT may aid in the selection of responders to CRT for an organ preservation approach such as 'watch-and-wait'.

Assessment of tumour perfusion by DCE-MRI showed that K^{trans} quantiles at all time-points were higher in non-responders than responders, suggesting increased tumour angiogenesis in non-responders, although this was not statistically significant.

2. Multi-parametric MRI for prediction of 2 year disease-free survival in rectal cancer (3.0 tesla)

This PhD work identified DCE-MRI derived K^{trans} as a novel biomarker predictive of 2 year distant disease free survival (DFS) in rectal cancer. Patients with higher K^{trans} after CRT

(before surgery) or a greater ΔK^{trans} from before CRT to after CRT were at a significantly higher risk of developing distant metastases, and had lower 2 year DFS probability. The higher K^{trans} after CRT (pre-surgery) could indicate ongoing angiogenic activity in the tumour bed, facilitating and increasing the risk of haematogenous spread. There are currently no other published studies assessing K^{trans} as a biomarker for DFS in rectal cancer. This biomarker could be used for stratification of patients with high risk of distant relapse for intensification of systemic therapy in future studies.

DWI-MRI derived ADC was not useful for predicting DFS.

3. Ultra-high field MRI biomarker discovery in rectal cancer (11.7 tesla)

This PhD work established a discovery framework for screening Biobank tissue at ultra-high field *ex* vivo for novel MRI biomarkers of tumour heterogeneity, extent and response. This discovery framework incorporated a MRI-histopathology co-registration method for direct correlation of MRI findings with 'ground-truth' histopathology. Co-registration validation demonstrated that the Biobank tissue preparation methods used resulted in good preservation of tissue integrity, and alignment of tissue ROIs between DTI-MRI and histopathology, allowing for accurate correlation for MRI biomarker screening.

4. Diffusion tensor imaging MRI for assessment of rectal cancer tumour extent and heterogeneity ex vivo (11.7 tesla)

This is the first published study that explored the potential of DTI-MRI for evaluation of rectal cancer tumour extent and stromal heterogeneity. DTI-MRI derived fractional anisotropy (FA) was able assist in more accurate delineation of tumour heterogeneity and extent in rectal cancer *ex vivo*. DTI-MRI was useful for defining the extent of rectal cancer invasion into rectal wall. FA was able to differentiate tumour from muscularis propria, allowing for differentiation between stage T1 and T2 tumours. In addition, FA was able to differentiate between tumour, desmoplasia and fibrosis, a finding that could be useful for radiotherapy response prediction.

5. Future directions

DTI-MRI at 3.0 tesla of rectal cancer tissue *ex vivo* showed heterogeneity in FA at a clinically relevant field strength. Future work is underway focusing on the clinical translation of ultra-high field MRI findings to clinically relevant field strengths. Deep learning and super-resolution MRI methods could be explored for the MRI biomarker discovery pipeline.

Early work on the Australian-MRI Linac has shown the ability of the MRI-Linac to achieve images with good definition of rectal radiotherapy treatment targets and surrounding normal tissue. Future work should be directed at developing the MRI-Linac for targeting of biological tumour subregions. Ultimately, an MRI virtual whole tumour 'biopsy' of heterogeneity could be used for real-time tracking, adaptation and targeting of tumour function on the MRI-Linac.

References

1. Colorectal and other digestive-tract cancers. Cancer Series no 114. Canberra: Australian Institute of Health and Welfare; 2018.
2. Kapiteijn E, Marijnen CAM, Nagtegaal ID, Putter H, Steup WH, Wiggers T, et al. Preoperative Radiotherapy Combined with Total Mesorectal Excision for Resectable Rectal Cancer. New England Journal of Medicine. 2001;345(9):638-46.
3. Folkesson J, Birgisson H, Pahlman L, Cedermark B, Glimelius B, Gunnarsson U. Swedish Rectal Cancer Trial: long lasting benefits from radiotherapy on survival and local recurrence rate. J Clin Oncol. 2005;23(24):5644-50.
4. Sauer R, Becker H, Hohenberger W, Rödel C, Wittekind C, Fietkau R, et al. Preoperative versus Postoperative Chemoradiotherapy for Rectal Cancer. N Engl J Med. 2004;351(17):1731-40.
5. Sauer R, Liersch T, Merkel S, Fietkau R, Hohenberger W, Hess C, et al. Preoperative versus postoperative chemoradiotherapy for locally advanced rectal cancer: results of the German CAO/ARO/AIO-94 randomized phase III trial after a median follow-up of 11 years. J Clin Oncol. 2012;30(16):1926-33.
6. Abraha I, Aristei C, Palumbo I, Lupattelli M, Trastulli S, Cirocchi R, et al. Preoperative radiotherapy and curative surgery for the management of localised rectal carcinoma. Cochrane Database of Systematic Reviews. 2018(10).
7. Camma C, Giunta M, Fiorica F, Pagliaro L, Craxi A, Cottone M. Preoperative radiotherapy for resectable rectal cancer: A meta-analysis. Jama. 2000;284(8):1008-15.
8. Maas M, Nelemans PJ, Valentini V, Das P, Rödel C, Kuo L-J, et al. Long-term outcome in patients with a pathological complete response after chemoradiation for rectal cancer: a pooled analysis of individual patient data. Lancet Oncol. 2010;11(9):835-44.
9. Valentini V, Coco C, Cellini N, Picciocchi A, Fares MC, Rosetto ME, et al. Ten years of preoperative chemoradiation for extraperitoneal T3 rectal cancer: acute toxicity, tumor response, and sphincter preservation in three consecutive studies. Int J Radiat Oncol Biol Phys. 2001;51(2):371-83.
10. Valentini V, van Stiphout RGPM, Lammering G, Gambacorta MA, Barba MC, Bebenek M, et al. Nomograms for Predicting Local Recurrence, Distant Metastases, and Overall Survival for Patients With Locally Advanced Rectal Cancer on the Basis of European Randomized Clinical Trials. J Clin Oncol2011.
11. Dhadda AS, Bessell EM, Scholefield J, Dickinson P, Zaitoun AM. Mandard Tumour Regression Grade, Perineural Invasion, Circumferential Resection Margin and Post-chemoradiation Nodal Status Strongly Predict Outcome in Locally Advanced Rectal Cancer Treated with Preoperative Chemoradiotherapy. Clin Oncol. 2014;26(4):197-202.
12. van der Paardt MP, Zagers MB, Beets-Tan RGH, Stoker J, Bipat S. Patients Who Undergo Preoperative Chemoradiotherapy for Locally Advanced Rectal Cancer Restaged by Using Diagnostic MR Imaging: A Systematic Review and Meta-Analysis. Radiology. 2013;269(1):101-12.
13. Patterson DM, Padhani AR, Collins DJ. Technology insight: water diffusion MRI--a potential new biomarker of response to cancer therapy. Nat Clin Pract Oncol. 2008;5(4):220-33.

14. Barbaro B, Vitale R, Valentini V, Illuminati S, Vecchio FM, Rizzo G, et al. Diffusion-weighted magnetic resonance imaging in monitoring rectal cancer response to neoadjuvant chemoradiotherapy. Int J Radiat Oncol Biol Phys. 2012;83(2):594-9.
15. Lambrecht M, Vandecaveye V, De Keyzer F, Roels S, Penninckx F, Van Cutsem E, et al. Value of diffusion-weighted magnetic resonance imaging for prediction and early assessment of response to neoadjuvant radiochemotherapy in rectal cancer: preliminary results. Int J Radiat Oncol Biol Phys. 2012;82(2):863-70.
16. Monguzzi L, Ippolito D, Bernasconi DP, Trattenero C, Galimberti S, Sironi S. Locally advanced rectal cancer: value of ADC mapping in prediction of tumor response to radiochemotherapy. Eur J Radiol. 2013;82(2):234-40.
17. Genovesi D, Filippone A, Ausili Cefaro G, Trignani M, Vinciguerra A, Augurio A, et al. Diffusion-weighted magnetic resonance for prediction of response after neoadjuvant chemoradiation therapy for locally advanced rectal cancer: preliminary results of a monoinstitutional prospective study. Eur J Surg Oncol. 2013;39(10):1071-8.
18. Metcalfe P, Liney G, Holloway L, Walker A, Barton M, Delaney G, et al. The potential for an enhanced role for MRI in radiation-therapy treatment planning. Technol Cancer Res Treat. 2013;12(5):429-46.
19. Zahra MA, Hollingsworth KG, Sala E, Lomas DJ, Tan LT. Dynamic contrast-enhanced MRI as a predictor of tumour response to radiotherapy. Lancet Oncol. 2007;8(1):63-74.
20. George M, Dzik-Jurasz A, Padhani A, Brown G, Tait D, Eccles S, et al. Non-invasive methods of assessing angiogenesis and their value in predicting response to treatment in colorectal cancer. Br J Surg. 2001;88(12):1628-36.
21. de Vries A, Griebel J, Kremser C, Judmaier W, Gneiting T, Debbage P, et al. Monitoring of Tumor Microcirculation during Fractionated Radiation Therapy in Patients with Rectal Carcinoma: Preliminary Results and Implications for Therapy. Radiology. 2000;217(2):385-91.
22. de Lussanet QG, Backes WH, Griffioen AW, Padhani AR, Baeten CI, van Baardwijk A, et al. Dynamic contrast-enhanced magnetic resonance imaging of radiation therapy-induced microcirculation changes in rectal cancer. Int J Radiat Oncol Biol Phys. 2005;63(5):1309-15.
23. Yeo DM, Oh SN, Jung CK, Lee MA, Oh ST, Rha SE, et al. Correlation of dynamic contrast-enhanced MRI perfusion parameters with angiogenesis and biologic aggressiveness of rectal cancer: Preliminary results. J Magn Reson Imaging. 2013.
24. Oberholzer K, Menig M, Pohlmann A, Junginger T, Heintz A, Kreft A, et al. Rectal cancer: assessment of response to neoadjuvant chemoradiation by dynamic contrast-enhanced MRI. J Magn Reson Imaging. 2013;38(1):119-26.
25. Joye I, Debucquoy A, Deroose CM, Vandecaveye V, Cutsem EV, Wolthuis A, et al. Quantitative imaging outperforms molecular markers when predicting response to chemoradiotherapy for rectal cancer. Radiother Oncol. 2017;124(1):104-9.
26. Bulens P, Couwenberg A, Haustermans K, Debucquoy A, Vandecaveye V, Philippens M, et al. Development and validation of an MRI-based model to predict response to chemoradiotherapy for rectal cancer. Radiother Oncol. 2018;126(3):437-42.
27. De Felice F, Magnante AL, Musio D, Ciolina M, De Cecco CN, Rengo M, et al. Diffusion-weighted magnetic resonance imaging in locally advanced rectal cancer

treated with neoadjuvant chemoradiotherapy. Eur J Surg Oncol. 2017;43(7):1324-9.
28. Iannicelli E, Di Pietropaolo M, Pilozzi E, Osti MF, Valentino M, Masoni L, et al. Value of diffusion-weighted MRI and apparent diffusion coefficient measurements for predicting the response of locally advanced rectal cancer to neoadjuvant chemoradiotherapy. Abdom Radiol. 2016;41(10):1906-17.
29. Birlik B, Obuz F, Elibol FD, Celik AO, Sokmen S, Terzi C, et al. Diffusion-weighted MRI and MR- volumetry--in the evaluation of tumor response after preoperative chemoradiotherapy in patients with locally advanced rectal cancer. Magn Reson Imaging. 2015;33(2):201-12.
30. Palmisano A, Esposito A, Rancoita PMV, Di Chiara A, Passoni P, Slim N, et al. Could perfusion heterogeneity at dynamic contrast-enhanced MRI be used to predict rectal cancer sensitivity to chemoradiotherapy? Clinical radiology. 2018;73(10):911 e1- e7.
31. Tong T, Sun Y, Gollub MJ, Peng W, Cai S, Zhang Z, et al. Dynamic contrast-enhanced MRI: Use in predicting pathological complete response to neoadjuvant chemoradiation in locally advanced rectal cancer. J Magn Reson Imaging. 2015;42(3):673-80.
32. Petrillo A, Fusco R, Petrillo M, Granata V, Sansone M, Avallone A, et al. Standardized Index of Shape (SIS): a quantitative DCE-MRI parameter to discriminate responders by non-responders after neoadjuvant therapy in LARC. European radiology. 2015;25(7):1935-45.
33. Intven M, Monninkhof EM, Reerink O, Philippens ME. Combined T2w volumetry, DW-MRI and DCE-MRI for response assessment after neo-adjuvant chemoradiation in locally advanced rectal cancer. Acta oncol. 2015;54(10):1729-36.
34. De Cecco CN, Ciolina M, Caruso D, Rengo M, Ganeshan B, Meinel FG, et al. Performance of diffusion-weighted imaging, perfusion imaging, and texture analysis in predicting tumoral response to neoadjuvant chemoradiotherapy in rectal cancer patients studied with 3T MR: initial experience. Abdom. Radiol. 2016;41(9):1728-35.
35. Enkhbaatar NE, Inoue S, Yamamuro H, Kawada S, Miyaoka M, Nakamura N, et al. MR Imaging with Apparent Diffusion Coefficient Histogram Analysis: Evaluation of Locally Advanced Rectal Cancer after Chemotherapy and Radiation Therapy. Radiology. 2018;288(1):129-37.
36. Choi MH, Oh SN, Rha SE, Choi JI, Lee SH, Jang HS, et al. Diffusion-weighted imaging: Apparent diffusion coefficient histogram analysis for detecting pathologic complete response to chemoradiotherapy in locally advanced rectal cancer. J Magn Reson Imaging. 2016;44(1):212-20.
37. Cho SH, Kim GC, Jang YJ, Ryeom H, Kim HJ, Shin KM, et al. Locally advanced rectal cancer: post-chemoradiotherapy ADC histogram analysis for predicting a complete response. Acta Radiol. 2015;56(9):1042-50.
38. Yamada I, Hikishima K, Miyasaka N, Kato K, Kojima K, Kawano T, et al. Gastric carcinoma: Evaluation with diffusion-tensor MR imaging and tractography ex vivo. Magn Reson Imaging. 2016;34(2):144-51.

39. Yamada I, Miyasaka N, Hikishima K, Kato K, Kojima K, Kawano T, et al. Gastric Carcinoma: Ex Vivo MR Imaging at 7.0 T–Correlation with Histopathologic Findings. Radiology. 2015;275(3):841-8.
40. Yamada I, Miyasaka N, Hikishima K, Tokairin Y, Kawano T, Ito E, et al. Ultra-high-resolution MR imaging of esophageal carcinoma at ultra-high field strength (7.0T) ex vivo: correlation with histopathologic findings. Magn Reson Imaging. 2015;33(4):413-9.
41. Ryan R, Gibbons D, Hyland J. Pathological response following long course neoadjuvant chemoradiotherapy for locally advanced rectal cancer. Histopathology. 2005;47:141-6.
42. Edge S BD, Compton C, Fritz A, Green F, Trotti A (Editors). AJCC Cancer Staging Manual 7th Edition. 2012.
43. Tofts PS, Brix G, Buckley DL, Evelhoch JL, Henderson E, Knopp MV, et al. Estimating kinetic parameters from dynamic contrast-enhanced T(1)-weighted MRI of a diffusable tracer: standardized quantities and symbols. J Magn Reson Imaging. 1999;10(3):223-32.
44. (RCPA) RCoPoA. Colorectal Cancer Structured Reporting Protocol 2nd edition. Sydney: RCPA. 2012.
45. Just N. Improving tumour heterogeneity MRI assessment with histograms. British journal of cancer. 2014;111(12):2205-13.
46. Trakarnsanga A, Gönen M, Shia J, Nash GM, Temple LK, Guillem JG, et al. Comparison of Tumor Regression Grade Systems for Locally Advanced Rectal Cancer After Multimodality Treatment. JNCI Journal of the National Cancer Institute. 2014;106(10):dju248.
47. Intven M, Reerink O, Philippens ME. Dynamic contrast enhanced MR imaging for rectal cancer response assessment after neo-adjuvant chemoradiation. J Magn Reson Imaging. 2015;41(6):1646-53.
48. Martens MH, Subhani S, Heijnen LA, Lambregts DMJ, Buijsen J, Maas M, et al. Can perfusion MRI predict response to preoperative treatment in rectal cancer? Radiother Oncol. 2015;114(2):218-23.
49. Intven M, Monninkhof EM, Reerink O, Philippens MEP. Combined T2w volumetry, DW-MRI and DCE-MRI for response assessment after neo-adjuvant chemoradiation in locally advanced rectal cancer. Acta oncol. 2015;54(10):1729-36.
50. DeVries AF, Kremser C, Hein PA, Griebel J, Krezcy A, Öfner D, et al. Tumor microcirculation and diffusion predict therapy outcome for primary rectal carcinoma. Int J Radiat Oncol Biol Phys. 2003;56(4):958-65.
51. Nie K, Shi L, Chen Q, Hu X, Jabbour SK, Yue N, et al. Rectal Cancer: Assessment of Neoadjuvant Chemoradiation Outcome based on Radiomics of Multiparametric MRI. Clin Cancer Res. 2016;22(21):5256-64
52. DeVries AF, Piringer G, Kremser C, Judmaier W, Saely CH, Lukas P, et al. Pretreatment evaluation of microcirculation by dynamic contrast-enhanced magnetic resonance imaging predicts survival in primary rectal cancer patients. Int J Radiat Oncol Biol Phys. 2014;90(5):1161-7.
53. Shukla-Dave A, Obuchowski NA, Chenevert TL, Jambawalikar S, Schwartz LH, Malyarenko D, et al. Quantitative imaging biomarkers alliance (QIBA) recommendations for improved precision of DWI and DCE-MRI derived

biomarkers in multicenter oncology trials. J Magn Reson Imaging. 2019;49(7):e101-e121.
54. DCE MRI Technical Committee. DCE MRI Quantification Profile, Quantitative Imaging, Biomarkers Alliance Version 1.0. Reviewed Draft. QIBA, July 1, 2012. Available from: http://rsna.org/QIBA_.aspx.
55. Tuncbilek N, Tokatli F, Altaner S, Sezer A, Ture M, Omurlu IK, et al. Prognostic value DCE-MRI parameters in predicting factor disease free survival and overall survival for breast cancer patients. Eur J Radiol. 2012;81(5):863-7.
56. Pickles MD, Manton DJ, Lowry M, Turnbull LW. Prognostic value of pre-treatment DCE-MRI parameters in predicting disease free and overall survival for breast cancer patients undergoing neoadjuvant chemotherapy. Eur J Radiol. 2009;71(3):498-505.
57. Beckonert O, Coen M, Keun HC, Wang Y, Ebbels TM, Holmes E, et al. High-resolution magic-angle-spinning NMR spectroscopy for metabolic profiling of intact tissues. Nature protocols. 2010;5(6):1019-32.
58. Swanson MG, Zektzer AS, Tabatabai ZL, Simko J, Jarso S, Keshari KR, et al. Quantitative analysis of prostate metabolites using 1H HR-MAS spectroscopy. Magn Reson Med. 2006;55(6):1257-64.
59. Caixeiro N, Aghmesheh M, de Souza P, Lee CS. The Centre for Oncology Education and Research Translation (CONCERT) Biobank. Open Journal of Bioresources. 2015;2(1):e3.
60. Liu Z, Zhang X-Y, Shi Y-J, Wang L, Zhu H-T, Tang Z, et al. Radiomics Analysis for Evaluation of Pathological Complete Response to Neoadjuvant Chemoradiotherapy in Locally Advanced Rectal Cancer. Clin Cancer Res. 2017;23(23):7253-62.
61. Bibault J-E, Giraud P, Housset M, Durdux C, Taieb J, Berger A, et al. Deep Learning and Radiomics predict complete response after neo-adjuvant chemoradiation for locally advanced rectal cancer. Sci Rep. 2018;8(1):12611.
62. Vallieres M, Zwanenburg A, Badic B, Cheze Le Rest C, Visvikis D, Hatt M. Responsible Radiomics Research for Faster Clinical Translation. J Nucl Med. 2018;59(2):189-93.
63. Zwanenburg A, Leger S, Vallières M, Löck S. Image biomarker standardisation initiative - feature definitions. Version 1.1. 2016
64. Cunningham C. Transanal excision. Colorectal Dis. 2019;21(S1):41-4.
65. Sun Myint A, Stewart A, Mills J, Sripadam R, Whitmarsh K, Roy R, et al. Treatment: the role of contact X-ray brachytherapy (Papillon) in the management of early rectal cancer. Colorectal Dis. 2019;21(S1):45-52.
66. Balyasnikova S, Brown G. The MRI assessment of SPECC (significant polyps and early colorectal cancer) lesions. Colorectal Dis. 2019;21(S1):19-22.
67. Balyasnikova S, Read J, Wotherspoon A, Rasheed S, Tekkis P, Tait D, et al. Diagnostic accuracy of high-resolution MRI as a method to predict potentially safe endoscopic and surgical planes in patients with early rectal cancer. BMJ Open Gastroenterol. 2017;4(1):e000151.
68. Renehan AG, Malcomson L, Emsley R, Gollins S, Maw A, Myint AS, et al. Watch-and-wait approach versus surgical resection after chemoradiotherapy for patients with rectal cancer (the OnCoRe project): a propensity-score matched cohort analysis. Lancet Oncol. 2016;17(2):174-83.

69. Habr-Gama A, Perez RO, Sao Juliao GP, Proscurshim I, Gama-Rodrigues J. Nonoperative approaches to rectal cancer: a critical evaluation. Semin Radiat Oncol. 2011;21(3):234-9.
70. Maas M, Beets-Tan RG, Lambregts DM, Lammering G, Nelemans PJ, Engelen SM, et al. Wait-and-see policy for clinical complete responders after chemoradiation for rectal cancer. Journal of Clinical Oncology. 2011;29(35):4633-40.
71. Myint AS, Smith FM, Gollins SW, Wong H, Rao C, Whitmarsh K, et al. Dose escalation using contact X-ray brachytherapy (Papillon) for rectal cancer: does it improve the chance of organ preservation? Br J Radiol. 2017;90(1080):20170175.
72. Myint AS, Lee CD, Gerard JP "Chapter 25 Rectal Cancer" in The GEC ESTRO Handbook of Brachytherapy (2nd Edition). Limbergen EV, Potter R, Hoskin P, Baltas D (Eds.) 2014.
73. Lyu Q, You C, Shan H, Wang G. Super-resolution MRI through deep learning https://arxiv.org/abs/1810.067762018 [16/10/2018:[
74. Yang W, Zhang X, Tian Y, Wang W, Xue J-H, Liao Q. Deep learning for single image super-resolution: a brief review. IEEE Transactions on Multimedia. 2019;2019.
75. Liu T, de Haan K, Rivenson Y, Wei Z, Zeng X, Zhang Y, et al. Deep learning-based super-resolution in coherent imaging systems. Sci Rep. 2019;9(1):3926.
76. Chaudhari AS, Fang Z, Kogan F, Wood J, Stevens KJ, Gibbons EK, et al. Super-resolution musculoskeletal MRI using deep learning. Magn Reson Med. 2018;80(5):2139-54.
77. Chen Y, Xie Y, Zhou Z, Shi F, Christodoulou A, Li D, editors. Brain MRI super resolution using 3D deep densely connected neural networks. 2018 IEEE 15th International Symposium on Biomedical Imaging (ISBI 2018); 2018 24/5/2018; Washington, D.C., USA: IEEE; 2018.
78. Keall PJ, Barton M, Crozier S. The Australian magnetic resonance imaging-linac program. Semin Radiat Oncol. 2014;24(3):203-6.
79. Liney GP, Dong B, Weber E, Rai R, Destruel A, Garcia-Alvarez R, et al. Imaging performance of a dedicated radiation transparent RF coil on a 1.0 tesla inline MRI-linac. Phys Med Biol. 2018;63:135005.
80. Liney GP, Jelen U, Byrne H, Dong B, Roberts T, Kuncic Z, et al. The first live treatment on a 1.0 tesla inline MRI-linac. Med Phys. 2019;46(7):3254-8.
81. Vaupel P. Tumour microenvironmental physiology and its implications for radiation oncology. Sem Radiat Oncol. 2004;14(3):198-206.

Appendices

APPENDIX 1 – Rectal multi-parametric MRI - study sequences (Version 3 - 17.4.2015)

Patient Preparation

- MRI safety form
- Doctor to check suitability for gadolinium-based contrast. Patients with eGFR <60ml/min/1.73m2 or prior allergic reaction to gadolinium-based contrast are not suitable contrast. Exclude the Flip angle and DCE sequence in these patients.
- ***Gadolinium-based contrast***: Calculated per body weight as prescribed by doctor. 0.1mM/kg (nb Optimark strength: 0.5mmol/ml), capped at a maximum of 15ml (7.5mmol)
- Ensure patient is comfortable and pain-free. *Amount of contrast needs to be same across all timepoints for each patient.*
- Allow the patient to empty the bladder/bowel before the procedure.
- No bowel preparation, air insufflations, antispasmodic or intrarectal contrast agents required.
- Nursing checks for buscopan and IV contrast must be done prior to commencing MRI scanning.

Patient Positioning

- Supine and feet-first
- Curved couch
- 18 channel phase array coil placed *firmly* around the pelvis and strapped to ensure good compression and reduction in abdominal movement with respiration. Ensure that the pelvic coil is centred optimally to ensure adequate coverage of the rectum, mesorectum and anal sphincter complex. There should be adequate coverage from the level of the sacral promontory to below the symphysis pubis.

Important note on field of view for week 3 and 11-12 scans

- *The field of view (FOV) for MRIs performed during weeks 3 and 11-12 should be the same as the baseline/Pre-CRT MRI. This is required to assess changes in MRI endpoints.*
- *The FOV should NOT be reduced, even in the case of tumour regression. Ie. The FOV for MRI and all three time-points needs to be identical.*

Sequences:

LOCALISER

- 3 plane localiser
- Used to plan the sagittal sequence below

SEQUENCE 1: T2-WEIGHTED Sagittal:

- FOV 24cm to encompass primary and nodes - from inner pelvic sidewall to sidewall
- 2mm slice thickness
- No fat saturation
- Bandwidth 444Hz/Px
- Phase encoding direction H-F
- Phase oversampling 60%
- Distance factor 0%
- 1 concatenation
- iPAT GRAPPA 2
- Averages 2
- 'Prescan normalize' ON

SEQUENCE 2: T2-WEIGHTED Axial Oblique (Short axis):

- **Axial Angulation**: the axial T2-weight sequence should be angulated perpendicular to the longest tumour axis as identified on the sagittal images.

- High resolution
- FOV 22cm to encompass primary and nodes – from L5/S1 junction to anal verge
- 2mm slice thickness
- No fat saturation
- Bandwidth 444Hz/Px
- Phase encoding direction R-L
- Distance factor 0%
- 1 concatenation
- iPAT GRAPPA 2
- Averages 2
- 'Flow Comp' ON
- 'Prescan normalize' ON

SEQUENCE 3: T2-WEIGHTED Axial Orthogonal:

- As per sequence 2 above, but angle – Axial Orthogonal (Straight transverse)

SEQUENCE 4: T2-WEIGHTED Coronal Haste (Long axis):

- Angulation:
    - Mid-high rectal tumours (5-15cm from anal verge) – coronal plane should be angulated parallel to long axis of tumour
    - Low rectal tumours (<5cm) coronal plane should be angulated parallel to the long axis of the anal canal
- FOV 16cm – from posterior pubic symphysis to S2
- HASTE
- Bandwidth 444Hz/Px
- Phase encoding direction R-L (may need to individualise)
- Distance factor 0%
- 1 concatenation
- 'Prescan normalize' ON

Administer Buscopan 20mg IV, and prepare the contrast lines prior to the DWI and FA/DCE sequences below.

SEQUENCE 5: DIFFUSION-WEIGHTED IMAGING RESOLVE (DWI)

- **Axial (Orthogonal)**
- RESOLVE
- b-values: 50 and 800 s/mm2.
- Tick box 'calculated image' 1400s/mm2
- FOV (coverage of ***primary tumour)***: 22cm - aim coverage of primary tumour. If all of tumour does not fit, then scan through the central part of tumour.
- *Copy isocentre from T2W axial orthogonal images.*
- 1 acquisition only.
- Slices per slab: 20
- Slice thickness 4mm
- Bandwidth 870Hz/Px
- Phase encoding direction: A>>P
- Distance factor 0%
- 1 concatenation
- Averages 1 & 3

OPTIONAL for tumours greater than 8cm vertical length:

- ***Coupled graphics on***
- Number slice groups: 2
- Slices: 13 (Therefore total 26 slices)
- PM: FIX
- Everything else, as per DWI above.

Important note re: sequences 6 and 7 – flip angle scans and DCE below:

- *The flip angle (2° and 15°) and DCE all need to be IDENTICAL slice positions and number of slices.*

- *The 'copy parameters' links only works if all 3 series (flip angles and DCE) are dragged over to the scan queue together.*
- *Copy scans isocentre and same slice locations – see below*
- *Check that the table positions (TP) are identical for FA 2, FA 15 and DCE. This can be done by opening 'System' --> 'Miscellaneous' --> 'TP'*
- *Phase oversampling has been set to '80%'. If this is changed, it must be changed for all 3 series: FA2, FA15, and DCE.*

SEQUENCE 6: FLIP ANGLE SCANS *(exclude in patients not suitable for MRI contrast)*

- **Axial (orthogonal)**
- **PM: - REF** 2°**, FIX** 15° : ***copy 'measurement parameters'* from 2°**
- For both flip angles the following to be identical:
- Slices per slab: 26
- FOV: 22cm
- Phase FOV 100%
- Slice thickness 4mm
- Resolution: 1.1x 1.1 x 4.0
- Bandwidth: 440 Hz/Px
- TR 4.09ms
- TE 1.35ms
- ***Phase encoding direction: R-L***
    - Perform two flip angle scans T1 VIBE

SEQUENCE 7: DYNAMIC CONTRAST ENHANCED (DCE) *(exclude in patients not suitable for MRI contrast)*

- **Axial (orthogonal)**
- **PM: FIX**
- ***Copy 'slice centre + sat regions' from flip angle 2°***. Slices per slab, slice positions, and FOV to be **IDENTICAL** to flip angle scans
- Check the TP is identical to above FAs.
- Slices per slab: 26

- FOV 22cm
- Phase FOV 100%
- Slice thickness 4mm
- Resolution: 1.1 x 1.1 x 4.0
- TWIST
- Bandwidth: 440Hz/Px
- TR: 3.67ms
- TE: 1.48ms
- ***Phase encoding direction: R-L***
- Temporal Resolution 5.28s.
- Distance factor 0%
- 1 concatenation
- ***Commence scanning for 3 measurements, prior to injection of contrast. Inject contrast AFTER the 3rd measurement is almost complete, and just before 4th measurement. Scan for total 60 timepoints.***
- Injection of contrast, 4ml / second, 20ml flush.
- Save DCE images under one folder.

SEQUENCE 8: POST CONTRAST T1 VIBE DIXON

- Post-contrast fat sat sequence
- **Axial (orthogonal)**
- FOV – Primary and nodes 30cm, from L5 to Anal verge
- Phase encoding direction A>>P
- 2mm slice thickness
- Distance factor 0%
- 1 concatenation

APPENDIX 2 - Acute toxicity scoring form

Common terminology criteria for adverse events (CTCAE) version 4.0

Patient Name

MRN

DOB

DATE OF ASSESSMENT:

	Grade				
Toxicity	**0**	**1**	**2**	**3**	**4**
Dermatitis radiation	Nil	Faint erythema or dry desquamation	Moderate to brisk erythema; patchy moist desquamation, mostly confined to skin folds and creases; moderate edema	Moist desquamation in areas other than skin folds and creases; bleeding induced by minor trauma or abrasion	Life-threatening consequences; skin necrosis or ulceration of full thickness dermis; spontaneous bleeding from involved site; skin graft indicated
GASTRO-INTESTINAL					
Abdominal Pain	Nil	Mild pain	Moderate pain; limiting instrumental ADL	Severe pain; limiting self care	
Diarrhoea	Nil	Increase of <4 stools per day over baseline; mild increase in ostomy output compared to baseline	Increase of 4 - 6 stools per day over baseline; moderate increase in ostomy output compared to baseline	Increase of >=7 stools per day over baseline; incontinence; hospitalization indicated; severe increase in ostomy	Life-threatening consequences; urgent intervention indicated

	Grade				
Toxicity	**0**	**1**	**2**	**3**	**4**
				output compared to baseline; limiting self care ADL	
Enterocolitis A disorder characterized by inflammation of the small and large intestines.	Nil	Asymptomatic; clinical or diagnostic observations only; intervention not indicated	Abdominal pain; mucus or blood in stool	Severe or persistent abdominal pain; fever; ileus; peritoneal signs	Life-threatening consequences; urgent intervention indicated
Faecal incontinence	Nil	Occasional use of pads required	Daily use of pads required	Severe symptoms; elective operative intervention indicated	-
Flatulence	Nil	Mild symptoms; intervention not indicated	Moderate; persistent; psychosocial sequelae	-	-
Nausea	Nil	Loss of appetite without alteration in eating habits	Oral intake decreased without significant weight loss, dehydration or malnutrition	Inadequate oral caloric or fluid intake; tube feeding, TPN, or hospitalization indicated	-
Proctitis A disorder characterized by inflammation of the rectum.	Nil	Rectal discomfort, intervention not indicated	Symptoms (e.g., rectal discomfort, passing blood or mucus); medical intervention indicated; limiting instrumental ADL	Severe symptoms; fecal urgency or stool incontinence; limiting self care ADL	Life-threatening consequences; urgent intervention indicated

	Grade				
Toxicity	**0**	**1**	**2**	**3**	**4**
Rectal Pain	Nil	Mild pain	Moderate pain; limiting instrumental ADL	Severe pain; limiting self care ADL	-
Rectal Haemorrhage	Nil	Mild; intervention not indicated	Moderate symptoms; medical intervention or minor cauterization indicated	Transfusion, radiologic, endoscopic, or elective operative intervention indicated	Life-threatening consequences; urgent intervention indicated
Rectal obstruction	Nil	Asymptomatic; clinical or diagnostic observations only; intervention not indicated	Symptomatic; altered GI function; limiting instrumental ADL	Hospitalization indicated; elective operative intervention indicated; limiting self care ADL; disabling	Life-threatening consequences; urgent operative intervention indicated
Small intestinal obstruction	Nil	Asymptomatic; clinical or diagnostic observations only; intervention not indicated	Symptomatic; altered GI function; limiting instrumental ADL	Hospitalization indicated; elective operative intervention indicated; limiting self care ADL; disabling	Life-threatening consequences; urgent operative intervention indicated
GENITOURINARY					
Cystitis noninfective	Nil	Microscopic hematuria; minimal increase in frequency, urgency, dysuria, or nocturia; new onset of incontinence	Moderate hematuria; moderate increase in frequency, urgency, dysuria, nocturia or incontinence; urinary catheter placement or	Gross hematuria; transfusion, IV medications or hospitalization indicated; elective endoscopic, radiologic or operative	Life-threatening consequences; urgent radiologic or operative intervention indicated

	Grade				
Toxicity	**0**	**1**	**2**	**3**	**4**
			bladder irrigation indicated; limiting instrumental ADL	intervention indicated	
Haematuria	Nil	Asymptomatic; clinical or diagnostic observations only; intervention not indicated	Symptomatic; urinary catheter or bladder irrigation indicated; limiting instrumental ADL	Gross hematuria; transfusion, IV medications or hospitalization indicated; elective endoscopic, radiologic or operative intervention indicated; limiting self care ADL	Life-threatening consequences; urgent radiologic or operative intervention indicated
Urinary retention	Nil	Urinary, suprapubic or intermittent catheter placement not indicated; able to void with some residual	Placement of urinary, suprapubic or intermittent catheter placement indicated; medication indicated	Elective operative or radiologic intervention indicated; substantial loss of affected kidney function or mass	Life-threatening consequences; organ failure; urgent operative intervention indicated
OTHER					
Fatigue	Nil	Fatigue relieved by rest	Fatigue not relieved by rest; limiting instrumental ADL	Fatigue not relieved by rest, limiting self care ADL	-
Weight loss	Nil	5 to <10% from baseline;	10 - <20% from baseline;	>=20% from baseline; tube	-

	Grade				
Toxicity	**0**	**1**	**2**	**3**	**4**
		intervention not indicated	nutritional support indicated	feeding or TPN indicated	
OTHER TOXICITY	Nil	Mild; asymptomatic or mild symptoms; clinical or diagnostic observations only; intervention not indicated.	Moderate; minimal, local or noninvasive intervention indicated; limiting age-appropriate instrumental ADL*.	Severe or medically significant but not immediately life-threatening; hospitalization or prolongation of hospitalization indicated; disabling; limiting self care ADL**	Life-threatening consequences; urgent intervention indicated.

APPENDIX 3 - Histopathology reporting form

1. ypT and N staging.
2. Tumour Regression Grade (AJCC 7th Edition) (41)

Description	Tumour Regression Grade
No viable cancer cells	0 (Complete response)
Single cells or small groups of cancer cells	1 (Moderate response)
Residual cancer outgrown by fibrosis	2 (Minimal response)
Minimal or no tumour kill; extensive residual cancer	3 (Poor response)

   Tumour regression should be assessed only in the primary tumour; lymph node metastases should not be included in the assessment.
3. Size of primary
4. Positive nodes
5. Apical node involvement
6. Total nodes
7. Histology
8. Tumour in bowel wall at line of resection (yes/no)
9. Tumour at circumferential line of resection (yes/no)
10. Distance from circumferential line of resection (mm)
11. Closest circumferential line of resection (anterior/posterior/left/right/peritonealised rectum)
12. Perforation
13. Venous invasion
14. Arterial invasion
15. Perineural invasion
16. Adenoma contiguous with primary
17. IHC: PLK1, TIL, MSI